Heterogeneity and plasticity of the CD4 T cell compartment in viral infections

Inauguraldissertation

zur

Erlangung der Würde eines Doktors der Philosophie

vorgelegt der

Philosophisch-Naturwissenschaftlichen Fakultät

der Universität Basel

von

Marco Künzli

aus Strengelbach, Schweiz

2020

Genehmigt von der Philosophisch-Naturwissenschaftlichen Fakultät auf Antrag von

---

(Mitglieder des Dissertationskomitees: Prof. Dr. C. Hess, Prof. Dr. C. King, Dr. M. Linterman)

Basel, den 13.10.2020

Prof. Dr. Martin Spiess

Dekan

Table of Contents

ACKNOWLEDGEMENTS

First and foremost, I'm deeply indebted to my brilliant supervisor and mentor Carolyn King for giving me the opportunity to join your team. You provided me with encouragement, relentless support & unwavering enthusiasm. Thank you for your guidance and your profound belief in my abilities, it was a privilege to do research under your supervision and learn from you. You are truly an inspiration to me and shaped me scientifically but also personally.

I would like to extend my deepest gratitude to my fellow lab mates: Nivedya, David, Tamara, Ludivine, Joelle, Helene, Daniel, Clemens, and Gideon for the awesome time and the unforgettable moments we had in the last 5 years. Thank you very much for all the exciting scientific and non-scientific discussions and for providing a friendly atmosphere in the lab.

I'm extremely grateful to Daniel Pinschewer for your support and encouragement throughout my PhD. Many thanks also to the Pinschewer lab members Anna, Benedict, Cornelia, Karen, Karsten, Katrin, Kerstin, Magdalena, Marianna, Mehmet, Min, Mirela, Peter, Weldy, and Yusuf for the warm welcome in your lab during my civilian service and for all the funny moments we shared during my stay.

Additionally, I had the pleasure of working with many collaborators whose contribution are truly appreciated: Jonas Lötscher, Julien Roux, Florian Geier, Roman Jakob, Timm Maier, Christoph Hess und Justin Taylor.

I would also like to thank Michelle Linterman for agreeing to act as an external supervisor and Jean Pieters for being part of my thesis committee. Thank you for your insightful comments during committee meetings.

Finally, I would like to thank my parents Esther & Dieter and my sister Carina for their endless support not only during my PhD but also throughout my whole life. This work would not have been possible without you and I cannot thank you enough.

ABBREVIATIONS

ACD	Asymmetric cell division
AID	activation-induced cytidine deaminase
AKT	Protein kinase B
AP-1	Activator protein 1
APL	Altered peptide ligand
APC	Antigen presenting cell
ASC	Antibody secreting cell
BAFF	B cell activating factor
BCR	B cell receptor
CCR7	C-C chemokine receptor type 7
CD	Cluster of differentiation
CSR	Class switch recombination
CTL	Cytotoxic T lymphocytes
CTLA4	Cytotoxic T lymphocyte antigen 4
DZ	Dark zone
ER	Endoplasmic reticulum
FDC	Follicular dendritic cell
FOXO	Forkhead-Box-Protein
FR4	Folate receptor 4
GC	Germinal center
GP	Glycoprotein
HA	Hemagglutinin
HBV	Hepatitis B virus
HCV	Hepatitis C virus
HIV	Human immunodeficiency virus
ICOS	Inducible T cell costimulator
IFN-γ	Interferon- γ
ILC	Innate lymphoid cell
IL-2	Interleukin-2
IL-4	Interleukin-4
IL-17	Interleukin-17
IL-21	Interleukin-21
ITAM	Immunoreceptor tyrosine-based activation motif
LAT	Linker for activation of T cells
LCMV	Lymphocytic choriomeningitis virus

LLPC	Long lived plasma cell
LZ	Light zone
MHC	Major histocompatibility complex
mTOR	Mammalian target of rapamycin
NF-κB	Nuclear factor-κB
NFAT	Nuclear factor of activated T cells
PALS	Periarteriolar lymphoid sheaths
PAMP	Pathogen-associated molecular pattern
PD1	Programmed cell death 1
PDK1	Pyruvate Dehydrogenase Kinase 1
pMHC	Peptide bound to MHC
PI3K	Phosphoinositide 3-kinase
PIP_2	Phosphatidylinositol (4,5)-bisphosphate
PIP_3	Phosphatidylinositol (3,4,5)-trisphosphate
PKB	Protein kinase B
PRR	Pathogen recognition receptors
PSGL1	P-selectin glycoprotein ligand-1
S1PR	Sphingosine-1-phosphate receptor
SHM	Somatic hypermutation
SLAM	Signaling lymphocytic activation molecule
SLO	Secondary lymphoid organ
SLPC	Short lived plasma cell
Tb	Tuberculosis
TCR	T cell receptor
Tfh	Follicular B helper T cell
Th1	T helper 1 cell

SUMMARY

Project #1: Long-lived Tfh cells

The CD4 memory compartment has been subdivided into 3 distinct subsets that have different functions: inflammatory T effector memory (Tem), T central memory (Tcm), and tissue resident memory (Trm) cells. Whether T follicular helper (Tfh) cells that orchestrate the humoral response persist after the pathogen is cleared is controversial. We were able to show that Tfh cells are long-lived but extremely susceptible to NAD induced cell death (NICD) and therefore have previously been overlooked. Further characterization of Tfh cells revealed that folate receptor 4 (FR4) is a superior marker to CXCR5 in identifying Tfh memory cells. Surprisingly, Tfh memory cells maintain an anabolic state characterized by increased glucose uptake and mTORc1 activity yet retain full developmental plasticity. Furthermore, we identified a previously unknown functional role of Tfh memory cells in contributing to the maintenance of the humoral immune response beyond effector time points.

Project #2: GP61 variants

Upon a viral infection, naïve CD4 T cells differentiate into inflammatory T helper 1 (Th1) cells and Tfh cells which shape the antibody response. The role of the T cell receptor (TCR) signal strength on Th1 vs Tfh cell differentiation in a viral infection model is incompletely understood. Here, we developed a new tool that allows us to address this question in both acute and chronic viral infections. We generated LCMV strains with point mutations in the GP61 epitope, which is part of the LCMV glycoprotein and is recognized by TCR transgenic SMARTA cells. In acute infections, TCR signal strength positively correlated with Th1 induction. In contrast, chronic infections preferentially induced Tfh cells with increasing TCR signal strength and led to acquisition of surface markers associated with chronic T cell stimulation. Thus, depending on the immune context, TCR signals exerts opposite effects on the Th1 versus Tfh generation.

1. GENERAL INTRODUCTION

1.1. The adaptive immune system

The adaptive immune system is triggered by vaccines or by pathogens that are able to evade the innate immune system, the body's first cellular line of defense. In contrast to the innate immune response, which relies on the recognition of broadly conserved pathogen-associated molecular patterns (PAMPs) through pattern recognition receptors (PRRs), adaptive immunity is highly specific to the invading pathogen and provides a tailored response to the threat. Adaptive immunity usually provides long-lasting protection by forming immunological memory that allows the body to "remember" the pathogen, and is therefore also referred to as acquired immunity. The presence of immunological memory leads to accelerated detection of a subsequent infection by the same pathogen and immediately triggers an enhanced response that leads to more efficient clearance of the pathogen (*1*). Immunological memory also forms the foundation of vaccination, one of the most-successful interventions created by human mankind in the fight and control of infectious diseases to reduce death and morbidity (*2-4*). The first well-documented successful vaccination was performed in 1796, when Edward Jenner inoculated a 8-year-old boy called James with pustule from milk-maids infected with cowpox to protect against smallpox infections (*5*). In 1977, smallpox was officially eradicated (*5*). In the coming year, vaccines not only led to the eradication of smallpox, but also to the elimination of measles, poliomyelitis, rubella, and mumps from most parts of the world (*6, 7*). However, despite the enormous success of vaccines, there are numerous deadly infections for which there is no vaccine, e.g. HIV, malaria and tuberculosis (*8*). Historically, vaccines have been developed by a trial and error approach. To generate efficient vaccines against the above-mentioned diseases, we need to improve our understanding of the adaptive immunity in order to come up with novel and more systematic approaches (*9-11*).

The adaptive immune system consists of two major arms: the cell-mediated response is characterized by the killing of pathogen-infected host cells through activation of cytotoxic CD8 T cells and innate phagocytic cells. The humoral response impairs the spread of the infection in the extracellular compartment by inhibiting pathogen cell-entry through antibodies, which are pathogen-specific immunoglobulins secreted by B cells. Adaptive immune responses are initiated by a specialized subset of cells termed “antigen presenting cells” (APC). APCs consist of dendritic cells, macrophages and B cells, and their purpose is to degrade engulfed pathogens into small epitope peptides and present these on major histocompatibility complex (MHC) proteins to T cells (*12*). Subsequently, CD4 T helper cells differentiate into distinct effector subsets, thereby regulating the extent of both the cell-mediated and humoral responses.

In a viral infection, the adaptive immune response is regulated through early bifurcation of naïve CD4 T helper cells into Th1 and T follicular helper (Tfh) effector subsets. Th1 cells potentiate cell-mediated CD8 and macrophage cytotoxicity, while Tfh provide survival and proliferation signals to antibody producing B cells (*13*). Once an infection is cleared, most T and B effector cells die. However, the rest are long-lived and represent the immunological memory that facilitates the enhanced secondary response to subsequent infections (*1*).

1.2. CD4 T cell differentiation

It is well established that three signals are needed to activate naïve CD4 T cells, and the integration of these signals leads to extensive clonal expansion and differentiation into functionally distinct effector subsets (*14*). These three signals are composed of the signals received through the T cell receptor (TCR), the co-stimulatory receptors, and cytokine receptors.

Naïve CD4 T cells migrate between secondary lymphoid organs (SLO) and the blood system via the lymph(*15, 16*). Upon activation through cognate antigen in periarteriolar lymphoid sheaths (PALS) of secondary lymphoid organs (SLO), naïve CD4 T cells stop

migrating and enter a clonal expansion phase, during which one single naïve T cell can give rise to more than 1000 daughter cells (*17*). To meet the bioenergetic needs during the proliferation phase, CD4 T cells have to generate not only enough ATP but also the metabolic intermediates needed to produce biomass. Thus, proliferating T cells change their metabolic programming towards glycolysis and production of proteins, lipids, and nucleic acids (*18-21*). Simultaneously, depending on the environmental cues they are exposed to, T cells differentiate into specialized subsets by undergoing distinct transcriptional programming regulated by subset-specific master transcription factors. Classically, 5 distinct CD4 effector subsets have been described, each requiring different cues and generating specific cytokines that have different functions (Figure 1). Th1 cells have been shown to be important in the control of intracellular bacteria and viruses and produce interferon-γ (IFN-γ). Th2 cells fight helminth and parasite infection by secreting interleukin-4 (IL-4), and Th17 generate IL-17 to combat fungal and extracellular bacterial pathogens (*22*). In contrast, Tfh cells are generated regardless of the encountered pathogen and mainly secrete IL-21. Lastly, immunosuppressive regulatory T cells (Tregs) secrete IL-10 and are important for the maintenance of self-tolerance by dampening the immune response and inflammation (*22*). While secretion of cytokines is only one of several ways helper T cells elicit their effector functions, they are helpful for characterizing the response.

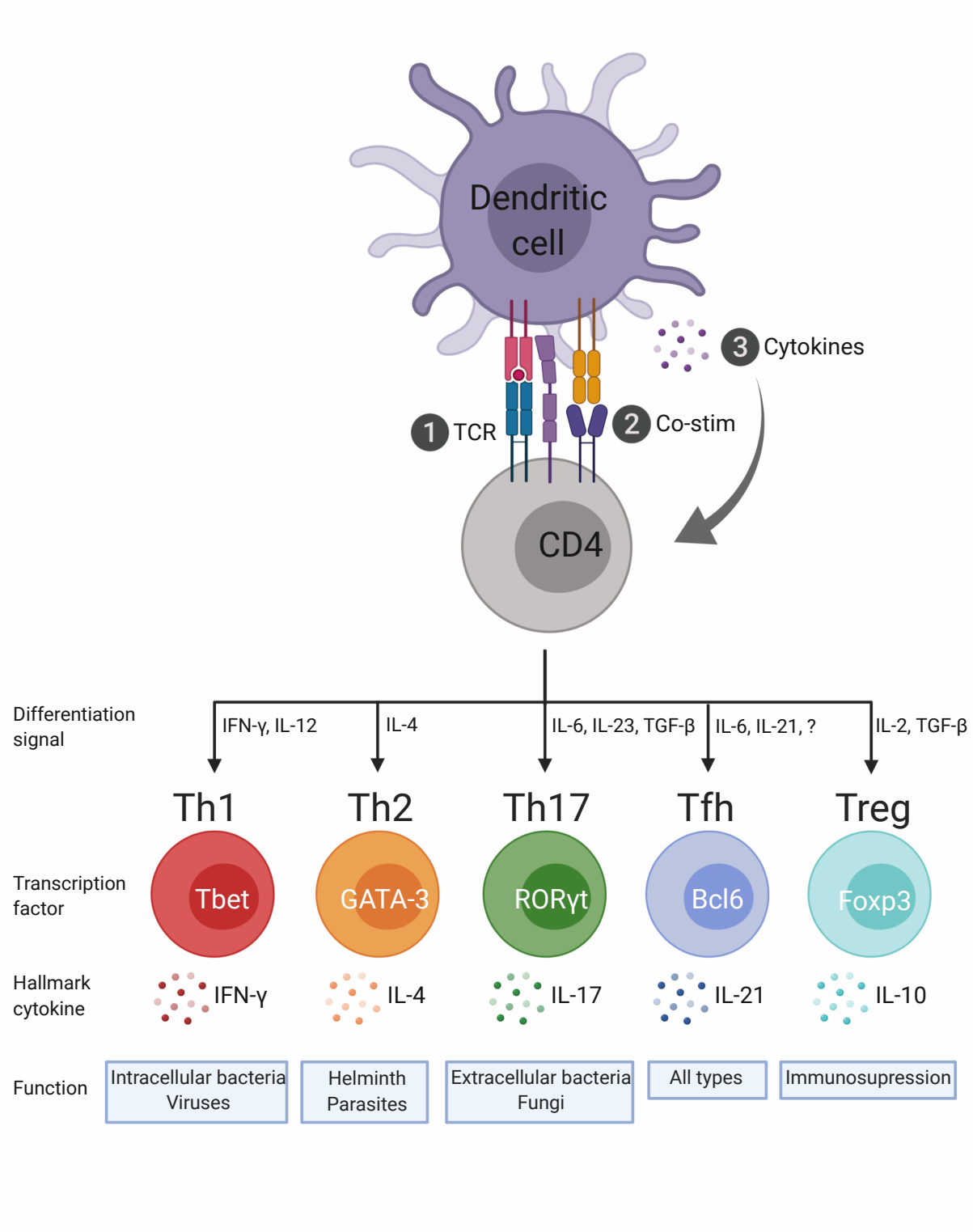

Figure 1: CD4 T cell heterogeneity. Upon receiving the 3 signals needed for full activation, naïve CD4 T cells can extensively proliferate and simultaneously differentiate into distinct effector subsets. Each effector subset needs different cytokine stimulation, expresses a different master transcription factor, secretes its hallmark cytokine, and is useful in different infection settings.

T cell receptor signal

The TCR signal is the most specific signal received by the T cell and the TCR defines its antigen-specificity. Each αβ T cell bears a unique heterodimeric TCR which was generated through the rearrangement of the DNA segments V, D and J for the β-chain and V and J for the α-chain during thymic development (*23*). CD4 T cells use their TCR to survey for antigen in the form of short peptides bound to major histocompatibility complex class II molecules (pMHC). pMHC is displayed on the surface of antigen presenting cells (APC) including dendritic cells (DC), B cells and macrophages (*12*). The TCR can interact with foreign and self-peptides presented by MHCII at a broad range of intensities (*24-26*). In fact, weak interactions with self-antigens are required for positive selection during T cell development in the thymus, and peripheral T cells also rely on interactions with endogenous pMHC to receive survival signals (*27-31*). Interactions with self pMHC are typically only 10-fold weaker than with non-self pMHC, but this small yet crucial difference can be accurately sensed by the highly evolved TCR signaling apparatus (*32, 33*).

Upon binding of antigen through the TCR α/β chains, TCR signal transduction is mediated by the T cell co-receptor protein complex CD3 consisting of a CD3 γ-chain, a δ-chain, two ε-chains and two ζ-chains. Each chain contains at least one immunoreceptor tyrosine-based activation motif (ITAM) that gets phosphorylated by the CD4-bound tyrosine kinase Lck through the activation of the phosphatase CD45 (*34-36*). Subsequently, phosphorylated ITAMs recruit ZAP70 kinases via the Src homology 2 (SH2) binding domain to the TCR thereby triggering several intracellular signal transduction pathways (*37*). ZAP70 phosphorylates linker for activation of T cells (LAT) which leads to the recruitment of more adaptor proteins, an increase in intracellular calcium and subsequently to the activation of calcineurin, protein kinase C (PKC) and the mitogen-activated protein (MAP) kinases (*38*). This ultimately leads to the activation of three important transcription factors: nuclear factor of activated T cells (NFAT), nuclear factor-κB (NF-κB), and activator protein 1 (AP-1), which in cooperation with co-stimulation and cytokine receptor signals lead to the full activation and

differentiation of T cells. Stronger TCR signal induces a stronger response and increased activity of the 3 transcription factors (*39-41*). Factors that influence TCR signal strength are the potency of the TCR/pMHC interaction (off rate), the duration of T cell-APC contacts (dwell time) and density of pMHC (affected by antigen dose and affinity of peptide for MHC) (*42-44*).

Although co-stimulation and cytokines can also impact CD4 T cell differentiation, TCR signal strength seems to play a major role in early CD4 T cell fate determination (*39, 41, 45-55*). This was shown in an elegant study by Tubo, et. al. where the early bifurcation of Th1 and Tfh cells in monoclonal vs polyclonal settings was assessed (*54*). While TCR-transgenic monoclonal CD4 T cells underwent a reproducible differentiation pattern following *Listeria monocytogenes* infection, the polyclonal endogenous compartment showed a more variable/heterogenous differentiation. In both settings, the environmental factors were similar, highlighting that the microenvironment by itself is not sufficient to dictate CD4 T cell differentiation bias towards Th1 or Tfh cells. Despite being more physiologically relevant, the impact of TCR signal strength on polyclonal populations is not well understood due to technical limitations. The detection of antigen-specific polyclonal CD4 T cells relies on the use of tetramers, a reagent consisting of 4 recombinant pMHC molecules conjugated to a fluorophore. While tetramers are an invaluable tool for the field, only T cells bearing a high affinity TCR to the tetramer are able to bind them, leaving low affinity CD4 T cells undetectable (*56*). However, it was shown that low affinity T cells can make up a big part of the antigen-specific CD4 pool when using Nur77 expression as a readout for TCR engagement in the tetramer negative fraction (*56*). Therefore, to enable the study of T cells expressing a low affinity TCR, the field has mainly relied on the adoptive transfer of cells from naïve TCR transgenic mice. While earlier studies suggested that high affinity T cell preferentially give rise to Tfh cells, growing evidence supports the idea that weak TCR signal can also generate Tfh cells (*39, 41, 47, 48, 50, 51*). Notably, these contradictory results might be a result of the infection or immunization model used. A recent study performed in humans further highlighted the importance of the TCR in CD4 T cell fate determination. By performing TCR sequencing in combination with peptide recognition, the authors were able to show that Tfh cells in tonsils

and blood are clonally convergent but show minimal clonal overlap with non-Tfh CD4 T cells (*57*).

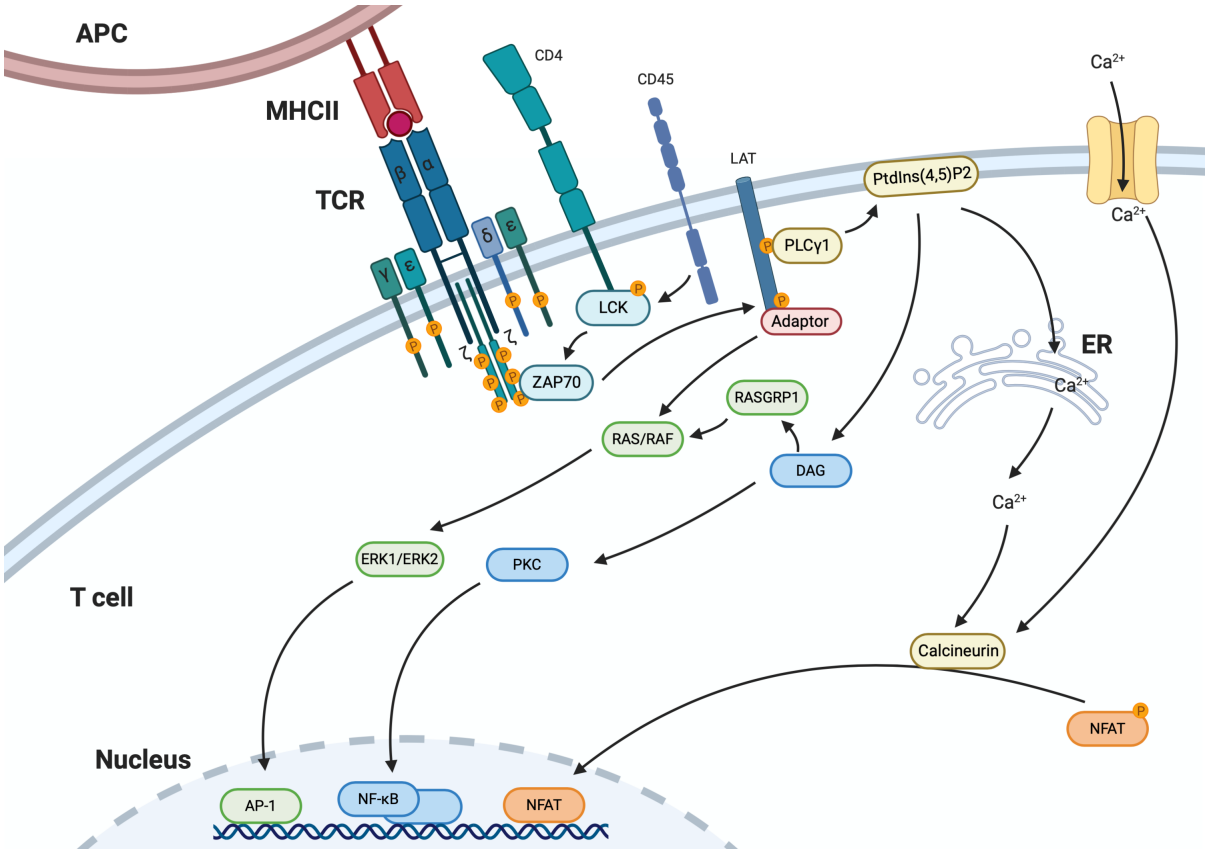

Figure 2: TCR signaling: Binding of the antigen by TCR α/β chains induces phosphorylation of Lck by CD45. This in turn leads to phosphorylation of the ITAM motifs of the CD3 complex and leads to the recruitment of ZAP70. Subsequently ZAP70 phosphorylates LAT and thereby triggers 3 intracellular pathways: The MAP kinase pathway leading to AP-1 activation, PKC pathway with NF-κB activation and calcineurin pathway with NFAT translocation into the nucleus. *Adapted from Gaud et al.* (*36*).

Co-stimulatory signals

While TCR engagement is crucial for activation, it became apparent in the field that TCR signaling alone is not sufficient for complete activation of T cells, as cytotoxic T lymphocytes (CTL) are incapable of inducing an immune response to alloantigens (*58, 59*). In fact, it was later found that stimulation of the TCR alone results in T cell anergy, a state that renders T cells unresponsive (*60*). This led to the corroboration of an old hypothesis that a second signal is necessary to overcome anergy induction (*61*). Soon thereafter, the surface protein CD28 was identified as the molecule delivering the co-stimulatory signal required for full T cell activation after engagement of the ligand B7-1 (also known as CD80) expressed on

B cells (*62-64*). Later, an additional ligand for CD28 termed B7-2 (also known as CD86) was identified (*65-67*). CD28 is constitutively expressed on T cells, and signaling leads to the activation of AP-1 and NF-κB (*68-71*). Mechanistically, binding of CD28 ligands by the extracellular CD28 domain leads to the recruitment of intracellular binding proteins with SH 2 and 3 domains to one of the intracellular YMNM motif of CD28, e.g. phosphatidylinositol 3-kinase (PI3K) (*72-74*). PI3 kinases are heterodimeric kinases and in lymphocytes PI3Kδ is the most abundantly expressed isoform which is composed of a p85 regulatory subunit and a p110δ catalytic subunit (*75*). The p85 regulatory subunit contains an SH2 domain that binds to the YMNM motif, thereby allowing localization of p110δ to the plasma membrane. Activation of p110δ leads to the phosphorylation of phosphatidylinositol to phosphatidylinositol (3,4)-biphosphate (PIP_2) and phosphatidylinositol (3,4,5)-triphosphate (PIP_3), and these lipids in turn activate downstream pathways by the recruitment of proteins with a PH binding domain (*76*). One of these downstream pathways involves the activation of phosphoinositide-dependent protein kinase 1 (PDK1) and the protein kinase B (AKT/PKB) that successively regulate multiple pathways involved in metabolism and survival like glycolysis, mammalian target of rapamycin (mTOR), glycogen synthase kinase 3 (GSK3), or activation of forkhead box O (FOXO) transcription factors among others but also the production of the cytokine IL-2 (*71, 77-81*).

Coinhibitory receptors also exist to balance the activating capacity of costimulatory receptors. CTLA4, also belonging the CD28 family, binds to the same ligands as CD28 (*82, 83*). However, it binds the ligands with a greater avidity and provides an inhibitory rather than a stimulatory signal (*83*). It does so by inhibiting TCR- and CD28-mediated signal transduction, inhibition of IL-2 synthesis and cell cycle arrest (*84*). In contrast to CD28, CTLA4 is not constitutively expressed but is rapidly upregulated upon T cell activation (*85*).

Inducible T cell costimulator (ICOS) is, as the name implies, another receptor for co-stimulatory signal that is expressed upon activation through TCR/CD28 stimulation (*86, 87*). It's ligand, ICOSL, is constitutively expressed on all professional APCs (*86, 88, 89*). ICOS, like CD28, induces PI3K activity but with an enhanced production of PIP_3 resulting in a stronger

Akt phosphorylation than CD28 which is due to a mutation in the intracellular motif (YMFM for ICOS) (*90, 91*). ICOS and ICOS ligand deficient mice show a profound impairment of class-switched antibodies concomitant with reduced number and size of GCs (*92*) . However, the disruption of the ICOS-PI3K pathway in T cells does not fully mirror the ICOS knockout phenotype suggesting that ICOS activates other pathways in addition to PI3K (*93, 94*). Indeed, an additional intracellular signaling motif named IProx was found in the intracellular domain of ICOS which is absent CD28 (*95*). IProx recruits TBK1 which was shown to play a crucial role in the transition of a Tfh cell to a GC-resident Tfh cell, although the exact role of TBK1 remains elusive (*95*).

Cytokines

Cytokines provide signal 3 to naïve CD4 T cells to fine-tune the adaptive immune response by inducing different types of immune responses that eliminate specific types of pathogens. The type of the immune response elicited might be influenced by the type of innate lymphoid cells (ILCs) activated early in the response (*96*). Type 1 responses induce the activation of ILC1s, which produce IFN-γ, and the secretion of IL-12 by dendritic cells and macrophages. These cytokines generate an environment that promotes the differentiation of naïve CD4 T-cells to Th1 cells to fight intracellular bacterial infections or viruses (*97, 98*). Following stimulation of IL-12 and IFN-γ, signaling transducer and activator of transcription (STAT) family protein members 4 respectively 1 are activated and Tbet, the lineage-defining transcription factor of Th1, is induced (*97-99*). Tbet, like other master transcription factors, induces lineage-specific genes while simultaneously repressing genes promoting alternate lineages, thereby stabilizing the Th1 cell fate (*100, 101*). Helminth and parasite infections lead to ILC2 activation and consequently to the secretion of IL-4 facilitating the generation of Th2 cells (*102*). IL-4 induces the activation of STAT6 and the expression of the Th2 master transcription factor GATA-3 (*103-107*). Type 3 responses are directed against fungi or extracellular bacteria and are characterized by the induction of Th17 cells and the activity of STAT3 through IL-6/IL-23 to induce ROR-γt expression (*108, 109*). Interestingly, Tfh cells

which are induced in all types of immune responses, share the dependency of STAT3 signaling with Th17 cells, yet require stimulation of Il-21 through IL-21 receptor and rely on the lineage defining transcription factor Bcl6 (*110-116*). Lastly, Treg cells rely on the IL-2-STAT5 axis and TGF-β signaling to express Foxp3 and mediate their immunosuppressive functions (*117-120*).

1.3. CD4 T cell response to viral infections

The CD4 T cell response to viral infections can be divided into 3 phases: expansion, contraction, and memory. Activation of naïve CD4 T cells leads to clonal burst and differentiation into the effector subsets Th1 and Tfh that help the immune system clear the virus. Once the late effector stage is reached (end of expansion phase) and the infection is cleared, Th1 and Tfh cells undergo clonal contraction leaving behind a small population of long-lived memory cells that exhibit improved functions upon reactivation (*121*). In contrast, chronic infections with persisting antigen lead to a state of T cell dysfunction termed exhaustion, which may serve to limit immunopathology.

Th1 and Tfh cells stimulate the two different arms of the adaptive immune system, namely the cell-mediated and the humoral arm respectively. The two subsets provide help via distinct mechanisms and also differ strongly in their differentiation programs and migration patterns. How and when the bifurcation of Th1 and Tfh cell differentiation occurs is still not fully resolved. Previous reports showed that some CD4 T cells early after infection co-express both Bcl6 and Tbet at high levels, which is somewhat counterintuitive due to their opposite effects on gene transcription (*122-124*). One possibility is that Bcl6/Tbet co-expressing cells may become Th1 cells after Bcl6 downregulation (*124*). On the other hand, a recent study using Tbet fate reporter mice found that a subset of Tfh cells in germinal centers previously expressed Tbet and to a certain degree retains Th1 helper capacity (*125*). Therefore, Th1 and Tfh cells early during the expansion phase most likely undergo a

transitional stage during differentiation with shared characteristics before committing to one lineage.

T helper 1 cells

Following immunization, CD4 T cells induce a potent CD8 response that helps to control infections. The ability of CD4 to help CD8 T cells is mainly attributed Th1 cells in a viral infection model. As already described above, naïve CD4 T cells differentiate into Th1 cells upon interaction with dendritic cells in the presence of IL-12 and IFN-γ leading to the up-regulation of STAT 1 and 4 and concomitant expression of Tbet, the master transcriptional regulator of Th1 cells (*97-99*). Tbet further induces IFN-γ production which leads to the expression of IL-12 receptor allowing specific expansion of Th1 cells (*98*) while repressing alternate cell fates like Th2/Th17 through gene expression inhibition (*126-128*). Besides Tbet, the Runt-related transcription factors Runx1 and Runx3 play an important role in the Th1 differentiation process. Both Runx transcription factors can repress GATA3 activity, either through repression of gene transcription or through direct protein interaction (*129, 130*).

Once the Th1-fate is stabilized, Th1 effectors help shape the CD8 response in several ways, stimulating CD8s either directly or indirectly (*131*). As an example of indirect stimulation of CD8 responses, Th1 cells can “license” dendritic cells to increase antigen-presentation and expression of co-stimulatory ligands, therefore potentiating DCs to stimulate CD8 T cells (*132, 133*). Furthermore, DC licensing induces the secretion of the chemokines CCL3 and CCL4 which attracts naïve CD8 T, providing an explanation for how a rare CD8 population can efficiently be activated (*134*). Th1 cells license DCs via CD40-stimulation through CD40L expression (*135-137*). However, CD40:CD40L interactions can also occur between Th1 cells and CD8 T cells directly although this seems to be more important for the generation of a long-lived memory compartment than for potentiating primary responses (*138*). The secretion of cytokines by Th1 cells is an example of direct stimulation of the cytotoxic T cell response. CD4 T cells have been shown to be a major source of IL-2, allowing expansion and enhanced

survival of CD8 T, but also increasing secondary responsiveness of CD8s (*139-143*). However, it is noteworthy that IL-2 concentrations can be modulated by the immunosuppressive CD4 Treg compartment. High consumption of IL-2 by Tregs can decrease the availability of IL-2 and thereby suppress CD8 T cell expansion, but it also improves the responsiveness of memory T cells to secondary infections through the inhibition of terminal differentiation (*144-147*). Th1 cells act not only on CD8 T cells but also activate and potentiate the cytotoxicity of macrophages. They achieve this by providing CD40L as well as stimulation through IFN-γ secretion, the two essential signals needed for macrophage activation (*148-151*). Subsequently, macrophages take on antimicrobial effector cell function via ROS-production and induce TNF-α secretion in macrophages (*149, 150*).

Another important feature of Th1 cells is their migration pattern. Licensing of DCs in SLOs is important, but effector functions directly at the site of inflammation in the infected organs are crucial for the full potential of Th1 cells (*152*). Migration of Th1 cells from SLOs to infected peripheral organs is mediated in two ways. First, T cells lose the expression of CCR7 and CD62L, which retain T-cells in the T cell zone of SLOs (*153-155*). Furthermore, upregulation of sphingosine 1-phosophate receptor (S1PR), P-selectin glycoprotein ligand-1 (PSGL-1), and CXCR3 allows SLO egress, migration along blood vessels and tissue entry at the site of inflammation through endothelial cells (*153-155*). In summary, the distinct migration properties of Th1 cells allows this subset to not only act in SLOs but also to coordinate cell-mediated killing in inflamed tissue, highlighting their systemic effect in orchestrating the cytotoxic response.

T follicular helper cells

In the year 2000, a new helper subset was identified that localizes in the B cell follicle where it promotes B cell responses, and was therefore termed T follicular helper cell (Tfh) (*156, 157*). At the time, it was unclear whether this newly identified subpopulation truly represented a distinct CD4 T cell lineage. This view changed with the identification of Bcl6 as

the master transcription factor for Tfh cells (*114-116*) and the discovery of distinct signals required for the differentiation of Tfh cells (*110*). Tfh differentiation from a naïve CD4 T cell is described as a multistage process involving interactions with both DCs and B cells, although this has recently been challenged by a study using a malaria infection model that implies that B cells alone are sufficient to prime Tfh cells (*158-160*). The classical Tfh differentiation process as currently understood is initiated by initial DC priming of naïve CD4 T cells resulting in early Tfh fate commitment (*160-162*). Expression of the chemokine receptor CXCR5 and Bcl6 through IL-6 stimulation allows migration of Tfh precursor cells from the T cell zone to the T-B border of B cell follicles (*114, 160, 163, 164*). Mechanistically, IL-6 stimulation induces Bcl6 expression which in turn represses CC chemokine receptor 7 (CCR7) and P-selectin glycoprotein 1 (PSGL-1) expression while simultaneously stabilizing CXCR5 expression (*165-168*). Further antigenic and ICOS stimulation via B cells is essential for the maintenance of Tfh cell fate and their ultimate localization in the germinal centers (GC) (*158, 162*).

Tfh cells play a crucial role in shaping the B cell response. Starting with the first interaction at the T-B border, Tfh cells instruct B cells to either differentiate into short-lived plasma cells (also referred to as extrafollicular plasma cells or GC-independent plasma cells), GC-independent memory B cells or GC B cells (*169-172*). These B cell subsets have distinct functions: extrafollicular plasma cells provide the first round of antibodies to limit the spread of the infection, GC-independent memory B cells might represent a stem-like reservoir for secondary GC reactions, and the GC B cells undergo class-switch and affinity maturation, ultimately generating a highly efficient and long-lasting humoral response (*158, 173*). Germinal centers are composed of two distinct zones in which GC B cells can circulate: the light zone (LZ) and the dark zone (DZ). GC B cells in the dark zone undergo a process called somatic hypermutation, in which activation-induced cytidine deaminase (AID) induces mutations in the B cell receptor (BCR) to alter the affinity of the BCR to the antigen that is present in the GC (*174*). Furthermore, the mutated B cells undergo clonal expansion before they migrate from the DZ to the LZ (*175*). In the LZ, GC B cells pick up antigen from FDCs and present it to Tfh cells via peptide:MHC complexes. The more antigen that is presented to the Tfh cell, the more

survival signals the GC B cell will get before returning to the DZ for the next round of affinity maturation. The number of additional cell divisions and mutations GC B cells undergo was found to directly correlate with the help provided by Tfh cells (*176*). Alternatively, GC B cells can exit the GC to differentiate into memory B cells or plasma cells, and this fate decision seems to be dependent on their affinity, although the mechanism of how the cell fate is decided is incompletely understood (*169, 177-185*). Germinal center B cells that do not receive the required stimulus from Tfh cells because of the expression of low-affinity BCRs are negatively selected and undergo apoptosis (*173, 186*). The Tfh cells thus select for high affinity B cells while restricting low-affinity B cells (*175, 187*). Additionally, Tfh cells were shown to regulate the size of GCs (*93, 115, 188*). Tfh were also found to be present in the DZ, however, their functional role remains to be elucidated (*189*).

How do Tfh cells provide help to GC B cells? The signals consist of both cytokines (IL-21, IL-4) and direct cell-to-cell interaction (CD40L, signaling lymphocytic activation molecule (SLAM)). However, the amount of Tfh help is not determined solely by TCR engagement but also by distinct costimulatory and coinhibitory signals through the interaction with the GC B cell (*158*). The importance of the proper regulation of help delivered by Tfh cells is highlighted by the finding that excessive Tfh help impairs clonal selection and affinity maturation leading to lower affinity antibodies over time (*175*). One of these regulators is SLAM expressed on LZ GC B cells (*190*). SLAM engagement on Tfh cells was shown to be required for cytokine production, as SLAM-associated protein (SAP) deficient Tfh cells are defective in both IL-4 and IL-21 production (*191*). SAP transduces the signal received through SLAM and has shown to be important for T cell B cell adhesion (*192*). SAP was also shown to play an important role in the establishment of long-term humoral immunity but not in early antibody responses (*193*). ICOS triggering was identified as another important factor for cytokine production by Tfh cells, since blocking ICOS-signaling abrogated IL-21 production (*194*). Both IL-4 and IL-21 are important for the survival of B cells, induction of B cell proliferation, induction of class switch recombination (CSR), and plasma cell differentiation(*182, 195, 196*). These functions can also be attributed to CD40L, which is probably the best characterized B cell helper signal (*197-*

200). Additionally, CD40L plays a role in stabilizing T:B interactions. Most interactions between Tfh cells and GC B cells have been shown to be rather short (*201, 202*). However, these interactions might be elongated through CD40L expression on Tfh cells as it can transiently enhance SLAM expression and thereby provide a feedforward loop to enhance T:B entanglement (*183*). In contrast, programmed cell death 1 (PD1) signaling received by PD1-ligand expressed on B cells dampens the TCR signal in Tfh cells and thereby limits help (*203*). This is important as Tfh cells are constantly exposed to TCR stimulation due to the continuous presence of antigen and therefore must remain sensitive to TCR signaling to distinguish small differences in number of pMHC molecules expressed on GC B cells and subsequently deliver the appropriate amount of help.

Because of the crucial role Tfh cells play in the generation of efficient antibody responses, Tfh cells are important in control of pathogens. However, it is noteworthy that Tfh hyperactivation can lead to misdirected B cell differentiation or antibody maturation which can also have negative consequences for the host. Tfh cells have been implicated in a number of autoimmune disease and allergies (*177*).

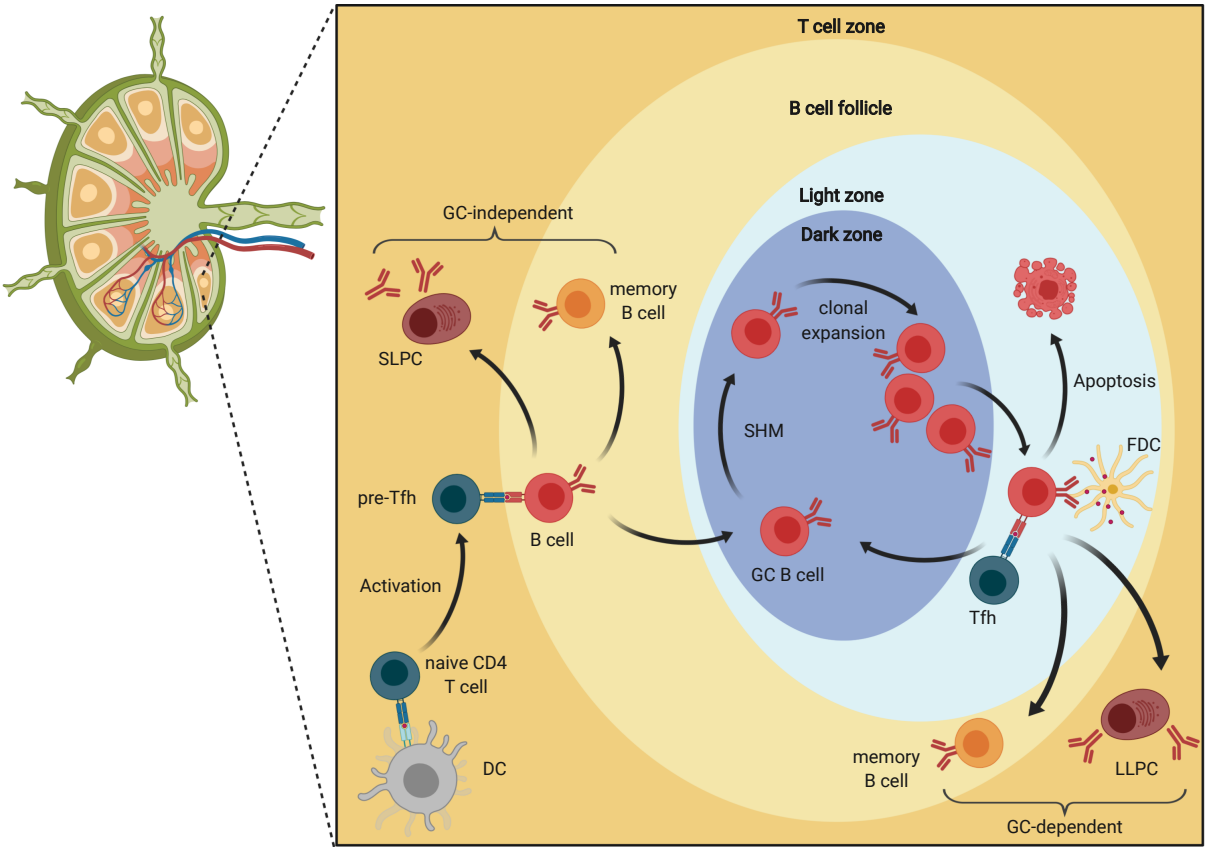

Figure 3: Germinal center response. Naïve CD4 T cells get activated by DCs in the T cell zone and pre-Tfh cells subsequently migrate to the T:B border. Pre-Tfh cells interact with activated B cells that recognized cognate antigen. Upon proliferation, B cells either become extrafollicular SLPCs, GC-independent memory B cells or migrate to the GC with Tfh cells and become GC B cells. In the DZ of the GC, GC B cells undergo SHM and clonal expansion before migrating to the LZ. In the LZ, upon antigen capture from FDC and cognate interaction with Tfh cells. After the affinity selection process in the LZ, GC B cells are either fated to die, become memory B cells or LLPCs, or undergo an additional round of affinity maturation. DZ: dark zone, FDC: follicular dendritic cell, GC: germinal center, LLPC: long lived plasma cell, LZ: light zone, SHM: somatic hypermutation, SLPC: short lived plasma cell. *Adapted from Mesin et al. (204).*

T cell memory

Once pathogens are cleared from the host, effector CD4 T cells undergo clonal contraction, leaving most of the expanded cells fated to die (*205*). However, a few pathogen specific CD4 T cells survive and are long-lived, and are termed CD4 memory T cells. When and how memory CD4 T cells are generated needs to be further investigated. First, whether memory T cells arise from effectors late in the immune response, or whether memory precursor cells bifurcate early after activation from effector T cells is still under debate (*160, 206-212*). Furthermore, several hypotheses exist on how early bifurcation of effector and

memory T cells would be achieved mechanistically. For example, memory cells could arise from asymmetric cell division (ACD), however since ACD is a rare event, it can likely not explain early bifurcation to full extent, but might contribute to it (*213*).

Memory T cells are classically defined to have the following characteristics: upon a subsequent infection of the same pathogen, these cells can be re-activated and reacquire effector functions quickly, proliferate earlier than primary activated T cells, and display higher extent of effector function which can be attributed to the increased precursor frequencies compared to their naïve counterparts (*121*). However, most studies have focused on the CD8 memory compartment, whereas the CD4 memory cells remain understudied. CD4 memory cells have classically been subdivided into T effector memory cells (Tem) and T central memory cells (Tcm) based on their expression of migratory markers CCR7 and CD62L (*214*). While Tem were shown to maintain limited expansion potential but acquire imminent effector function and are able to survey tissues (Th1 characteristics), Tcm cells are able to secrete IL-2 and can proliferate extensively before acquiring effector functions and mainly circulate in lymph (*214*). More recently, a third memory population has been described that takes up permanent residency in organs and was subsequently called tissue resident memory T cell (Trm). Trm act as a first line of defense upon reinfection in tissues (*215*). In addition to these subsets, it was shown that memory CD4 cells can promote secondary B cell responses, suggesting that Tfh cells persist for a prolonged time even though previous studies failed to identify bona fide Tfh memory cells (*163, 216-219*) . The discrepancy might be explained with the fact that effector Tfh cells gradually lose their hallmark surface proteins including CXCR5 and PD1 (*163, 208, 216, 220, 221*). Furthermore, Tfh cells have a substantial overlap with Tcm in regards to surface markers (CXCR5, ICOS) and transcription factors (TCF1, STAT3 and ID3) making it difficult to clearly discriminate the two subsets (*216, 222-226*). The shared characteristics likely explains the different results obtained with respect to plasticity (the ability to adapt a new lineage, e.g. Tfh becoming a Th1 cell) of the distinct CD4 memory subsets upon re-activation. Recently, Thpok was identified as an important transcription factor for functional fitness of Tcm cells and a distinct memory precursor population expressing Thpok

was identified early after infection (*207*). The gene signature of Thpok expressing cells included the lymphoid homing marker Ccr7 and the survival factor Bcl2 among others. However, this gene signature was absent in Tfh effector cells, indicating an early bifurcation of Tcm precursor and Tfh memory cells. This idea is further supported by the fact that the TCR repertoire of Tfh cells in humans is distinct from non-Tfh cells (*57*). Whether these long-lived Tfh cells represent a bona fide memory population capable of self-renewal or whether they represent remnants from the effector response requires further investigation.

T cell exhaustion

In cases where the pathogen doesn't get cleared from the host but persists and establishes a chronic infection, T cells can acquire yet another state called T cell exhaustion. This dysfunctional state is characterized by a) limited proliferation potential, b) limited cytokine secretion and c) expression of co-inhibitory receptors like PD-1, Lag3, Tim3, CTLA4 and others (*227, 228*). Although most studies on T cell exhaustion have focused on the CD8 compartment, CD4 cells acquire similar characteristics in chronic infections (*229-232*). From an evolutionary point of view, T cell exhaustion most likely represents a safety program of the body to circumvent extensive immunopathology caused by excessive inflammation. For example, in an experimental setup that allows for the reactivation of a high number of inflammatory Th1 cells before the exhaustion program is acquired triggers lethal immunopathology (*233*).

However, heterogeneous populations of exhausted T cells exist, and the developmental relationship of these distinct subsets have been identified (*234*). Terminally exhausted T cells exhibit an irreversible transcriptional and epigenetic state that cannot be reprogrammed to re-acquire effector functions (*235*). In contrast, chronic infections also lead to the emergence of a stem-like CD8 population expressing intermediate levels of PD-1, CXCR5, and other proteins associated with a Tfh phenotype (*236, 237*). Despite their dormant state, stem-like CD8 T cells can be re-invigorated by PD-1 blockade leading to proliferation

and increased effector functions representing a major advancement in the treatment of cancer and other chronic diseases (*237-240*). However, re-activated stem-like CD8 T cells retain their exhaustion phenotype on an epigenetic level upon PD-1 blockade therapy, and whether these cells can also be reprogrammed at the chromatin level remains unknown (*241*). How the T cell exhaustion program is induced remained an open question until TOX was identified as a master regulator (*242-246*). Interestingly, TOX expressing cells can be identified early after infection suggesting an early divergency of exhausted T cells from effector or memory T cells. Whether TOX plays a role in CD4 T cell exhaustion and whether the CD4 exhaustion compartment is as heterogenous as the CD8 counterpart has not been investigated yet.

1.4. Viral infections

Broadly speaking, viral infections can be classified into two major types: acutely resolved and persistent viruses. Persistent infections can be further classified into active versus latent persistent infections. The hallmark feature of latent chronic infections are the alternating states of active viral replication and quiescent non-replicating phases. Several factors like viral replicative capacity, tropism, immune evasion strategies and others determine whether the outcome of an infection is acute or persistent (*247*).
Continuous productive replication is used by viruses like human immunodeficiency virus (HIV) and hepatitis B and C virus (HBV/HCV) in humans. In mice, lymphocytic choriomeningitis virus (LCMV) belongs in the former virus category, although different strains with different infection outcomes exist (*248*). The LCMV model has been widely used to study cell-mediated and humoral responses in acute and chronic settings, and several key concepts have been identified using LCMV (*248*). LCMV was also the infection model used in both projects described in this thesis.

Lymphocytic Choriomeningitis virus

LCMV belongs to the family of Arenaviruses and is a naturally occurring infection in mice. The virus is a non-cytopathic bi-segmented ambisense single-stranded RNA virus (*249*). The two segments of the viral genome each encode for two proteins. The L segment encodes for the RNA polymerase (L protein) and the matrix protein (Z protein) (*249*). The small S segment encodes for the nucleoprotein (NP) and the glycoprotein (GP) precursor which is cleaved into the extracellular subunit GP1 and the transmembrane subunit GP2 which then form the homotrimeric glycoprotein (*250*). The GP then facilitates infection of cells mainly through the interaction with the widely expressed glycoprotein α-dystroglycan (α-DG) (*251*). After binding, the virus particles are then taken up in smooth-walled vesicles and fused with acidified endosomes (*252*). The viral RNA then reaches the cytoplasm where the NP and L proteins induce viral replication followed by assembly and budding of virions mediated by the Z protein (*253-255*).

LCMV was shown to infect macrophages, dendritic cells, fibroblasts, fibroblastic reticular cells, endothelial cells, and hepatocytes (*256-260*). However, several distinct LCMV strains exist and they exhibit differences in viral tropism and replicative capacity that can result in either acute or chronic infections (*261*). For example, LCMV Armstrong induces an acute infection, whereas Clone-13 leads to a persistent infection. Interestingly, the acute Armstrong strain and the chronic Clone-13 strain only differ in two amino acids with a functional impact (*262*). The first mutation in the glycoprotein increases affinity towards α-DG leading to an improved infectivity of dendritic cells (*263*). The second mutation in the polymerase increases the viral replicative capacity and was reported to be the primary determinant for viral persistence (*262*). Having two viral strains that are highly similar to each other yet generate different outcomes represents one of the major advantages of LCMV because it allows the comparison of acute and chronic viral infections side by side. Furthermore, due to the simple organization of the genome, LCMV rescue systems exist that allow the study of various mutations in the virus and its functional consequences for the host, making LCMV an ideal infection model to study immune responses (*264*).

2. AIM OF THE PROJECTS

2.1. Project #1: Long-lived Tfh cells

The existence of bona fide Tfh memory cells is controversial and is complicated by the down-regulation of hallmark Tfh proteins like CXCR5 and PD1 and the vast overlap of additional markers associated with both Tfh and Tcm subsets: ICOS, Bcl6, STAT3, TCF1, Id3 etc. (*208, 216, 223-226*). Therefore, the aim of this project was to investigate whether Tfh cells are long-lived, how they can be discriminated from Tcm cells and to further characterize this compartment. Specifically, we wanted to address survival requirements of Tfh memory cells, investigate their potential to trans-differentiate into other subsets like Th1, and to assess their function.

2.2. Project #2: GP61 variants

Upon viral infection, naïve CD4 T cells receive signals through the TCR, co-stimulatory receptors and cytokines to differentiate into inflammatory Th1 cells and Tfh cells that support the generation of an efficient humoral response. How a naïve CD4 T cell decides to either become a Th1 or a Tfh cell is incompletely understood. However, several reports indicate that the TCR plays a crucial role (*39, 41, 47, 48, 50, 51, 54, 55*). Furthermore, how persistent antigen impacts CD4 differentiation hasn't been addressed yet. Here we aimed to generate a new tool that allows us to investigate the impact of TCR signal strength on CD4 differentiation in acute versus chronic viral infections.

3. RESULTS

3.1. Project #1: Long-lived T follicular helper cells retain plasticity and help sustain humoral immunity

T CELLS

Long-lived T follicular helper cells retain plasticity and help sustain humoral immunity

Marco Künzli[1]*, David Schreiner[1]*, Tamara C. Pereboom[1], Nivedya Swarnalekha[1], Ludivine C. Litzler[1], Jonas Lötscher[2], Yusuf I. Ertuna[3], Julien Roux[2,4], Florian Geier[2,4], Roman P. Jakob[5], Timm Maier[5], Christoph Hess[2,6], Justin J. Taylor[7], Carolyn G. King[1†]

CD4$^+$ memory T cells play an important role in protective immunity and are a key target in vaccine development. Many studies have focused on T central memory (T_{cm}) cells, whereas the existence and functional significance of long-lived T follicular helper (T_{fh}) cells are controversial. Here, we show that T_{fh} cells are highly susceptible to NAD-induced cell death (NICD) during isolation from tissues, leading to their underrepresentation in prior studies. NICD blockade reveals the persistence of abundant T_{fh} cells with high expression of hallmark T_{fh} markers to at least 400 days after infection, by which time T_{cm} cells are no longer found. Using single-cell RNA-seq, we demonstrate that long-lived T_{fh} cells are transcriptionally distinct from T_{cm} cells, maintain stemness and self-renewal gene expression, and, in contrast to T_{cm} cells, are multipotent after recall. At the protein level, we show that folate receptor 4 (FR4) robustly discriminates long-lived T_{fh} cells from T_{cm} cells. Unexpectedly, long-lived T_{fh} cells concurrently express a distinct glycolytic signature similar to trained immune cells, including elevated expression of mTOR-, HIF-1–, and cAMP-regulated genes. Late disruption of glycolysis/ICOS signaling leads to T_{fh} cell depletion concomitant with decreased splenic plasma cells and circulating antibody titers, demonstrating both unique homeostatic regulation of T_{fh} and their sustained function during the memory phase of the immune response. These results highlight the metabolic heterogeneity underlying distinct long-lived T cell subsets and establish T_{fh} cells as an attractive target for the induction of durable adaptive immunity.

INTRODUCTION

Vaccination and infection lead to the generation of protective immune responses mediated by memory T and B cells (*1*). Two major subsets of memory T cells have been described on the basis of differential expression of lymphoid homing receptors: CCR7$^+$ central memory (T_{cm}) cells and CCR7$^-$ effector memory (T_{em}) cells (*2*). After challenge infection, T_{cm} cells produce interleukin-2 (IL-2) and maintain the capacity to proliferate and generate secondary effector cells. In contrast, T_{em} cells can immediately produce inflammatory cytokines but have more limited expansion. In addition to these subsets, CD4$^+$ T follicular helper (T_{fh}) memory cells can promote secondary B cell expansion and class switching (*3*–*7*). The number of circulating T_{fh} cells correlates with the number of blood plasmablasts after vaccination in humans and can be boosted to improve long-lived antibody production (*8*–*10*). These data suggest targeted generation of long-lived T_{fh} cells as a rational approach for improving vaccine design. However, despite the importance of T_{fh} cells for supporting antibody responses, the signals promoting maintenance and survival of these cells are not well understood. In addition, it is unclear whether T_{fh} cells retain the capacity to differentiate into diverse secondary effectors (*3*, *5*, *6*, *11*). Analysis of long-lived T_{fh} cells is complicated by a gradual loss of phenotypic markers typically associated with T_{fh} effector cells, including programmed cell death protein 1 (PD1) and CXCR5, as well as the apparent decline of the CD4$^+$ memory compartment compared with CD8$^+$ memory cells over time (*3*, *6*, *12*–*14*). Moreover, the relationship between T_{cm} cells and T_{fh} effector cells, which share several surface markers and transcription factors including CXCR5, inducible T-cell costimulator (ICOS), T cell factor 1 (TCF1), signal transducers and activators of transcription 3 (STAT3), and DNA-binding protein inhibitor ID-3 (ID3), is not well established (*3*, *15*–*19*). Recently, a T_{cm} precursor signature, including markers for lymphoid homing (*Ccr7*) and survival (*Bcl2*), was identified among antigen-specific effector cells responding to viral infection (*20*). This signature, however, was not detected in T_{fh} effector cells, suggesting an early divergence between precursors of T_{cm} and long-lived T_{fh}. Nevertheless, it remains unclear whether T_{fh} cells found at later phases are remnants of a primary effector response or whether they represent a distinct population of self-renewing T_{cm} cells that share differentiation requirements and phenotypic characteristics with T_{fh} cells.

Although informative, T cell receptor (TCR) transgenic models used to unravel these questions demonstrate intrinsically biased differentiation tendencies and may not reveal the full palette of CD4$^+$ heterogeneity (*21*). In addition, many such studies require transferring high numbers of donor cells, which could affect T cell differentiation (*3*, *22*). Using tetramers to study the polyclonal T cell response, we determined that T_{fh} cells are particularly susceptible to nicotinamide adenine dinucleotide (NAD)–induced cell death (NICD) during isolation. By blocking NICD, we observed that T_{fh} cells persist in high numbers to at least 400 days after infection, whereas T_{cm} cells decline. Transcriptional and epigenetic profiling revealed that long-lived T_{fh} cells constitutively engage glycolytic metabolism while remaining stem-like. Consistent with these findings, transfer experiments revealed that long-lived T_{fh} cells, but not T_{cm} cells, can generate the full spectrum of secondary effectors. Although long-lived T_{fh} cells

[1]Immune Cell Biology Laboratory, Department of Biomedicine, University of Basel, University Hospital Basel, CH-4031 Basel, Switzerland. [2]Department of Biomedicine, University of Basel, University Hospital Basel, CH-4031 Basel, Switzerland. [3]Department of Biomedicine, University of Basel, CH-4031 Basel, Switzerland. [4]Swiss Institute of Bioinformatics, Basel, Switzerland. [5]Biozentrum, University of Basel, Basel, Switzerland. [6]Department of Medicine, CITIID, University of Cambridge, Cambridge, UK. [7]Vaccine and Infectious Disease Division, Fred Hutchinson Cancer Research Center, Seattle, WA, USA.
*These authors contributed equally as first authors.
†Corresponding author. Email: carolyn.king@unibas.ch

can survive in the absence of antigen, they depend on sustained ICOS signals to preserve glycolytic and Tcf7-dependent gene expression. A reduction in T_{fh} cell numbers induced by late ICOS blockade led to a reduction in circulating antibody titers and splenic plasma cells, highlighting an underestimated contribution of long-lived T_{fh} cells to late phase humoral immune responses.

RESULTS

T_{fh} cells are susceptible to death during isolation

T_{fh} cells were recently described to express high levels of the purinergic receptor P2X7 receptor (*23*, *24*). P2X7R is an adenosine 5′-triphosphate–gated cation channel that can be adenosine 5′-diphosphate ribosylated by the cell surface enzyme ARTC2.2, rendering certain cell types, including regulatory T cells and resident memory T (T_{rm}) cells, susceptible to NICD during isolation from the tissue (*25*, *26*). Injection of an ARTC2.2-blocking nanobody (NICD protector) before organ harvest protects these subsets from NICD and improves their recovery from lymphoid organs (*27*, *28*). To determine whether inhibition of ARTC2.2 could also improve the recovery of T_{fh} cells at effector and memory time points, we harvested antigen-specific T cells from NICD protector–treated mice after infection with lymphocytic choriomeningitis virus (LCMV). Polyclonal LCMV-specific $CD4^+$ T cells were enriched using tetramer staining for IA^b:nucleoprotein $(NP)_{309–328}$ (NP specific) or IA^b:glycoprotein $(GP)_{66–77}$ (GP66 specific) and analyzed for expression of T_{fh}-associated surface markers; a variety of gating strategies was used to place the results in the context of previous studies assessing LCMV-induced T_{fh} cells (*3*, *12*). In untreated mice, T_{fh} effector cells were clearly identified at day 15 after infection but were largely absent by day 43 (Fig. 1A and fig. S1A). In contrast, treatment with NICD protector resulted in a significant recovery of T_{fh} cells at all time points and with both T cell specificities, indicating a larger expansion and more prolonged survival of T_{fh} cells than previously appreciated (Fig. 1, A to C). As the number of GP66-specific T_{fh} cells was about fourfold higher than NP-specific T_{fh} cells, we focused subsequent analyses on the GP66-specific T cell compartment (fig. S1B). Two-dimensional visualization of the cytometry data by *t*-distributed stochastic neighbor embedding (*t*SNE) confirmed that NICD protector preferentially rescued cells with high expression of P2X7R (Fig. 1B). NICD protector also significantly improved the recovery of P-selectin glycoprotein ligand-1 $(PSGL1)^{hi}Ly6C^{lo}$ memory cells but had minimal impact on more terminally differentiated $PSGL1^{hi}Ly6C^{hi}$ (hereafter T_H1) memory cells, in line with the levels of P2X7R expression on these subsets (Fig. 1, C and D, and fig. S1C). In addition, NICD protector improved the recovery of $Ly6c^{lo}$ and $CXCR5^+$ cells after infection with *Listeria monocytogenes*, again correlating with P2X7R expression (fig. S1, D to G). After day >400, T_{fh} cells identified by all gating strategies persisted in LCMV-infected mice, whereas $Ly6C^{lo}PSGL1^{hi}$ memory cells, a heterogeneous population previously shown to contain a substantial proportion of T_{cm}, were nearly absent (Fig. 1, A and C, and fig. S1C) (*12*). These data suggest either a survival defect or conversion of $Ly6C^{lo}PSGL1^{hi}$ memory into one of the remaining memory cell subsets. T_{fh} cells isolated at late time points after infection were further phenotyped by flow cytometry and characterized by high expression of folate receptor 4 (FR4), CD73, CXCR4, ICOS, and Bcl6 compared with T_H1 and $Ly6C^{lo}PSGL1^{hi}$ memory cells (Fig. 1D). Although a similar phenotype was observed on polyclonal NP-specific T_{fh} cells isolated from LCMV-infected mice (fig. S1A), experiments using monoclonal T cells from NICD-protected SMARTA or NIP TCR transgenic strains generated substantially fewer long-lived T_{fh} cells (fig. S1H). These observations agree with previous reports showing a gradual decline of T_{fh}-associated markers on transferred monoclonal populations and highlight the value of studying polyclonal responses, particularly given the tendency of different types of TCR transgenic T cells to undergo distinct and more limited patterns of differentiation (*3*, *12*, *21*).

FR4 discriminates long-lived T_{fh} from transcriptionally distinct T_{cm}

To further investigate $CD4^+$ T cell heterogeneity and regulation at memory time points, we performed single-cell RNA sequencing (scRNA-seq) on GP66-specific T cells isolated at day >35 after infection. To assess the effect of NICD protector using a transcriptional readout, we sequenced cells from NICD protector–treated and untreated mice and found that treatment leads to an increase in proportions of T_{fh}-like clusters (fig. S2A). To ensure consistency with other experiments, we performed further scRNA-seq analyses using the run with NICD protector. Principal components analysis (PCA) was used for dimension reduction, hierarchical clustering of the cells, and *t*SNE visualization (Fig. 2A and fig. S2B). Seven distinct clusters were enriched for genes associated with the following: T_{fh} cells (clusters 1 to 3, 37% of cells), T_{cm} cells (clusters 4 and 5, 45% of cells), and T_H1 cells (clusters 6 and 7, 18% of cells) (Fig. 2, A and B, and fig. S2B). The top defining genes in the T_{fh} clusters included established T_{fh} markers such as *Izumo1r*, *Pdcd1*, and *Sh2d1a*, as well as transcription factors expressed by $CD4^+$ memory cells, including *Klf6*, *Jun*, and *Junb* (Fig. 2, B and C) (*23*, *29*). T_{cm} and T_H1 clusters (4 to 7) exhibited higher expression of *Il7r*, *S100a4*, *S100a6*, *Selplg*, and various integrins (Fig. 2, B and D), whereas clusters 6 and 7 were enriched for genes associated with T_H1 differentiation including *Cxcr6*, *Ccl5*, *Nkg7*, and *Id2* (Fig. 2, B and E). Among T_H1 clusters, cluster 7 represented the subset highest in *Selplg*, *Ly6c2*, and *Il7r*, whereas cluster 6 expressed higher levels of *Cxcr6* and *Id2* along with signatures of dysfunction and exhaustion (fig. S2, C to E) (*20*, *30*). Cluster cell type identities were confirmed by scoring each cell for signature genes obtained from publicly available datasets and examining the scores across clusters (Fig. 2F and fig. S2F). T_{fh} and T_H1 signatures matched well with clusters 1 to 3 and 6 to 7, respectively, whereas clusters 4, 5, and 7 were enriched for the T_{cm} precursor signature reported by Ciucci *et al.* (*20*) (Fig. 2F).

Within T_{fh} clusters 1 to 3, we observed stable expression of *Izumo1r*, which encodes FR4. Although the function of this receptor on T cells is not well understood, it has been shown to be expressed on T_{fh} effector and memory cells, as well as on anergic and regulatory $CD4^+$ T cells (*23*, *31*, *32*). Compared with *Cxcr5* and *Pdcd1*, *Izumo1r* served as a much cleaner transcriptional marker of the boundary between T_{fh} and non-T_{fh} cells (Fig. 2, G and H). Unlike *Izumo1r*, *Cxcr5* expression was also detected in non-T_{fh} clusters, although with a slight decrease from T_{cm} to T_H1 (Fig. 2H). These findings were confirmed at the protein level, where $CXCR5^{hi}$ gating includes both $FR4^{hi}$ and $FR4^{lo}$ cells, whereas $FR4^{hi}$ gating largely excludes $CXCR5^{lo}$ cells (Fig. 2K). Unexpectedly, *Ccr7* expression, highest in clusters 4 and 5, was negatively correlated with *Cxcr5* in cells from animals treated with NICD protector (in the bottom 4% of all genes), whereas cells from untreated animals showed a slight positive correlation (in the top 27% of all genes) (Fig. 2G). This trend was mainly driven by

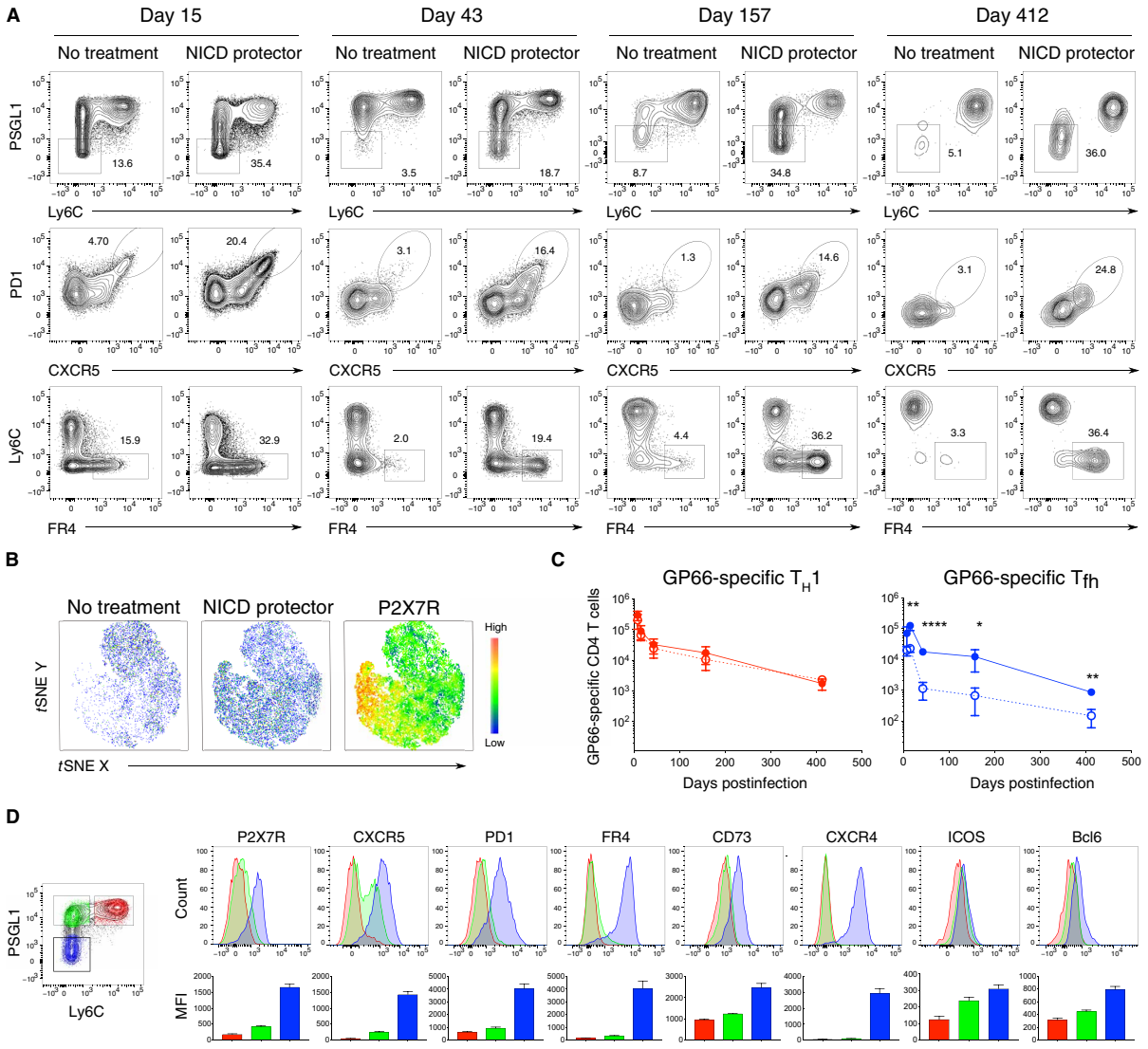

Fig. 1. T_{fh} cells are susceptible to death during isolation. (**A**) Flow cytometry analysis of GP66-specific $CD4^+$ T cells isolated from the spleen at indicated time points after infection, with or without NICD protector using different gating strategies to identify long-lived T_{fh} cells ($Ly6C^{lo}PSGL1^{lo}$, $CXCR5^{hi}PD1^{hi}$, or $FR4^{hi}Ly6C^{lo}$). (**B**) *t*SNE plots of the GP66-specific $CD4^+$ memory compartment with (middle and right) or without NICD protector (left) and overlaid P2X7R expression with red indicating the highest expression level (right). (**C**) Quantification of GP66-specific T_H1 memory (red, $Ly6C^{hi}PSGL1^{hi}$) or long-lived T_{fh} cell (blue, $Ly6C^{lo}PSGL1^{lo}$) numbers over time with (solid lines) or without (dashed lines) NICD protector gated as in Fig. 1D. Thin lines represent the means ± SD. (**D**) Representative flow cytometry plots and geometric mean fluorescence intensity (hereafter MFI) of the indicated marker in GP66-specific $CD4^+$ memory cell subsets T_H1 (red), $Ly6C^{lo}PSGL1^{hi}$ (green), and T_{fh} (blue) >40 days after infection. Data represent $N = 2$ independent experiments for (D) with $n = 3$ to 5 mice per group. Unpaired two-tailed Student's *t* test was performed on each individual time point (C). $^*P < 0.05$, $^{**}P < 0.01$, $^{****}P < 0.0001$.

the bona fide T_{fh} clusters (1 to 3) preferentially rescued from NICD, as illustrated by imputed expression levels of *Cxcr5* versus *Ccr7* (Fig. 2I). A similar negative correlation was found between protein expression levels for CCR7 and CXCR5, with the highest CCR7-expressing cells falling within the $Ly6C^{lo}PSGL1^{hi}$ (hereafter T_{cm}) compartment (Fig. 2J and fig. S2G). Long-lived GP66-specific T_{fh} cells found in lymph nodes also expressed lower levels of CCR7 compared with T_{cm}, consistent with the idea that T_{fh} cells generated in lymphoid organs are a noncirculating population similar to resident memory cells (fig. S2H) (*33*). T_{fh} cells have a higher expression of CD69 and enrichment for residency-associated genes (fig. S2, I and J) (*34*–*36*). Together, the use of FR4 as a marker for long-term T_{fh} identity

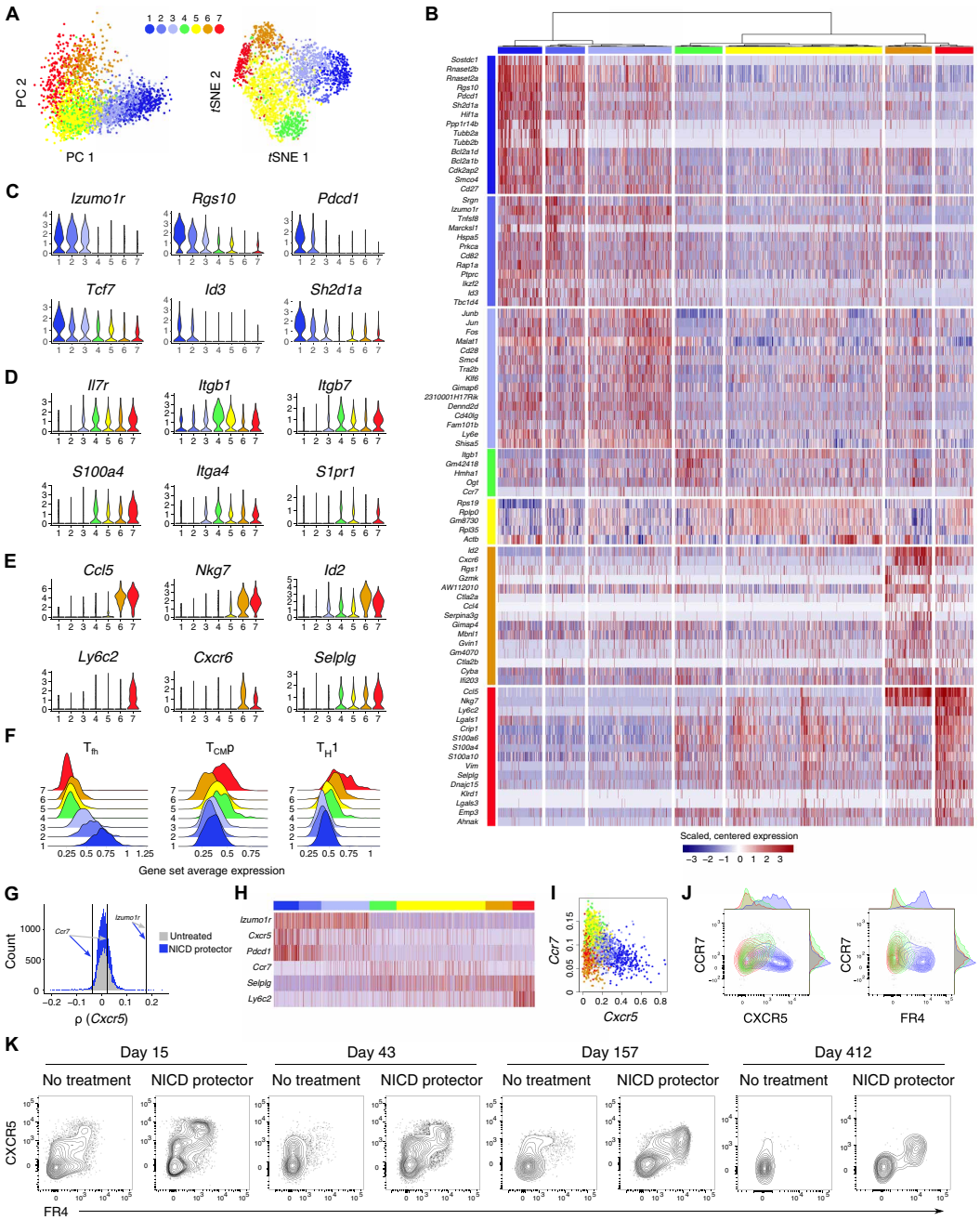

Fig. 2. FR4 discriminates long-lived T_{fh} from transcriptionally distinct T_{cm}. (**A**) Unsupervised hierarchical clustering using Ward's method: PCA and *t*SNE dimension reductions. (**B**) Heatmap showing scaled, centered single-cell expression of top 15 genes sorted according to cluster average log fold change (FC) , adjusted *P* value of <0.05. (**C** to **E**) Log-normalized expression of genes typical for T_{fh} (C), T_{cm} (D), and T_H1 (E) populations. (**F**) Log-normalized average expression of published $CD4^+$ signatures obtained by analysis of d7 effectors: T_{fh}, T_{cm} precursors, and T_H1. (**G**) scRNA-seq: Rank of *Ccr7* and *Izumo1r* (encoding FR4) among Spearman's rank correlation coefficients between *Cxcr5* and all other genes, NICD protector versus untreated. (**H**) Scaled, centered single-cell expression of *Izumo1r* in comparison with other common gating markers. (**I**) scRNA-seq: Cxcr5 versus Ccr7 on imputed data, colored by cluster. Dropout imputed using Seurat::AddImputedScore. (**J** and **K**) Flow cytometry analysis of CCR7, CXCR5, and FR4 on GP66-specific $CD4^+$ memory subsets >50 days after infection gated as in Fig. 1D (J) or at the indicated time points after infection, with or without NICD protector (K). Data represent $N = 2$ independent experiments with $n = 4$ mice (J).

improves upon previous gating strategies, which either allocate too many T_{cm} cells into a T_{fh} gate or depend upon markers like PD1, which is known to decline over time. We additionally noted that *Hif1a*, a transcription factor normally associated with glycolysis, was one of the top genes expressed by T_{fh} cells, consistent with the recently reported enrichment of this transcription factor in T_{fh} effectors and resident memory cells (Fig. 2B) (*37*–*39*). Together, these data highlight clear transcriptional distinctions between T_{cm} cells and the ultimately more persistent NICD-rescued T_{fh} cells.

Long-lived T_{fh} cells are constitutively glycolytic

In addition to *Hif1a* expression, long-lived T_{fh} cells were enriched for mammalian target of rapamycin (mTOR)– and cyclic adenosine 3′,5′-monophosphate (cAMP)–regulated genes, suggesting a metabolic signature similar to that observed in trained immune cells (Fig. 3A and fig. S3, A to C) (*40*–*44*). Enhanced activation of mTOR-regulated genes was also observed in secondary analysis of microarray data on bulk sorted SMARTA T_{fh} memory cells (where PD1 protein expression was negative) and in recently published single-cell data from GP66-specific T_{fh} memory cells (fig. S3, D and E) and was further confirmed by quantitative polymerase chain reaction (qPCR) of mTOR-regulated genes in sorted $CD4^+$ GP66-specific memory T cell populations (Fig. 3B) (*3*, *20*, *43*). These data indicate that long-lived T_{fh} cells may constitutively engage a glycolytic metabolism. To assess mTORC1 activity, we measured phosphorylation of TORC1 target ribosomal protein S6 (p-S6) directly after T cell isolation (Fig. 3C and fig. S3F). Both GP66-specific T_{fh} cells and $CD44^+$ T_{fh} cells, which are phenotypically similar to antigen-specific T_{fh} cells (fig. S3G), exhibited increased p-S6 compared with T_H1 memory cells (Fig. 3C and fig. S3F). To exclude modulation of p-S6 due to tetramer-induced activation, we conducted experiments on ice with dasatinib, a tyrosine kinase inhibitor shown to temporarily block TCR-mediated signal transduction (*45*). Consistent with mTOR activation, long-lived T_{fh} cells had increased uptake of the fluorescent glucose analog 2-(*N*-(7-nitrobenz-2-oxa-1,3-diazol-4-yl)amino)-2-deoxyglucose) (2-NBDG) and an increased baseline extracellular acidification rate (ECAR) compared with T_H1 memory cells (Fig. 3, D and E). However, alongside this apparent increase in glycolytic metabolism, long-lived T_{fh} cells had slightly decreased expression of the amino acid transporter CD98 and the transcription factor c-myc (classically viewed as activation markers) compared with T_H1 memory cells, indicating that not all measures of anabolic activity are increased (Fig. 3, F and G).

To determine whether the shift toward glycolysis by long-lived T_{fh} cells was accompanied by a reduction in oxidative metabolism, we also assessed their baseline oxygen consumption rate (OCR). Although we observed a slight reduction in basal respiration by long-lived T_{fh} cells compared with T_H1 memory cells, the maximum respiration and spare respiratory capacity were similar between these two populations (Fig. 3H). Transcriptionally, long-lived T_{fh} cells were also enriched for genes associated with oxidative phosphorylation and mitochondrial respiration, a signature associated with $CD8^+$ memory T cell survival (fig. S3H). Because T_{fh} effectors were previously reported to have decreased mTOR activation and reduced glycolysis (*46*), we also assessed the metabolic capacity of cells isolated at day 10 after infection, reasoning that NICD protector might improve their survival and fitness. At this time point, T_{fh} effectors had slightly reduced basal ECAR compared with T_H1 effectors but demonstrated normal glycolytic flux after the addition of carbonyl cyanide *p*-trifluoromethoxyphenylhydrazone (Fig. 3I). Similar to long-lived T_{fh} cells, T_{fh} effectors had equivalent baseline and maximal respiratory capacity to T_H1 effectors, indicating that in contrast to an earlier report, T_{fh} cells isolated at earlier time points are also metabolically fit (Fig. 3J) (*12*). To test whether these discrepancies can be explained by the effect of NICD protector, we compared cell viability and 2-NBDG uptake with or without NICD protector from T cells isolated at days 10 (effector) and 110 (memory) after infection. NICD protector predominantly improved the viability of the T_{fh} subset as measured by annexin V staining (fig. S3, I and J). In addition, annexin V–negative T_{fh} cells from unprotected mice failed to take up 2-NBDG, demonstrating a fundamental metabolic difference from NICD-protected T_{fh} cells (fig. S3K). These results indicate that both T_{fh} effector and memory cells have greater metabolic capacity than previously appreciated.

To assess whether glycolysis/mTOR signaling are required to maintain long-lived T_{fh} cells, we examined T_{fh} cell survival in mice treated with the glycolysis inhibitor 2-deoxyglucose (2-DG) and rapamycin starting at day >40 after LCMV infection. After 2 weeks of 2-DG/rapamycin treatment, both the proportion and number of long-lived T_{fh} cells were significantly decreased, with the remaining T_{fh} cells showing reduced size consistent with less mTOR activation (Fig. 3, K and L, and fig. S3L) (*46*). Signaling through P2X7R was recently suggested to restrain mTOR activation, leading to improved survival of $CD8^+$ memory T cells (*47*). In contrast, P2X7R signals have been shown to restrain accumulation of T_{fh} effectors in Peyer's patches (*24*). To assess whether P2X7R signals promote or restrain long-lived T_{fh} cell survival, we generated radiation bone marrow chimeras with a mixture of wild-type and P2X7R-deficient bone marrow. Sixty days after LCMV infection, P2X7R-deficient T cells generated an increased proportion of all memory cells, with the most significant increase in the T_{fh} compartment (Fig. 3, M and N). These data demonstrate that P2X7R is a key negative regulator of long-lived T_{fh} cell accumulation and are consistent with a role for P2X7R in restraining mTOR activation.

Antigen is not required for the survival of long-lived T_{fh} cells

Glycolytic metabolism in T cells is often associated with activation and effector cell proliferation. To understand whether long-lived T_{fh} cells are responding to ongoing antigen stimulation, we examined Nur77 expression in LCMV-infected Nur77 reporter mice. About 30% of $PSGL1^{lo}Ly6C^{lo}$ T_{fh} cells were Nur77 positive, with a slightly higher percentage in the $CXCR5^{hi}PD1^{hi}$ T_{fh} compartment (Fig. 4A). Whereas PD1 expression was moderately increased on $Nur77^+$ compared with $Nur77^-$ T_{fh} cells, it was much higher in both of these populations than in non-T_{fh} cells (Fig. 4B). Although these data indicate that a fraction of the long-lived T_{fh} compartment continues to respond to antigen, we did not observe a positive correlation between PD1 expression and 2-NBDG uptake. Glucose uptake within the T_{fh} compartment is thus unlikely to be related to antigen stimulation (fig. S4A). Furthermore, increased 2-NBDG uptake was maintained by long-lived T_{fh} cells at >400 days of infection, by which time PD1 expression by T_{fh} cells has decreased (fig. S4B). To understand whether the glycolytic metabolism observed in long-lived T_{fh} cells is related to proliferation, we administered bromo-2′-deoxyuridine (BrdU) in the drinking water of LCMV-infected mice beginning 40 days after infection. After 12 to 14 days, about 4 to 9% of T_{fh} cells incorporated BrdU, with a slightly higher proportion of $CXCR5^{hi}PD1^{hi}$ T_{fh} cells staining positive (Fig. 4C). FR4-negative

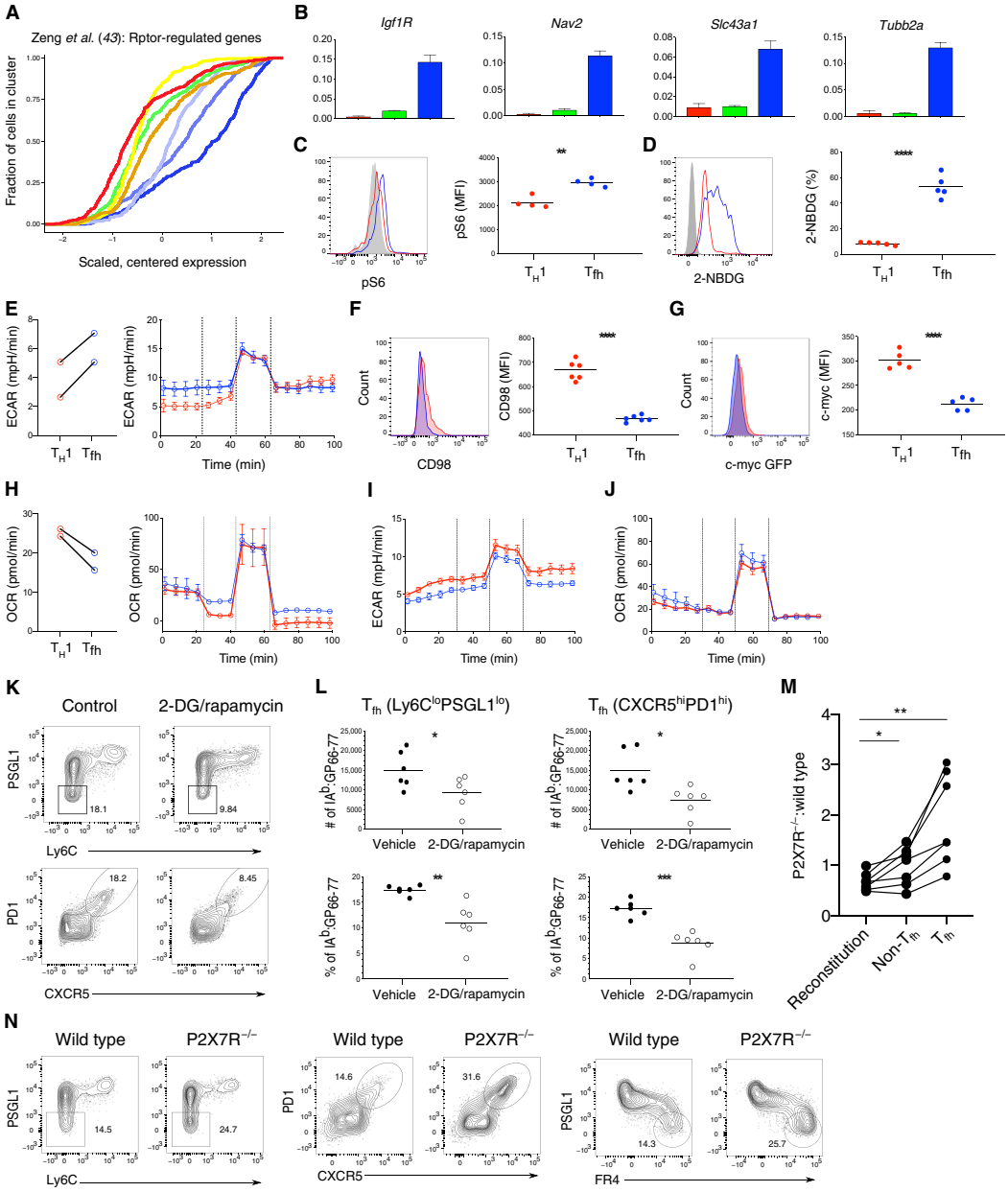

Fig. 3. Long-lived T_{fh} cells are constitutively glycolytic. (**A**) Cumulative distribution of scaled, centered mRNA expression of Rptor-regulated genes by cluster (*43*). (**B**) qPCR of genes (arbitrary units relative to Rpl13a) in sort-purified GP66-specific T_H1 memory (red), T_{cm} (green), and long-lived T_{fh} (blue) cells gated as in Fig. 1D. (**C** and **D**) Representative histograms and quantification of phospho-S6 Ser240/244 on long-lived CD44$^+$ T_H1 or T_{fh} cells compared with naïve CD4$^+$ T cells (gray) (C) and 2-NBDG uptake (D) on GP66-specific cells >30 days after infection compared with unstained control (gray). (**E**) Basal ECAR and ECAR profile in response to Mito Stress test in T_H1 memory and long-lived T_{fh} cells pooled from 20 to 30 mice. (**F** and **G**) Histogram and MFI of CD98 (F) or c-myc GFP (G) in GP66-specific memory T_H1 and long-lived T_{fh}. (**H**) Basal respiration and OCR profile in response to Mito Stress test on sorted CD44$^+$ T_H1 memory and long-lived T_{fh}. (**I** and **J**) ECAR profile (I) and OCR profile (J) in response to Mito Stress test in T_H1 and T_{fh} effector cells (day 10 after infection) pooled from $n = 12$ to 14 mice. Representative flow cytometry plots (**K**) and quantification (**L**) of GP66-specific cells treated with vehicle or 2-DG/rapamycin. (**M** and **N**) P2X7R$^{-/-}$ to wild-type ratio of GP66-specific T_{fh} cells >60 days after infection (M) and analysis (**N**) using different gating strategies. Data are representative of $N = 2$ independent experiments depicting the means ± SD of $n = 3$ technical replicates (B) or 4 to 7 mice per group [(C) to (G) and (K) to (N)]. Dots represent cells from individual mice, and the line represents the mean. Unpaired (C, D, F, G, and L) or paired (M) two-tailed Student's *t* test was performed with *$P < 0.05$, **$P < 0.01$, ***$P < 0.001$, ****$P < 0.0001$.

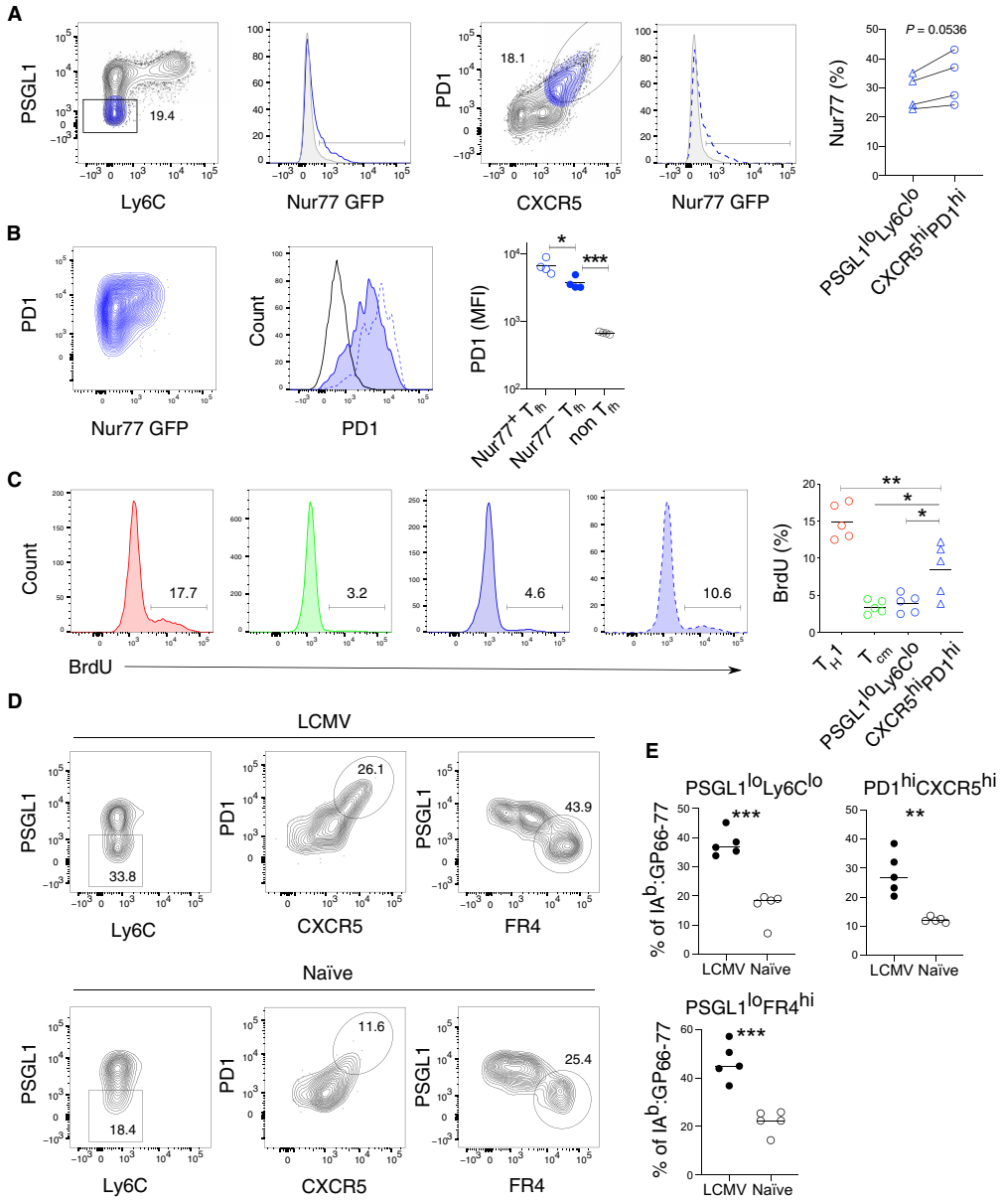

Fig. 4. Antigen is not required for the survival of long-lived T_{fh} cells. (**A**) Flow cytometry analysis of Nur77 expression by GP66-specific long-lived T_{fh} cells for the indicated gating strategies. (**B**) Representative flow cytometry plots (left) and MFI (right) depicting PD1 expression on Nur77$^+$ (blue dotted line) and Nur77$^-$ (tinted blue line) T_{fh} cells, gated as depicted in (A). (**C**) Flow cytometry plots (left) and quantification (right) of BrdU incorporation by GP66-specific CD4$^+$ memory subsets after providing BrdU for 12 days in drinking water. (**D** and **E**) Total GP66-specific CD4$^+$ T cells isolated at day 10 after LCMV infection and transferred into congenic infection-matched (LCMV) or naïve mice. Donor cell phenotype analyzed at day 30 after infection. Representative flow cytometry plots (D) and quantification (E) with gating for PSGL1^{lo} Ly6C^{lo} (left), PD1^{hi}CXCR5^{hi} (middle), and PSGL1^{lo}FR4^{hi} (right). Dots represent cells from individual mice, and the line depicts the mean. Data represent $N = 2$ independent experiments with $n = 4$ to 5 mice. Paired (A) or unpaired two-tailed Student's t test (B, C, and E) was performed with $^*P < 0.05$, $^{**}P < 0.01$, $^{***}P < 0.001$.

T_{cm} cells containing a mixture of CXCR5$^+$ and CXCR5$^-$ cells showed a similar level of in vivo cycling with about 3% of cells staining for BrdU, whereas 15% of T_H1 memory cells stained positive, demonstrating more extensive proliferation by this subset (Fig. 4C). The glycolytic phenotype observed in long-lived T_{fh} cells is thus not strongly correlated with extensive cell division, although the slightly increased BrdU incorporation by CXCR5^{hi}PD1^{hi} T_{fh} cells may be related to ongoing antigen stimulation. To better understand the contribution of antigen to maintaining the long-lived T_{fh} compartment, we transferred LCMV-specific effector cells isolated at day 10 after infection into either LCMV infection matched or naïve recipients, followed by analysis of donor T cell phenotype. Thirty days after primary infection, T_H1 memory cells were nearly absent in both transfer scenarios, indicating that T_H1 effector cells survive poorly in this setting (Fig. 4D). In contrast, GP66-specific T_{fh} cells were detected in both antigen-free (naïve) and infection-matched mice. Although fewer T_{fh} cells (with dampened expression of CXCR5 and PD1) were recovered from naïve mice, this may be partially due to ongoing expansion of T_{fh} effector cells in LCMV-infected recipients between days 10 and 15 after transfer (Figs. 1C and 4, D and E). The

long-lived donor T_{fh} cells maintained high expression of FR4 with or without antigen, consistent with scRNA-seq data identifying *Izumo1r*/FR4 as a superior marker for long-lived T_{fh} cells (Figs. 2, C and H, and 4, D and E). Together, these data indicate that although T_{fh} cells with high expression of CXCR5 and PD1 survive optimally in the presence of antigen, they nevertheless persist in its absence and without classical signs of activation or proliferation.

T_{fh} cells generate multiple cell fates upon recall

Despite maintaining a glycolytic phenotype, long-lived T_{fh} cells are enriched for genes regulated by *Tcf7* (encoding TCF1) and highly express *Cd27*, a marker associated with memory T cell survival, cytokine production potential, and stemness (Fig. 5, A and B) (*48*–*50*). Although higher expression of *Tcf7* in long-lived T_{fh} cells matched higher expression of TCF1 protein, CD27 protein expression was substantially lower in T_{fh} compared with T_H1 memory cells (Fig. 5, C and D). To determine whether the discrepancy between the CD27 gene expression and protein expression was due to P2X7R-mediated shedding, we examined CD27 on memory cells isolated from LCMV-infected mixed bone marrow chimeras reconstituted with an equal mixture of P2X7R-deficient and wild-type bone marrow cells (*51*). We observed higher expression of CD27 on P2X7R-deficient long-lived T_{fh} cells compared with both wild-type T_{fh} and T_H1 memory cells (Fig. 5D). Consistent with high expression of both *Tcf7* and *Cd27*, T_{fh} cells were also enriched for "early memory"–associated genes (fig. S5A) (*52*). In addition, construction of a cell developmental trajectory indicated that T_{fh} and T_H1 memory cells occupied opposite ends of a pseudotime trajectory, predicting enhanced differentiation plasticity in one of these subsets (Fig. 5E and fig. S5, B and C) (*53*). To test this in vivo, long-lived T_{fh} ($FR4^{hi}PSGL1^{lo}Ly6C^{lo}$), T_H1 memory ($FR4^{lo}PSGL1^{hi}Ly6C^{hi}$), and T_{cm} ($FR4^{lo}PSGL1^{hi}Ly6C^{lo}$) cells were sorted from LCMV-infected mice and transferred into naïve congenic recipients, followed by secondary challenge with LCMV (Fig. 5F). To prevent tetramer-induced activation, we stained cells for transfer in the presence of dasatinib. Twelve days after recall infection, transferred T_{fh} cells differentiated into both T_{fh} and T_H1 effectors, demonstrating lineage flexibility (Fig. 5, G and H). Consistent with a stem-like character, transferred T_{fh} donor cells also expanded most upon reactivation, generating the largest pool of each secondary effector subset (Fig. 5I). In contrast, T_{cm} cells maintained the capacity to differentiate into both $Ly6C^{hi}$ and $Ly6C^{lo}$ effectors, but generated few T_{fh} effectors, suggesting more limited plasticity (Fig. 5, G to I). Consistent with several reports, T_H1 memory cells almost exclusively gave rise to $Ly6C^{hi}$ effectors, indicating more terminal differentiation of these cells (Fig. 5, G to I) (*3*, *6*). Together, these data demonstrate that despite engaging an anabolic metabolism often associated with effector cell proliferation and differentiation, long-lived T_{fh} cells have a stem-like, early memory signature and maintain the capacity to differentiate into multiple types of effectors after secondary challenge.

Epigenetic regulation of long-lived T_{fh} cells

To assess whether the distinct transcriptional signatures observed in T_{fh} and T_H1 memory cells were also apparent at the epigenetic level, we compared chromatin accessibility of T_H1 memory, long-lived T_{fh}, and naïve T cells by assay for transposase-accessible chromatin using sequencing (ATAC-seq) (*54*). The majority of called peaks were shared among these three populations, with the highest number of unique peaks present in naïve $CD4^+$ T cells (fig. S6A). PCA revealed that T_{fh} and T_H1 memory cells are set apart from naïve T cells along PC1 yet separated from each other along PC2, indicating distinct accessibility profiles (Fig. 6A). Whereas T_H1 memory cells had more differentially open peaks annotated to exons, introns, and distal intergenic regions, long-lived T_{fh} cells had about 50% more differentially accessible peaks in promoter regions (fig. S6B). We thus focused on the significantly differentially accessible promoter regions with a high fold change ($\log_2$ fold change > 1 and false discovery rate < 0.05) between at least two of the T cell subsets and performed hierarchical clustering. This resulted in clusters of genes with common accessibility patterns: e.g., up in naïve, up in memory, and up in naïve and long-lived T_{fh} (Fig. 6B and fig. S6C). For example, the *Foxp1* promoter was exclusively accessible in naïve $CD4^+$ T cells, consistent with its role as a gatekeeper of the naïve to memory T cell transition (*55*). Integrative analysis of ATAC-seq and RNA-seq data (in silico pseudo-bulk samples derived from scRNA-seq data) revealed a correlation between the promoter accessibility and expression of genes defining T_{fh} and T_H1 memory cell subsets (Fig. 6C) (*3*). Consistent with a study that assessed the DNA methylation status of various cytokine loci in T_{fh} and T_H1 memory cells (*3*), we observed that the *Gzmb* promoter was exclusively accessible in T_H1 memory cells, whereas the *Ifny* promoter was accessible in both populations, albeit at slightly lower levels in long-lived T_{fh} cells (Fig. 6D). In contrast to this earlier study, however, the promoter accessibility of the hallmark T_{fh} cytokine, *Il21*, was restricted to long-lived T_{fh} cells (Fig. 6D). In addition, one of the most accessible cytokine promoter regions in long-lived T_{fh} cells was the epidermal growth factor–like ligand amphiregulin (*Areg*), notable for its role in restoring tissue integrity after infection (*56*). To further assess differences in the transcriptional regulation of T_{fh} and T_H1 memory cells, we analyzed enriched binding motifs in called peaks using Hypergeometric Optimization of Motif EnRichment (HOMER) (*57*). In agreement with the scRNA-seq data, long-lived T_{fh} cells were enriched for motifs belonging to the TCF transcription factor family and activating protein 1 (AP1) family members, which are known to be similarly regulated in $CD8^+$ memory cells (Fig. 6E) (*58*, *59*). In contrast, T_H1 memory peaks exhibited increased Runx and T-box transcription family member binding sites, consistent with the cooperation of these transcription factors in regulating interferon-γ and stabilizing T_H1 fate in $CD4^+$ T cells (Fig. 6F) (*60*, *61*). These observations were further validated by applying single-cell regulatory network inference and clustering to the scRNA-seq data, which highlighted TCF/AP1 and Runx family members as regulators in long-lived T_{fh} and T_H1 memory, respectively (fig. S6D). We next assessed functional pathways in the ATAC-seq data by running gene set enrichment analysis (GSEA) on differentially accessible promoter regions in long-lived T_{fh} compared with T_H1 memory cells using both standard gene set categories and sets curated from relevant publications (fig. S6E). Here, we observed increased promoter accessibility in long-lived T_{fh} cells of *Rptor*- and *Tcf7*-regulated genes and genes activated in response to *cAMP*, suggesting that the anabolic and stem signatures of this population are strongly regulated at the epigenetic level (fig. S6E).Last, using Ingenuity Pathway Analysis (Qiagen, version 01-14) to probe the functional regulation of long-lived T_{fh} cells, we identified ICOS-inducible T-cell costimulator ligand (ICOSL) signaling as one of the top pathways enriched in both ATAC-seq and scRNA-seq datasets (fig. S6F) (*62*). These data raise the possibility that ICOS-mediated signals contribute to the maintenance and identity of long-lived T_{fh} via specific epigenetic modifications.

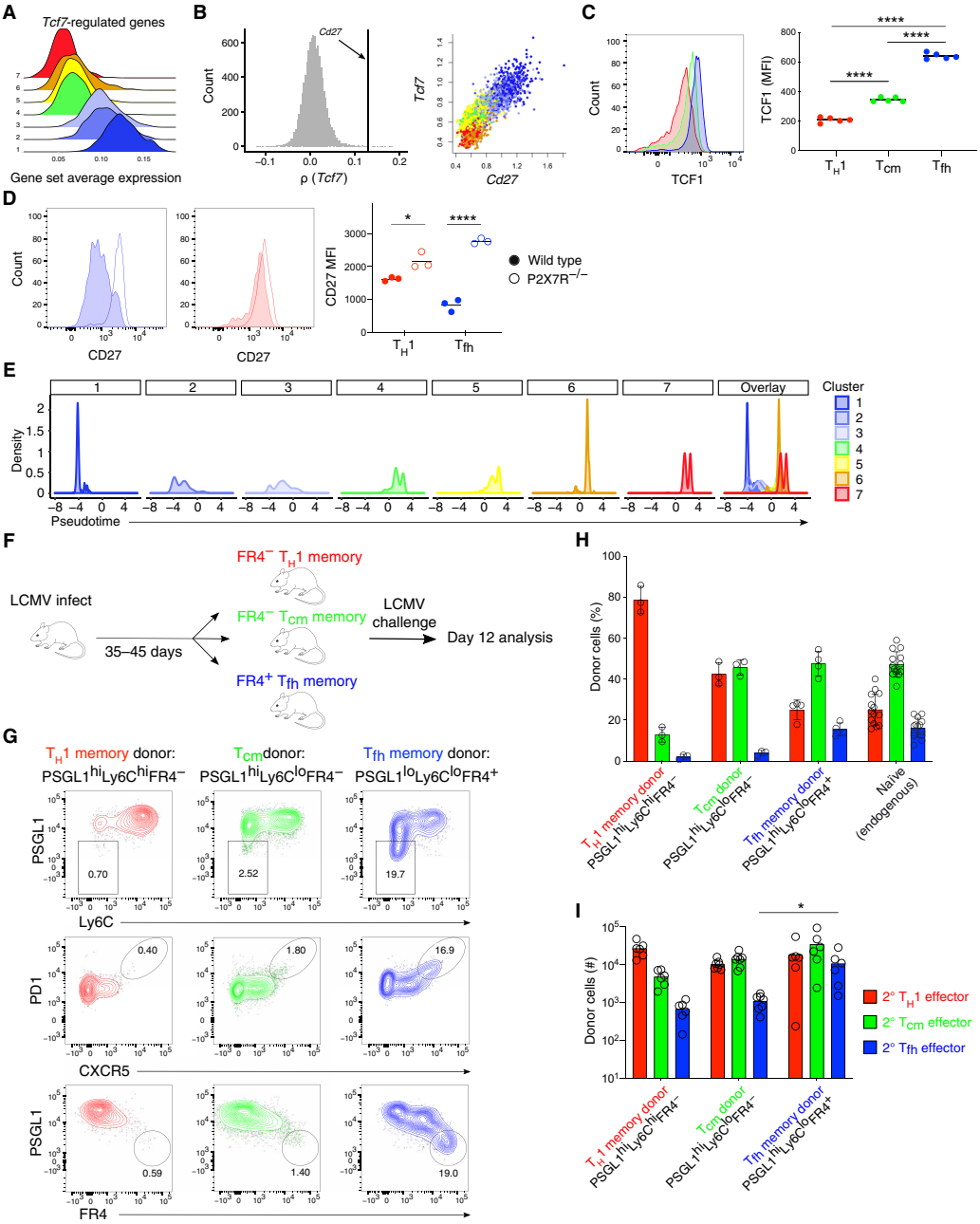

Fig. 5. T_{fh} cells generate multiple cell fates upon recall. (**A**) Log-normalized average expression of genes tracking with *Tcf7* (*90*). (**B**) scRNA-seq: Rank of *Cd27* among Spearman's rank correlation coefficients between *Tcf7* and all other genes (left). *Cd27* versus *Tcf7* on imputed data (right), colored by cluster. (**C** and **D**) Flow cytometry analysis of TCF1 (C) in wild type and CD27 (D) in mixed wild-type and P2X7R$^{-/-}$ bone marrow chimera mice in T_H1 (red), T_{cm} (green), and T_{fh} (blue) GP66-specific memory cells. (**E**) Density of cells in pseudotime using Monocle2 analysis. (**F**) GP66-specific T_H1, T_{cm}, or T_{fh} CD4$^+$ T cells sorted at days 35 to 45 after LCMV infection and transferred into congenic naïve mice. Recipient mice challenged with LCMV the following day. Donor cell phenotype analyzed at day 12 after infection. (**G**) Representative flow cytometry plots of T_H1, T_{cm}, or T_{fh} donor cell phenotype. (**H** and **I**) Quantification of proportions (H) and numbers (I) of T_H1 effectors (red), T_{cm} (green), and T_{fh} effectors (blue) from T_H1, T_{cm}, or T_{fh} donors compared with endogenous response. Data represent $N = 2$ independent experiments with $n = 5$ (C) or 3 to 14 (D to H) mice per group with the thin line depicting the mean and the dots representing cells from individual mice. (**I**) Summarizes $N = 2$ independent experiments with $n = 6$ to 7 mice. One-way analysis of variance (ANOVA) followed by Tukey's posttest for multiple comparisons (C) or unpaired two-tailed Student's *t* test (D and I) with $^*P < 0.05$ and $^{****}P < 0.0001$.

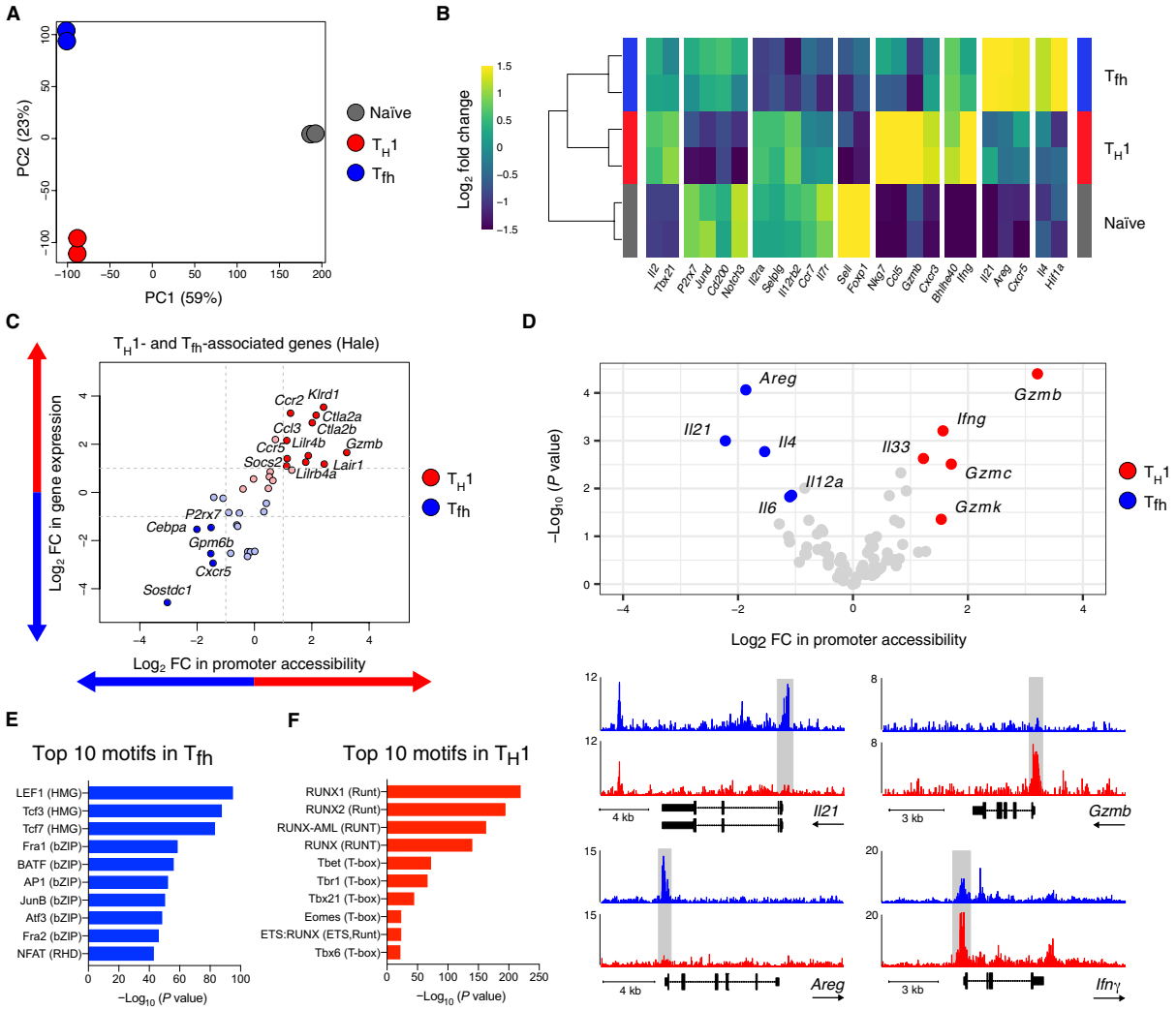

Fig. 6. Epigenetic regulation of long-lived T_{fh} cells. (**A**) PCA of ATAC-seq data on all peaks. (**B**) Heatmap of hierarchically clustered promoter regions of highlighted genes. Genes with absolute value (log_2 FC) > 1 are assigned the most extreme colors. (**C**) Scatter plots of ATAC-seq promoter log2 FC and in silico pseudo-bulk RNA-seq log_2 FC with blue and red arrows indicating enrichment in T_{fh} and T_H1 compartment, respectively. (**D**) Volcano plot of cytokine promoter region accessibility with blue and red dots indicating increased accessibility in T_{fh} and T_H1 compartment, respectively, and highlighted gene tracks. (**E** and **F**) Enriched motifs in long-lived T_{fh} (E) or T_H1 memory cells (F) found by HOMER.

ICOS signaling maintains T_{fh} cell identity at late time points

Although ICOS has an established role in primary T_{fh} responses, its role in maintaining $CD4^+$ T cells in the long term is less clear. ICOS signaling has been shown to induce the expression of *Tcf7* in Th17 memory cells that maintain the plasticity to differentiate after stimulation (*63*). ICOS can also induce mTORC1 activation in both T_{fh} effector and T follicular regulatory effector cells, leading to further stabilization of the follicular T cell program (*43*, *64*, *65*). To test the hypothesis that ICOS signals contribute to the integration of stemness and anabolic metabolism in long-lived T_{fh} cells, we treated LCMV-infected mice with anti-ICOSL starting at day >50 after infection (Fig. 7A). After 12 days of treatment, the number of GP66-specific T_{fh} cells was decreased in anti-ICOSL–treated mice (Fig. 7B). T_{fh} cells remaining after ICOS blockade had decreased expression of TCF1 and reduced activation of mTOR as measured by cell size (fig. S7, A and B). To further characterize the effects of anti-ICOSL blocking on long-lived T_{fh} cells, we performed RNA-seq at day 60 after infection on control and treated mice. Cells from mice treated with anti-ICOSL for 12 days before harvest exhibited lower transcription of key T_{fh} genes such as *Pdcd1*, *Cxcr5*, and *Bcl6*, whereas known T_H1 survival factors such as *Bcl2* and *Il7r* were increased (Fig. 7C). GSEA showed decline of T_{fh}-defining, resident memory, *Rptor*-regulated,

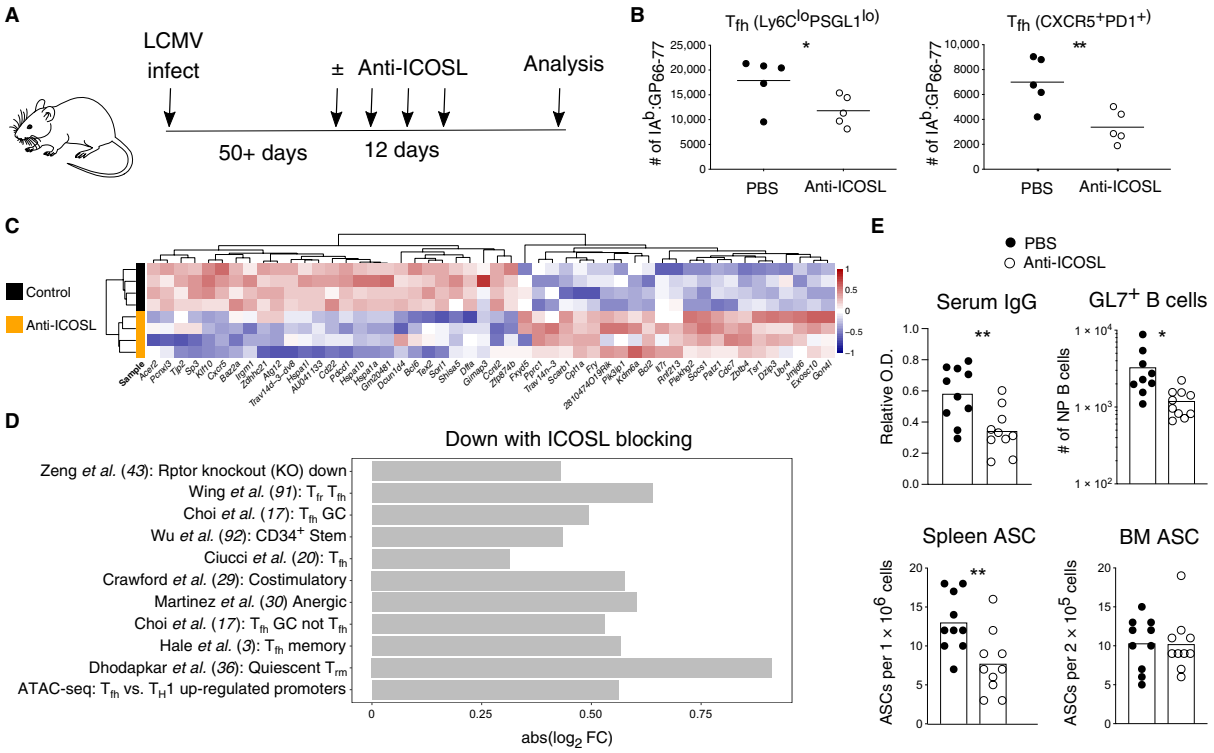

Fig. 7. ICOS signaling maintains T_{fh} cell identity. (**A**) Mice infected with LCMV followed by anti-ICOSL treatment at late time points after infection. LCMV-specific $CD4^+$ T and B cells analyzed after 12 days of treatment. (**B**) Cell numbers of GP66-specific long-lived T_{fh} cells in treated mice using different gating strategies. (**C**) Scaled, centered expression of 20 most significant differentially expressed transcripts in long-lived T_{fh} cells between control and anti-ICOSL–treated mice. (**D**) Most significantly down-regulated gene signatures with anti-ICOSL–blocking (false discovery rate < 0.2) (*3*, *17*, *20*, *29*, *30*, *36*, *43*, *91*, *92*). (**E**) NP-specific IgG serum titer [far left, optical density (O.D.) measured in 1:8100 dilution], numbers of NP-specific $GL7^+$ B cells (left), and NP-specific antibody-secreting cells (ASC) from the spleen (right) and bone marrow (far right). Data represent one of $N = 2$ independent experiments with $n = 5$ mice per group (B). Data summarize $N = 2$ independent experiments with $n = 9$ to 10 mice per group, and bars indicate the mean (E). Unpaired two-tailed Student's *t* test was performed for (B) and (E) with $^*P < 0.05$ and $^{**}P < 0.01$.

and stem cell–associated sets in treated samples compared with controls (Fig. 7D). These data emphasize the importance of ICOS signals in maintaining long-lived T_{fh} identity.

At late time points after LCMV infection, antibody titers are maintained by plasma cells present in the bone marrow (*66*, *67*). However, up to 1 year after infection, about 20% of the total plasma cell compartment is found in the spleen, with an estimated half-life of 172 days (*68*, *69*). The contribution of long-lived T_{fh} cells to plasma cell maintenance or antibody titers has not been considered due to the previous inability to detect T_{fh} cells at late time points. To assess whether late ICOS blockade and subsequent decline of the long-lived T_{fh} cell compartment affect late phase humoral responses, we measured LCMV-specific antibody titers in the serum of treated and control mice at day >60. Here, we observed an almost twofold decrease in NP-specific immunoglobulin G (IgG) antibody titers with ICOS blockade (Fig. 7E). To determine whether the decline in antibody titers correlated with fewer plasma cells in the bone marrow or spleen, we measured the number of NP-specific plasma cells by ELISpot. Here, we observed that anti-ICOSL treatment correlated with a twofold decrease in the number of splenic plasma cells, with no impact on the number of bone marrow plasma cells (Fig. 7E). Assuming that ICOS blocking is 100% efficient and that circulating IgG has a half-life of about 8 days, these data reveal a sizeable and ongoing contribution of splenic plasma cells to antibody maintenance at this time point (fig. S7C). Because both anti-ICOSL and 2-DG/rapamycin treatments result in decreased numbers of long-lived T_{fh} cells, we tested whether antibody titers decrease after 2-DG/rapamycin treatment. 2-DG/rapamycin did not affect circulating antibody titers (fig. S7D). One possible explanation is that the low dose of rapamycin used primarily inhibits mTORC1 signaling, whereas ICOS signals are additionally mediated by mTORC2 (*43*). In support of this idea, anti-ICOSL treatment decreased the expression of mTORC2 target proteins IL-7R and CCR7 on T_{fh} cells, whereas T_{fh} cells from 2-DG/rapamycin and control mice maintained higher levels of these proteins (fig. S7E).

To further assess humoral responses, we counted germinal centers (GCs) at late time points after LCMV infection using immunohistochemistry. Although GCs were clearly detected at day 15 after infection, their number at day 54 was comparable with the number in uninfected mice of a similar age (fig. S7F). We next used an NP tetramer to determine whether virus-specific B cells were affected by ICOSL blockade (*70*). Numbers of IgD, IgM, and isotype-switched

immunoglobulin (swIg) memory B cells were unaffected, but there was a significant decrease in the number and proportion of $GL7^+$ B cells (fig. S7G and Fig. 7E). These cells did not express Fas, a marker normally associated with active GC B cells and that, when absent, has been reported to preferentially support plasma cell differentiation (fig. S7H) (*71*). $GL7^+Fas^-$ B cells were also negative for CD38 and CD138, distinguishing them from B memory or plasmablasts (fig. S7I). In addition, most of these cells were double negative for IgM and IgD and expressed both CD73 and CD80, markers associated with prior participation in a GC reaction (fig. S7J) (*72*). Together, these data demonstrate an essential role for ICOS signaling in maintaining the long-lived T_{fh} compartment and plasma cell survival in the spleen.

DISCUSSION

In this study, we determined that the $CD4^+$ memory compartment contains an abundant and highly persistent population of long-lived T_{fh} cells with broad recall capacity after secondary challenge. The presence of T_{fh} memory has been controversial. Although cells with T_{fh} cell markers have been identified in the memory phase after infection, it is unclear whether they represent an ongoing immune response, whether they are "rested down" T_{fh} memory cells, or whether they are a distinct population of self-renewing T_{cm} cells with T_{fh}-like characteristics (*73*). Our data demonstrating the extreme susceptibility of T_{fh} cells to death during isolation from the tissue shed light on the previous difficulty in discriminating these possibilities. Earlier studies reporting that T_{fh} memory cells have a muted phenotype, with decreased or absent expression of CXCR5 and PD1, respectively, were conducted with monoclonal populations of TCR transgenic cells transferred in high numbers that may not accurately reflect the breadth in differentiation of a polyclonal repertoire (*3*, *12*, *21*). Consistent with the idea that T cell differentiation can be partially informed by TCR signals, a cell-intrinsic bias for various TCR transgenic strains has previously been reported (*21*). In addition to confirming more limited long-lived T_{fh} differentiation by two distinct TCR transgenic strains, we show that treatment with NICD protector rescues polyclonal T_{fh} cells at all time points, preserving their phenotype and exposing their metabolic fitness and unexpected longevity. In contrast, T_{cm} cells, generally considered to be self-renewing and multipotent, are largely absent at the latest time points after infection. Previous studies have suggested the existence of memory cells with a hybrid T_{fh}/T_{cm} phenotype, namely, dual expression of CXCR5 and CCR7 (*6*, *12*, *20*). Our data on NICD-susceptible samples confirm a population of $CXCR5^+CCR7^+$ memory cells that likely represents cells on the border of transition from T_{fh} to T_{cm}/T_H1. However, the addition of NICD protector reveals that these transitional cells constitute a small minority of the total $CD4^+$ population at memory time points. When cells are protected from NICD, CCR7 and CXCR5 are negatively correlated. In addition, we show that CXCR5 as a marker to define the T_{fh} memory compartment is complicated by the expression of this protein in non-T_{fh} subsets. Using scRNA-seq and flow cytometry, we demonstrate that long-lived T_{fh} and T_{cm} populations are more clearly discriminated by *Izumo1r*/FR4 expression.

We further show that long-lived T_{fh} cells require ongoing ICOS signals and mTOR/glycolysis for their survival. These observations suggest that maintenance of long-lived T_{fh} cells is an active process. In the absence of ICOS signaling, long-lived T_{fh} cells may re-localize and acquire T_H1 memory cell characteristics, as previously reported for T_{fh} effector cells (*74*). This idea is consistent with our experiments demonstrating the inherent plasticity of long-lived T_{fh} cells after transfer, although under unperturbed conditions, ICOS-mediated retention of long-lived T_{fh} cells in proximity with B cells may limit their secondary effector potential. These data are also in line with a recent study showing the importance of ICOS signals for the maintenance of lung-resident $CD4^+$ T cells induced by tuberculosis infection (*75*). Our scRNA-seq data reveal transcriptional similarity between long-lived T_{fh} and T_{rm} cells, both recognized as noncirculating subsets. As both residency and mTOR gene expression signatures are reduced in long-lived T_{fh} cells after ICOS blockade, it will be interesting to determine whether ICOS and mTOR signals are required to sustain T_{rm} cells after acute infection.

The constitutive glycolytic phenotype we observed in long-lived T_{fh} cells occurs together with high expression of TCF1 and CD27, both associated with self-renewal and plasticity. These data are notably in contrast to many studies showing a positive correlation between catabolic metabolism and stem-like features. In general, effector T cell differentiation is associated with a more glycolytic metabolism, whereas memory T cells exhibit a shift toward oxidative metabolism (*76*). Previous studies have shown that inhibition of mTOR signals promotes the generation of both $CD4^+$ and $CD8^+$ memory T cells (*77*–*79*). mTOR activation was also recently shown to mediate the differentiation of metabolically quiescent, TCF1-positive TH17 cells into inflammatory T_H1 effectors (*50*). On the other hand, $CD4^+$ memory T cells require Notch-dependent glucose uptake for survival, and $CD8^+$ T cells with enforced glycolytic metabolism are still able to generate memory T cells with robust recall capacity, albeit with a bias toward the $CD62L^{lo}$ T_{em} phenotype (*80*, *81*). Similarly, human $CD4^+$ T_{em} cells have an increased glycolytic reserve and depend on glycolysis to maintain mitochondrial membrane potential, regulating both survival and recall potential (*82*). Together, our findings suggest that engagement of a specific metabolic pathway does not universally underlie the differentiation of memory T cells and that different types of memory T cells may preferentially use metabolic pathways that are tuned to a particular immune context (e.g., availability of cytokines, nutrients, antigen, etc.).

Last, our data reveal an unexpected role for T_{fh} cells in supporting splenic plasma cells and systemic antibody titers at time points when the immune response has supposedly died down. Because of the apparent absence of long-lived T_{fh} cells without NICD protector, a role for T_{fh} cells was not previously considered. One possibility is that persistent antigen fuels the continuous differentiation of memory B cells into plasma cells (*83*). The observation of decreased NP-specific $GL7^+$ B cells after ICOS blockade is compatible with this idea, although $GL7^+$ B cells isolated at these late time points did not express Fas and therefore have an unusual phenotype. It is possible that $GL7^+Fas^-$ cells received fewer costimulatory signals (e.g., CD40 cross-linking), which would otherwise induce Fas expression, or that these cells are recent GC emigrants, which may later up-regulate CD38 and transition into the memory B cell compartment. We also did not see a change in NP-specific plasmablast numbers, although we cannot exclude effects of technical limitations. In addition, abundant T_{fh} cells were detected 400+ days after infection, which points to either astonishingly long antigen persistence or an alternative explanation. Another possibility is that ICOS blocking interferes with the structural organization of the spleen and/or plasma cell niche. Plasma cell survival depends on the availability of soluble factors, such as IL-6, IL-21, and B-cell activating factor (BAFF), all of which

can be produced by T_{fh} cells (*84*). Both $CD4^+$ T cells and BAFF were recently identified as key factors supporting the survival of splenic plasma cells, but the nature of $CD4^+$-derived signals was not reported (*85*). One way to discriminate the function of long-lived T_{fh} cells will be to understand where these cells are localized. During the effector phase, T_{fh} cells localize to B cell follicles by interacting with ICOSL expressed by bystander B cells (*86*). If long-lived T_{fh} cells support the conversion of memory B cells into plasma cells, we would expect this colocalization to continue at late time points after infection. On the other hand, if long-lived T_{fh} cells directly provide survival signals to plasma cells, they may be localized in or near the red pulp. In this scenario, long-lived T_{fh} cell interactions with $CD11c^+$ ICOSL- expressing antigen presenting cells would be impaired by ICOSL blockade, leading to a loss of T_{fh} cells (*87*).

The observation that ICOS blocking reduces NP-specific IgG titers roughly twofold is unexpected if splenic plasma cells make up only 20% of the total plasma cell pool, as has been previously estimated (*67*). One possibility is that this original calculation underestimates the number of splenic plasma cells at this time point; alternatively, antibody output from splenic plasma cells may be higher compared with bone marrow cells. With respect to the first possibility, the original estimate of 20% is based on the number of plasma cells in the mouse femur, under the assumption that all bone marrow compartments have equivalent plasma cell activity. However, a recent study in macaques demonstrated that plasma cells preferentially accumulate in the femur compared with other bones, suggesting that the current conversion factor for mice—based solely on counts from the femur—may overestimate the total number of bone marrow splenic cells (*88*).

In summary, our data establish long-lived T_{fh} cells as an attractive target for vaccination. The question remains, however, as to whether these cells can be termed memory cells. This debate assumes a classical definition of memory, hinging on questions of antigen availability and dependence. Although our experiments demonstrate that a large proportion of polyclonal T_{fh} cells can survive in the absence of antigen, their recovery is highest after transfer into infection-matched recipients. Nevertheless, at day 400+ after infection, when residual antigen is unlikely to play a major role, T_{fh} cells make up a substantial proportion of the antigen-specific compartment. When identified by the absence of CCR7 and CD62L, long-lived T_{fh} cells can be considered a T_{em} subset. $CD4^+$ T_{em} cells were recently shown to be generated in response to a universal influenza vaccination and to correlate with accelerated and improved cellular and humoral secondary responses after challenge (*89*). In contrast, the unanticipated scarcity of T_{cm} cells at late time points that we report here combined with their more limited recall potential indicates that vaccines targeting T_{cm} may not offer optimal long-term protection.

MATERIALS AND METHODS

Study design

The aim of this study was to understand the longevity and differentiation potential of distinct $CD4^+$ memory T cell subsets. We used the murine LCMV infection model and major histocompatibility complex II tetramers to identify polyclonal antigen-specific $CD4^+$ memory T cells. Detailed descriptions of experimental parameters (sample sizes, number of experimental replicates, and statistical analysis) can be found below or in figure legends. Infected mice were randomly assigned to treatment versus control groups. Analysis of the experimental data was conducted in an unblinded manner.

Mice

Mice were bred and housed under specific pathogen-free conditions at the University Hospital of Basel according to the animal protection law in Switzerland. For all experiments, male or female sex-matched mice that were at least 6 weeks old at the time point of infection were used. The following mouse strains were used: C57BL/6 CD45.2, C57BL/6 CD45.1, Nur77 green fluorescent protein (GFP), c-myc GFP (provided by T. Schroeder, Department of Biosystems Science and Engineering, Switzerland), T-bet ZsGreen (provided by J. Zhu, National Institutes of Health, USA), $P2X7R^{-/-}$ (provided by F. Grassi, Institute for Research in Biomedicine, Switzerland), SMARTA, and NIP (S. Crotty, La Jolla Institute for Allergy and Immunology, USA).

NICD protector

Mice were intravenously injected with 25 μg of commercial (BioLegend, no. 149802) or 12.5 μg of homemade ARTC2.2-blocking nanobody s+16 (NICD protector) 15 min before organ harvest. NICD protector was used in every experiment (including adoptive transfers) except for when the goal was to compare NICD protector treatment to no treatment (Fig. 1, A and C, and figs. S1, C to E and G, and S3, I to K).

Statistical analysis

For statistical analysis, the tests that were used are specified in each figure legend. In time course experiments, statistical analysis was performed for each individual time point. Error bars show SD centered on the mean unless otherwise indicated. Data were analyzed with GraphPad Prism software (version 7 or 8). $*P < 0.05$, $**P < 0.01$, $***P < 0.001$, $****P < 0.0001$. ns, not significant.

SUPPLEMENTARY MATERIALS

immunology.sciencemag.org/cgi/content/full/5/45/eaay5552/DC1

Methods

Fig. S1. T_{fh} cells are susceptible to death during isolation.

Fig. S2. FR4 discriminates long-lived T_{fh} from transcriptionally distinct T_{cm}.

Fig. S3. Long-lived T_{fh} cells are constitutively glycolytic.

Fig. S4. Antigen is not required for the survival of long-lived T_{fh} cells.

Fig. S5. T_{fh} cells generate multiple cell fates upon recall.

Fig. S6. Epigenetic regulation of long-lived T_{fh} cells.

Fig. S7. ICOS signaling maintains T_{fh} cell identity at late time points.

Fig. S8. Normalization of ATAC-seq data.

Table S1. Raw data file (Excel spreadsheet).

References (*93*–*105*)

View/request a protocol for this paper from *Bio-protocol*.

REFERENCES AND NOTES

1. R. Ahmed, D. Gray, Immunological memory and protective immunity: Understanding their relation. *Science* **272**, 54–60 (1996).
2. F. Sallusto, J. Geginat, A. Lanzavecchia, Central memory and effector memory T cell subsets: Function, generation, and maintenance. *Annu. Rev. Immunol.* **22**, 745–763 (2004).
3. J. S. Hale, B. Youngblood, D. R. Latner, A.-U.-R. Mohammed, L. Ye, R. S. Akondy, T. Wu, S. S. Iyer, R. Ahmed, Distinct memory $CD4^+$ T cells with commitment to T follicular helper- and T helper 1-cell lineages are generated after acute viral infection. *Immunity* **38**, 805–817 (2013).
4. M. K. MacLeod, A. David, A. S. McKee, F. Crawford, J. W. Kappler, P. Marrack, Memory CD4 T cells that express CXCR5 provide accelerated help to B cells. *J. Immunol.* **186**, 2889–2896 (2011).
5. K. Luthje, A. Kallies, Y. Shimohakamada, G. T. Belz, A. Light, D. M. Tarlinton, S. L. Nutt, The development and fate of follicular helper T cells defined by an IL-21 reporter mouse. *Nat. Immunol.* **13**, 491–498 (2012).
6. M. Pepper, A. J. Pagán, B. Z. Igyártó, J. J. Taylor, M. K. Jenkins, Opposing signals from the Bcl6 transcription factor and the interleukin-2 receptor generate T helper 1 central and effector memory cells. *Immunity* **35**, 583–595 (2011).

7. A. Asrir, M. Aloulou, M. Gador, C. Pérals, N. Fazilleau, Interconnected subsets of memory follicular helper T cells have different effector functions. *Nat. Commun.* **8**, 847 (2017).
8. S. E. Bentebibel, S. Lopez, G. Obermoser, N. Schmitt, C. Mueller, C. Harrod, E. Flano, A. Mejias, R. A. Albrecht, D. Blankenship, H. Xu, V. Pascual, J. Banchereau, A. Garcia-Sastre, A. K. Palucka, O. Ramilo, H. Ueno, Induction of $ICOS^+CXCR3^+CXCR5^+$ T_H cells correlates with antibody responses to influenza vaccination. *Sci. Transl. Med.* **5**, 176ra32 (2013).
9. S. Crotty, R. Ahmed, *Immune Memory and Vaccines: Great Debates* (Cold Spring Harbor perspectives in biology, Cold Spring Harbor Laboratory Press, Cold Spring Harbor, New York, 2018), pp. ix, 418 pages.
10. D. L. Hill, W. Pierson, D. J. Bolland, C. Mkindi, E. J. Carr, J. Wang, S. Houard, S. W. Wingett, R. Audran, E. F. Wallin, S. A. Jongo, K. Kamaka, M. Zand, F. Spertini, C. Daubenberger, A. E. Corcoran, M. A. Linterman, The adjuvant GLA-SE promotes human Tfh cell expansion and emergence of public TCRβ clonotypes. *J. Exp. Med.* **216**, 1857–1873 (2019).
11. S. Keck, M. Schmaler, S. Ganter, L. Wyss, S. Oberle, E. S. Huseby, D. Zehn, C. G. King, Antigen affinity and antigen dose exert distinct influences on CD4 T-cell differentiation. *Proc. Natl. Acad. Sci. U.S.A.* **111**, 14852–14857 (2014).
12. H. D. Marshall, A. Chandele, Y. W. Jung, H. Meng, A. C. Poholek, I. A. Parish, R. Rutishauser, W. Cui, S. H. Kleinstein, J. Craft, S. M. Kaech, Differential expression of Ly6C and T-bet distinguish effector and memory T_H1 $CD4^+$ cell properties during viral infection. *Immunity* **35**, 633–646 (2011).
13. D. Homann, L. Teyton, M. B. A. Oldstone, Differential regulation of antiviral T-cell immunity results in stable $CD8^+$ but declining $CD4^+$ T-cell memory. *Nat. Med.* **7**, 913–919 (2001).
14. M. A. Williams, E. V. Ravkov, M. J. Bevan, Rapid culling of the $CD4^+$ T cell repertoire in the transition from effector to memory. *Immunity* **28**, 533–545 (2008).
15. H. D. Marshall, J. P. Ray, B. J. Laidlaw, N. Zhang, D. Gawande, M. M. Staron, J. Craft, S. M. Kaech, The transforming growth factor beta signaling pathway is critical for the formation of CD4 T follicular helper cells and isotype-switched antibody responses in the lung mucosa. *eLife* **4**, e04851 (2015).
16. Y. Tian, M. Babor, J. Lane, V. Schulten, V. S. Patil, G. Seumois, S. L. Rosales, Z. Fu, G. Picarda, J. Burel, J. Zapardiel-Gonzalo, R. N. Tennekoon, A. D. De Silva, S. Premawansa, G. Premawansa, A. Wijewickrama, J. A. Greenbaum, P. Vijayanand, D. Weiskopf, A. Sette, B. Peters, Unique phenotypes and clonal expansions of human CD4 effector memory T cells re-expressing CD45RA. *Nat. Commun.* **8**, 1473 (2017).
17. Y. S. Choi, J. A. Gullicksrud, S. Xing, Z. Zeng, Q. Shan, F. Li, P. E. Love, W. Peng, H.-H. Xue, S. Crotty, LEF-1 and TCF-1 orchestrate T_{FH} differentiation by regulating differentiation circuits upstream of the transcriptional repressor Bcl6. *Nat. Immunol.* **16**, 980–990 (2015).
18. A. M. Siegel, J. Heimall, A. F. Freeman, A. P. Hsu, E. Brittain, J. M. Brenchley, D. C. Douek, G. H. Fahle, J. I. Cohen, S. M. Holland, J. D. Milner, A critical role for STAT3 transcription factor signaling in the development and maintenance of human T cell memory. *Immunity* **35**, 806–818 (2011).
19. C. S. Ma, D. T. Avery, A. Chan, M. Batten, J. Bustamante, S. Boisson-Dupuis, P. D. Arkwright, A. Y. Kreins, D. Averbuch, D. Engelhard, K. Magdorf, S. S. Kilic, Y. Minegishi, S. Nonoyama, M. A. French, S. Choo, J. M. Smart, J. Peake, M. Wong, P. Gray, M. C. Cook, D. A. Fulcher, J.-L. Casanova, E. K. Deenick, S. G. Tangye, Functional STAT3 deficiency compromises the generation of human T follicular helper cells. *Blood* **119**, 3997–4008 (2012).
20. T. Ciucci, M. S. Vacchio, Y. Gao, F. Tomassoni Ardori, J. Candia, M. Mehta, Y. Zhao, B. Tran, M. Pepper, L. Tessarollo, D. B. McGavern, R. Bosselut, The emergence and functional fitness of memory $CD4^+$ T cells require the transcription factor Thpok. *Immunity* **50**, 91–105.e4 (2019).
21. N. J. Tubo, A. J. Pagán, J. J. Taylor, R. W. Nelson, J. L. Linehan, J. M. Ertelt, E. S. Huseby, S. S. Way, M. K. Jenkins, Single naive $CD4^+$ T cells from a diverse repertoire produce different effector cell types during infection. *Cell* **153**, 785–796 (2013).
22. Y. S. Choi, J. A. Yang, I. Yusuf, R. J. Johnston, J. Greenbaum, B. Peters, S. Crotty, Bcl6 expressing follicular helper CD4 T cells are fate committed early and have the capacity to form memory. *J. Immunol.* **190**, 4014–4026 (2013).
23. S. S. Iyer, D. R. Latner, M. J. Zilliox, M. M. Causland, R. S. Akondy, P. Penaloza-MacMaster, J. S. Hale, L. Ye, A.-U.-R. Mohammed, T. Yamaguchi, S. Sakaguchi, R. R. Amara, R. Ahmed, Identification of novel markers for mouse $CD4^+$ T follicular helper cells. *Eur. J. Immunol.* **43**, 3219–3232 (2013).
24. M. Proietti, V. Cornacchione, T. Rezzonico Jost, A. Romagnani, C. E. Faliti, L. Perruzza, R. Rigoni, E. Radaelli, F. Caprioli, S. Preziuso, B. Brannetti, M. Thelen, K. D. McCoy, E. Slack, E. Traggiai, F. Grassi, ATP-gated ionotropic P2X7 receptor controls follicular T helper cell numbers in Peyer's patches to promote host-microbiota mutualism. *Immunity* **41**, 789–801 (2014).
25. F. Aswad, H. Kawamura, G. Dennert, High sensitivity of $CD4^+CD25^+$ regulatory T cells to extracellular metabolites nicotinamide adenine dinucleotide and ATP: A role for $P2X_7$ receptors. *J. Immunol.* **175**, 3075–3083 (2005).
26. D. Fernandez-Ruiz, W. Y. Ng, L. E. Holz, J. Z. Ma, A. Zaid, Y. C. Wong, L. S. Lau, V. Mollard, A. Cozijnsen, N. Collins, J. Li, G. M. Davey, Y. Kato, S. Devi, R. Skandari, M. Pauley, J. H. Manton, D. I. Godfrey, A. Braun, S. S. Tay, P. S. Tan, D. G. Bowen, F. Koch-Nolte, B. Rissiek, F. R. Carbone, B. S. Crabb, M. Lahoud, I. A. Cockburn, S. N. Mueller, P. Bertolino, G. I. McFadden, I. Caminschi, W. R. Heath, Liver-resident memory $CD8^+$ T cells form a front-line defense against malaria liver-stage infection. *Immunity* **45**, 889–902 (2016).
27. S. Hubert, B. Rissiek, K. Klages, J. Huehn, T. Sparwasser, F. Haag, F. Koch-Nolte, O. Boyer, M. Seman, S. Adriouch, Extracellular NAD^+ shapes the $Foxp3^+$ regulatory T cell compartment through the ART2–P2X7 pathway. *J. Exp. Med.* **207**, 2561–2568 (2010).
28. H. Borges da Silva, H. Wang, L. J. Qian, K. A. Hogquist, S. C. Jameson, ARTC2.2/P2RX7 signaling during cell isolation distorts function and quantification of tissue-resident $CD8^+$ T cell and invariant NKT subsets. *J. Immunol.* **202**, 2153–2163 (2019).
29. A. Crawford, J. M. Angelosanto, C. Kao, T. A. Doering, P. M. Odorizzi, B. E. Barnett, E. J. Wherry, Molecular and transcriptional basis of $CD4^+$ T cell dysfunction during chronic infection. *Immunity* **40**, 289–302 (2014).
30. G. J. Martinez, R. M. Pereira, T. Äijö, E. Y. Kim, F. Marangoni, M. E. Pipkin, S. Togher, V. Heissmeyer, Y. C. Zhang, S. Crotty, E. D. Lamperti, K. M. Ansel, T. R. Mempel, H. Lähdesmäki, P. G. Hogan, A. Rao, The transcription factor NFAT promotes exhaustion of activated $CD8^+$ T cells. *Immunity* **42**, 265–278 (2015).
31. L. A. Kalekar, S. E. Schmiel, S. L. Nandiwada, W. Y. Lam, L. O. Barsness, N. Zhang, G. L. Stritesky, D. Malhotra, K. E. Pauken, J. L. Linehan, M. G. O'Sullivan, B. T. Fife, K. A. Hogquist, M. K. Jenkins, D. L. Mueller, $CD4^+$ T cell anergy prevents autoimmunity and generates regulatory T cell precursors. *Nat. Immunol.* **17**, 304–314 (2016).
32. T. Yamaguchi, K. Hirota, K. Nagahama, K. Ohkawa, T. Takahashi, T. Nomura, S. Sakaguchi, Control of immune responses by antigen-specific regulatory T cells expressing the folate receptor. *Immunity* **27**, 145–159 (2007).
33. M. M. McCausland, S. Crotty, Quantitative PCR technique for detecting lymphocytic choriomeningitis virus in vivo. *J. Virol. Methods* **147**, 167–176 (2008).
34. L. K. Mackay, M. Minnich, N. A. M. Kragten, Y. Liao, B. Nota, C. Seillet, A. Zaid, K. Man, S. Preston, D. Freestone, A. Braun, E. Wynne-Jones, F. M. Behr, R. Stark, D. G. Pellicci, D. I. Godfrey, G. T. Belz, M. Pellegrini, T. Gebhardt, M. Busslinger, W. Shi, F. R. Carbone, R. A. W. van Lier, A. Kallies, K. P. J. M. van Gisbergen, Hobit and Blimp1 instruct a universal transcriptional program of tissue residency in lymphocytes. *Science* **352**, 459–463 (2016).
35. L. K. Mackay, A. Rahimpour, J. Z. Ma, N. Collins, A. T. Stock, M.-L. Hafon, J. Vega-Ramos, P. Lauzurica, S. N. Mueller, T. Stefanovic, D. C. Tscharke, W. R. Heath, M. Inouye, F. R. Carbone, T. Gebhardt, The developmental pathway for $CD103^+CD8^+$ tissue-resident memory T cells of skin. *Nat. Immunol.* **14**, 1294–1301 (2013).
36. C. S. Boddupalli, S. Nair, S. M. Gray, H. N. Nowyhed, R. Verma, J. A. Gibson, C. Abraham, D. Narayan, J. Vasquez, C. C. Hedrick, R. A. Flavell, K. M. Dhodapkar, S. M. Kaech, M. V. Dhodapkar, ABC transporters and NR4A1 identify a quiescent subset of tissue-resident memory T cells. *J. Clin. Invest.* **126**, 3905–3916 (2016).
37. S. H. Cho, A. L. Raybuck, J. Blagih, E. Kemboi, V. H. Haase, R. G. Jones, M. R. Boothby, Hypoxia-inducible factors in $CD4^+$ T cells promote metabolism, switch cytokine secretion, and T cell help in humoral immunity. *Proc. Natl. Acad. Sci. U.S.A.* **116**, 8975–8984 (2019).
38. Y. Zhu, Y. Zhao, L. Zou, D. Zhang, D. Aki, Y.-C. Liu, The E3 ligase VHL promotes follicular helper T cell differentiation via glycolytic-epigenetic control. *J. Exp. Med.* **216**, 1664–1681 (2019).
39. P. Hombrink, C. Helbig, R. A. Backer, B. Piet, A. E. Oja, R. Stark, G. Brasser, A. Jongejan, R. E. Jonkers, B. Nota, O. Basak, H. C. Clevers, P. D. Moerland, D. Amsen, R. A. W. van Lier, Programs for the persistence, vigilance and control of human $CD8^+$ lung-resident memory T cells. *Nat. Immunol.* **17**, 1467–1478 (2016).
40. S. Bekkering, R. J. W. Arts, B. Novakovic, I. Kourtzelis, C. D. C. C. van der Heijden, Y. Li, C. D. Popa, R. ter Horst, J. van Tuijl, R. T. Netea-Maier, F. L. van de Veerdonk, T. Chavakis, L. A. B. Joosten, J. W. M. van der Meer, H. Stunnenberg, N. P. Riksen, M. G. Netea, Metabolic induction of trained immunity through the mevalonate pathway. *Cell* **172**, 135–146.e9 (2018).
41. S.-C. Cheng, J. Quintin, R. A. Cramer, K. M. Shepardson, S. Saeed, V. Kumar, E. J. Giamarellos-Bourboulis, J. H. A. Martens, N. A. Rao, A. Aghajanirefah, G. R. Manjeri, Y. Li, D. C. Ifrim, R. J. W. Arts, B. M. J. W. van der Veer, P. M. T. Deen, C. Logie, L. A. O'Neill, P. Willems, F. L. van de Veerdonk, J. W. M. van der Meer, A. Ng, L. A. B. Joosten, C. Wijmenga, H. G. Stunnenberg, R. J. Xavier, M. G. Netea, mTOR- and HIF-1α–mediated aerobic glycolysis as metabolic basis for trained immunity. *Science* **345**, 1250684 (2014).
42. S. Saeed, J. Quintin, H. H. D. Kerstens, N. A. Rao, A. Aghajanirefah, F. Matarese, S.-C. Cheng, J. Ratter, K. Berentsen, M. A. van der Ent, N. Sharifi, E. M. Janssen-Megens, M. T. Huurne, A. Mandoli, T. van Schaik, A. Ng, F. Burden, K. Downes, M. Frontini, V. Kumar, E. J. Giamarellos-Bourboulis, W. H. Ouwehand, J. W. M. van der Meer, L. A. B. Joosten, C. Wijmenga, J. H. A. Martens, R. J. Xavier, C. Logie, M. G. Netea, H. G. Stunnenberg, Epigenetic programming of monocyte-to-macrophage differentiation and trained innate immunity. *Science* **345**, 1251086 (2014).
43. H. Zeng, S. Cohen, C. Guy, S. Shrestha, G. Neale, S. A. Brown, C. Cloer, R. J. Kishton, X. Gao, B. Youngblood, M. Do, M. O. Li, J. W. Locasale, J. C. Rathmell, H. Chi, mTORC1 and mTORC2 kinase signaling and glucose metabolism drive follicular helper T cell differentiation. *Immunity* **45**, 540–554 (2016).
44. D. K. Finlay, E. Rosenzweig, L. V. Sinclair, C. Feijoo-Carnero, J. L. Hukelmann, J. Rolf, A. A. Panteleyev, K. Okkenhaug, D. A. Cantrell, PDK1 regulation of mTOR and

hypoxia-inducible factor 1 integrate metabolism and migration of $CD8^+$ T cells. *J. Exp. Med.* **209**, 2441–2453 (2012).
45. A. Lissina, K. Ladell, A. Skowera, M. Clement, E. Edwards, R. Seggewiss, H. A. van den Berg, E. Gostick, K. Gallagher, E. Jones, J. J. Melenhorst, A. J. Godkin, M. Peakman, D. A. Price, A. K. Sewell, L. Wooldridge, Protein kinase inhibitors substantially improve the physical detection of T-cells with peptide-MHC tetramers. *J. Immunol. Methods* **340**, 11–24 (2009).
46. J. P. Ray, M. M. Staron, J. A. Shyer, P.-C. Ho, H. D. Marshall, S. M. Gray, B. J. Laidlaw, K. Araki, R. Ahmed, S. M. Kaech, J. Craft, The interleukin-2-mTORc1 kinase axis defines the signaling, differentiation, and metabolism of T helper 1 and follicular B helper T cells. *Immunity* **43**, 690–702 (2015).
47. H. Borges da Silva, L. K. Beura, H. Wang, E. A. Hanse, R. Gore, M. C. Scott, D. A. Walsh, K. E. Block, R. Fonseca, Y. Yan, K. L. Hippen, B. R. Blazar, D. Masopust, A. Kelekar, L. Vulchanova, K. A. Hogquist, S. C. Jameson, The purinergic receptor P2RX7 directs metabolic fitness of long-lived memory $CD8^+$ T cells. *Nature* **559**, 264–268 (2018).
48. J. Hendriks, L. A. Gravestein, K. Tesselaar, R. A. W. van Lier, T. N. M. Schumacher, J. Borst, CD27 is required for generation and long-term maintenance of T cell immunity. *Nat. Immunol.* **1**, 433–440 (2000).
49. M. Pepper, J. L. Linehan, A. J. Pagán, T. Zell, T. Dileepan, P. P. Cleary, M. K. Jenkins, Different routes of bacterial infection induce long-lived T_H1 memory cells and short-lived T_H17 cells. *Nat. Immunol.* **11**, 83–89 (2010).
50. P. W. F. Karmaus, X. Chen, S. A. Lim, A. A. Herrada, T.-L. M. Nguyen, B. Xu, Y. Dhungana, S. Rankin, W. Chen, C. Rosencrance, K. Yang, Y. Fan, Y. Cheng, J. Easton, G. Neale, P. Vogel, H. Chi, Metabolic heterogeneity underlies reciprocal fates of T_H17 cell stemness and plasticity. *Nature* **565**, 101–105 (2019).
51. H. Moon, H.-Y. Na, K. H. Chong, T. J. Kim, P2X7 receptor-dependent ATP-induced shedding of CD27 in mouse lymphocytes. *Immunol. Lett.* **102**, 98–105 (2006).
52. P. Muranski, Z. A. Borman, S. P. Kerkar, C. A. Klebanoff, Y. Ji, L. Sanchez-Perez, M. Sukumar, R. N. Reger, Z. Yu, S. J. Kern, R. Roychoudhuri, G. A. Ferreyra, W. Shen, S. K. Durum, L. Feigenbaum, D. C. Palmer, P. A. Antony, C. C. Chan, A. Laurence, R. L. Danner, L. Gattinoni, N. P. Restifo, Th17 cells are long lived and retain a stem cell-like molecular signature. *Immunity* **35**, 972–985 (2011).
53. C. Trapnell, D. Cacchiarelli, J. Grimsby, P. Pokharel, S. Li, M. Morse, N. J. Lennon, K. J. Livak, T. S. Mikkelsen, J. L. Rinn, The dynamics and regulators of cell fate decisions are revealed by pseudotemporal ordering of single cells. *Nat. Biotechnol.* **32**, 381–386 (2014).
54. J. D. Buenrostro, P. G. Giresi, L. C. Zaba, H. Y. Chang, W. J. Greenleaf, Transposition of native chromatin for fast and sensitive epigenomic profiling of open chromatin, DNA-binding proteins and nucleosome position. *Nat. Methods* **10**, 1213–1218 (2013).
55. P. Durek, K. Nordström, G. Gasparoni, A. Salhab, C. Kressler, M. de Almeida, K. Bassler, T. Ulas, F. Schmidt, J. Xiong, P. Glažar, F. Klironomos, A. Sinha, S. Kinkley, X. Yang, L. Arrigoni, A. D. Amirabad, F. B. Ardakani, L. Feuerbach, O. Gorka, P. Ebert, F. Müller, N. Li, S. Frischbutter, S. Schlickeiser, C. Cendon, S. Fröhler, B. Felder, N. Gasparoni, C. D. Imbusch, B. Hutter, G. Zipprich, Y. Tauchmann, S. Reinke, G. Wassilew, U. Hoffmann, A. S. Richter, L. Sieverling; DEEP Consortium, H. D. Chang, U. Syrbe, U. Kalus, J. Eils, B. Brors, T. Manke, J. Ruland, T. Lengauer, N. Rajewsky, W. Chen, J. Dong, B. Sawitzki, H. R. Chung, P. Rosenstiel, M. H. Schulz, J. L. Schultze, A. Radbruch, J. Walter, A. Hamann, J. K. Polansky, Epigenomic profiling of human $CD4^+$ T cells supports a linear differentiation model and highlights molecular regulators of memory development. *Immunity* **45**, 1148–1161 (2016).
56. D. M. W. Zaiss, W. C. Gause, L. C. Osborne, D. Artis, Emerging functions of amphiregulin in orchestrating immunity, inflammation, and tissue repair. *Immunity* **42**, 216–226 (2015).
57. S. Heinz, C. Benner, N. Spann, E. Bertolino, Y. C. Lin, P. Laslo, J. X. Cheng, C. Murre, H. Singh, C. K. Glass, Simple combinations of lineage-determining transcription factors prime *cis*-regulatory elements required for macrophage and B cell identities. *Mol. Cell* **38**, 576–589 (2010).
58. C. M. Lau, N. M. Adams, C. D. Geary, O.-E. Weizman, M. Rapp, Y. Pritykin, C. S. Leslie, J. C. Sun, Epigenetic control of innate and adaptive immune memory. *Nat. Immunol.* **19**, 963–972 (2018).
59. D. M. Moskowitz, D. W. Zhang, B. Hu, S. L. Saux, R. E. Yanes, Z. Ye, J. D. Buenrostro, C. M. Weyand, W. J. Greenleaf, J. J. Goronzy, Epigenomics of human CD8 T cell differentiation and aging. *Sci. Immunol.* **2**, eaag0192 (2017).
60. I. M. Djuretic, D. Levanon, V. Negreanu, Y. Groner, A. Rao, K. M. Ansel, Transcription factors T-bet and Runx3 cooperate to activate *Ifng* and silence *Il4* in T helper type 1 cells. *Nat. Immunol.* **8**, 145–153 (2007).
61. K. Kohu, H. Ohmori, W. F. Wong, D. Onda, T. Wakoh, S. Kon, M. Yamashita, T. Nakayama, M. Kubo, M. Satake, The Runx3 transcription factor augments T_h1 and down-modulates Th2 phenotypes by interacting with and attenuating GATA3. *J. Immunol.* **183**, 7817–7824 (2009).
62. A. Kramer, J. Green, J. Pollard Jr., S. Tugendreich, Causal analysis approaches in Ingenuity Pathway Analysis. *Bioinformatics* **30**, 523–530 (2014).
63. K. Majchrzak, M. H. Nelson, J. S. Bowers, S. R. Bailey, M. M. Wyatt, J. M. Wrangle, M. P. Rubinstein, J. C. Varela, Z. Li, R. A. Himes, S. S. L. Chan, C. M. Paulos, β-catenin and PI3Kδ inhibition expands precursor Th17 cells with heightened stemness and antitumor activity. *JCI Insight* **2**, 90547 (2017).
64. L. Xu, Q. Huang, H. Wang, Y. Hao, Q. Bai, J. Hu, Y. Li, P. Wang, X. Chen, R. He, B. Li, X. Yang, T. Zhao, Y. Zhang, Y. Wang, J. Ou, H. Liang, Y. Wu, X. Zhou, L. Ye, The kinase mTORC1 promotes the generation and suppressive function of follicular regulatory T cells. *Immunity* **47**, 538–551.e5 (2017).
65. J. Yang, X. Lin, Y. Pan, J. Wang, P. Chen, H. Huang, H.-H. Xue, J. Gao, X.-P. Zhong, Critical roles of mTOR Complex 1 and 2 for T follicular helper cell differentiation and germinal center responses. *eLife* **5**, e17936 (2016).
66. M. K. Slifka, R. Ahmed, Long-term antibody production is sustained by antibody-secreting cells in the bone marrow following acute viral infection. *Ann. N. Y. Acad. Sci.* **797**, 166–176 (1996).
67. M. K. Slifka, M. Matloubian, R. Ahmed, Bone marrow is a major site of long-term antibody production after acute viral infection. *J. Virol.* **69**, 1895–1902 (1995).
68. M. K. Slifka, R. Antia, J. K. Whitmire, R. Ahmed, Humoral immunity due to long-lived plasma cells. *Immunity* **8**, 363–372 (1998).
69. F. M. Ndungu, E. T. Cadman, J. Coulcher, E. Nduati, E. Couper, D. W. MacDonald, D. Ng, J. Langhorne, Functional memory B cells and long-lived plasma cells are generated after a single *Plasmodium chabaudi* infection in mice. *PLOS Pathog.* **5**, e1000690 (2009).
70. J. J. Taylor, K. A. Pape, M. K. Jenkins, A germinal center–independent pathway generates unswitched memory B cells early in the primary response. *J. Exp. Med.* **209**, 597–606 (2012).
71. D. Butt, T. D. Chan, K. Bourne, J. R. Hermes, A. Nguyen, A. Statham, L. A. O'Reilly, A. Strasser, S. Price, P. Schofield, D. Christ, A. Basten, C. S. Ma, S. G. Tangye, T. G. Phan, V. K. Rao, R. Brink, FAS inactivation releases unconventional germinal center B cells that escape antigen control and drive IgE and autoantibody production. *Immunity* **42**, 890–902 (2015).
72. A. T. Krishnamurty, C. D. Thouvenel, S. Portugal, G. J. Keitany, K. S. Kim, A. Holder, P. D. Crompton, D. J. Rawlings, M. Pepper, Somatically hypermutated *plasmodium*-specific IgM^+ memory B cells are rapid, plastic, early responders upon malaria rechallenge. *Immunity* **45**, 402–414 (2016).
73. Q. P. Nguyen, T. Z. Deng, D. A. Witherden, A. W. Goldrath, Origins of $CD4^+$ circulating and tissue-resident memory T-cells. *Immunology* **157**, 3–12 (2019).
74. J. P. Weber, F. Fuhrmann, R. K. Feist, A. Lahmann, M. S. Al Baz, L.-J. Gentz, D. Vu van, H. W. Mages, C. Haftmann, R. Riedel, J. R. Grün, W. Schuh, R. A. Kroczek, A. Radbruch, M.-F. Mashreghi, A. Hutloff, ICOS maintains the T follicular helper cell phenotype by down-regulating Krüppel-like factor 2. *J. Exp. Med.* **212**, 217–233 (2015).
75. A. O. Moguche, S. Shafiani, C. Clemons, R. P. Larson, C. Dinh, L. E. Higdon, C. J. Cambier, J. R. Sissons, A. M. Gallegos, P. J. Fink, K. B. Urdahl, ICOS and Bcl6-dependent pathways maintain a CD4 T cell population with memory-like properties during tuberculosis. *J. Exp. Med.* **212**, 715–728 (2015).
76. G. R. Bantug, L. Galluzzi, G. Kroemer, C. Hess, The spectrum of T cell metabolism in health and disease. *Nat. Rev. Immunol.* **18**, 19–34 (2018).
77. K. Araki, A. P. Turner, V. O. Shaffer, S. Gangappa, S. A. Keller, M. F. Bachmann, C. P. Larsen, R. Ahmed, mTOR regulates memory CD8 T-cell differentiation. *Nature* **460**, 108–112 (2009).
78. E. L. Pearce, M. C. Walsh, P. J. Cejas, G. M. Harms, H. Shen, L.-S. Wang, R. G. Jones, Y. Choi, Enhancing CD8 T-cell memory by modulating fatty acid metabolism. *Nature* **460**, 103–107 (2009).
79. L. Ye, J. Lee, L. Xu, A.-U.-R. Mohammed, W. Li, J. S. Hale, W. G. Tan, T. Wu, C. W. Davis, R. Ahmed, K. Araki, mTOR promotes antiviral humoral immunity by differentially regulating CD4 helper T cell and B cell responses. *J. Virol.* **91**, e01653-16 (2017).
80. Y. Maekawa, C. Ishifune, S.-i. Tsukumo, K. Hozumi, H. Yagita, K. Yasutomo, Notch controls the survival of memory $CD4^+$ T cells by regulating glucose uptake. *Nat. Med.* **21**, 55–61 (2015).
81. A. T. Phan, A. L. Doedens, A. Palazon, P. A. Tyrakis, K. P. Cheung, R. S. Johnson, A. W. Goldrath, Constitutive glycolytic metabolism supports $CD8^+$ T cell effector memory differentiation during viral infection. *Immunity* **45**, 1024–1037 (2016).
82. S. Dimeloe, M. Mehling, C. Frick, J. Loeliger, G. R. Bantug, U. Sauder, M. Fischer, R. Belle, L. Develioglu, S. Tay, A. Langenkamp, C. Hess, The immune-metabolic basis of effector memory $CD4^+$ T cell function under hypoxic conditions. *J. Immunol.* **196**, 106–114 (2016).
83. A. F. Ochsenbein, D. D. Pinschewer, S. Sierro, E. Horvath, H. Hengartner, R. M. Zinkernagel, Protective long-term antibody memory by antigen-driven and T help-dependent differentiation of long-lived memory B cells to short-lived plasma cells independent of secondary lymphoid organs. *Proc. Natl. Acad. Sci. U.S.A.* **97**, 13263–13268 (2000).
84. S. G. Tangye, Staying alive: Regulation of plasma cell survival. *Trends Immunol.* **32**, 595–602 (2011).
85. L.-H. Thai, S. Le Gallou, A. Robbins, E. Crickx, T. Fadeev, Z. Zhou, N. Cagnard, J. Mégret, C. Bole, J.-C. Weill, C.-A. Reynaud, M. Mahévas, BAFF and $CD4^+$ T cells are major survival factors for long-lived splenic plasma cells in a B-cell–depletion context. *Blood* **131**, 1545–1555 (2018).

86. J. Shi, S. Hou, Q. Fang, X. Liu, X. Liu, H. Qi, PD-1 controls follicular T helper cell positioning and function. *Immunity* **49**, 264–274.e4 (2018).
87. L. L. Teichmann, J. L. Cullen, M. Kashgarian, C. Dong, J. Craft, M. J. Shlomchik, Local triggering of the ICOS coreceptor by CD11c$^+$ myeloid cells drives organ inflammation in lupus. *Immunity* **42**, 552–565 (2015).
88. E. Hammarlund, A. Thomas, I. J. Amanna, L. A. Holden, O. D. Slayden, B. Park, L. Gao, M. K. Slifka, Plasma cell survival in the absence of B cell memory. *Nat. Commun.* **8**, 1781 (2017).
89. S. A. Valkenburg, O. T. W. Li, A. Li, M. Bull, T. A. Waldmann, L. P. Perera, M. Peiris, L. L. M. Poon, Protection by universal influenza vaccine is mediated by memory CD4 T cells. *Vaccine* **36**, 4198–4206 (2018).
90. D. T. Utzschneider, M. Charmoy, V. Chennupati, L. Pousse, D. P. Ferreira, S. Calderon-Copete, M. Danilo, F. Alfei, M. Hofmann, D. Wieland, S. Pradervand, R. Thimme, D. Zehn, W. Held, T cell factor 1-expressing memory-like CD8$^+$ T cells sustain the immune response to chronic viral infections. *Immunity* **45**, 415–427 (2016).
91. J. B. Wing, Y. Kitagawa, M. Locci, H. Hume, C. Tay, T. Morita, Y. Kidani, K. Matsuda, T. Inoue, T. Kurosaki, S. Crotty, C. Coban, N. Ohkura, S. Sakaguchi, A distinct subpopulation of CD25$^-$ T-follicular regulatory cells localizes in the germinal centers. *Proc. Natl. Acad. Sci. U.S.A.* **114**, E6400–E6409 (2017).
92. J. Q. Wu, M. Seay, V. P. Schulz, M. Hariharan, D. Tuck, J. Lian, J. Du, M. Shi, Z. Ye, M. Gerstein, M. P. Snyder, S. Weissman, Tcf7 is an important regulator of the switch of self-renewal and differentiation in a multipotential hematopoietic cell line. *PLOS Genet.* **8**, e1002565 (2012).
93. M. Battegay, Quantification of lymphocytic choriomeningitis virus with an immunological focus assay in 24 well plates. *ALTEX* **10**, 6–14 (1993).
94. J. J. Moon, H. H. Chu, J. Hataye, A. J. Pagán, M. Pepper, J. B. McLachlan, T. Zell, M. K. Jenkins, Tracking epitope-specific T cells. *Nat. Protoc.* **4**, 565–581 (2009).
95. R. Sommerstein, L. Flatz, M. M. Remy, P. Malinge, G. Magistrelli, N. Fischer, M. Sahin, A. Bergthaler, S. Igonet, J. ter Meulen, D. Rigo, P. Meda, N. Rabah, B. Coutard, T. A. Bowden, P.-H. Lambert, C.-A. Siegrist, D. D. Pinschewer, Arenavirus glycan shield promotes neutralizing antibody evasion and protracted infection. *PLOS Pathog.* **11**, e1005276 (2015).
96. O. Schweier, U. Aichele, A.-F. Marx, T. Straub, J. S. Verbeek, D. D. Pinschewer, H. Pircher, Residual LCMV antigen in transiently CD4$^+$ T cell-depleted mice induces high levels of virus-specific antibodies but only limited B-cell memory. *Eur. J. Immunol.* **49**, 626–637 (2019).
97. M. E. Ritchie, B. Phipson, D. Wu, Y. Hu, C. W. Law, W. Shi, G. K. Smyth, *limma* powers differential expression analyses for RNA-sequencing and microarray studies. *Nucleic Acids Res.* **43**, e47 (2015).
98. A. Liberzon, A. Subramanian, R. Pinchback, H. Thorvaldsdottir, P. Tamayo, J. P. Mesirov, Molecular signatures database (MSigDB) 3.0. *Bioinformatics* **27**, 1739–1740 (2011).
99. A. Subramanian, P. Tamayo, V. K. Mootha, S. Mukherjee, B. L. Ebert, M. A. Gillette, A. Paulovich, S. L. Pomeroy, T. R. Golub, E. S. Lander, J. P. Mesirov, Gene set enrichment analysis: A knowledge-based approach for interpreting genome-wide expression profiles. *Proc. Natl. Acad. Sci. U.S.A.* **102**, 15545–15550 (2005).
100. S. Aibar, C. B. González-Blas, T. Moerman, V. A. Huynh-Thu, H. Imrichova, G. Hulselmans, F. Rambow, J.-C. Marine, P. Geurts, J. Aerts, J. van den Oord, Z. K. Atak, J. Wouters, S. Aerts, SCENIC: Single-cell regulatory network inference and clustering. *Nat. Methods* **14**, 1083–1086 (2017).
101. M. R. Corces, A. E. Trevino, E. G. Hamilton, P. G. Greenside, N. A. Sinnott-Armstrong, S. Vesuna, A. T. Satpathy, A. J. Rubin, K. S. Montine, B. Wu, A. Kathiria, S. W. Cho, M. R. Mumbach, A. C. Carter, M. Kasowski, L. A. Orloff, V. I. Risca, A. Kundaje, P. A. Khavari, T. J. Montine, W. J. Greenleaf, H. Y. Chang, An improved ATAC-seq protocol reduces background and enables interrogation of frozen tissues. *Nat. Methods* **14**, 959–962 (2017).
102. S. K. Denny, D. Yang, C.-H. Chuang, J. J. Brady, J. S. Lim, B. M. Grüner, S.-H. Chiou, A. N. Schep, J. Baral, C. Hamard, M. Antoine, M. Wislez, C. S. Kong, A. J. Connolly, K.-S. Park, J. Sage, W. J. Greenleaf, M. M. Winslow, Nfib promotes metastasis through a widespread increase in chromatin accessibility. *Cell* **166**, 328–342 (2016).
103. A. Dobin, C. A. Davis, F. Schlesinger, J. Drenkow, C. Zaleski, S. Jha, P. Batut, M. Chaisson, T. R. Gingeras, STAR: Ultrafast universal RNA-seq aligner. *Bioinformatics* **29**, 15–21 (2013).
104. Y. Liao, G. K. Smyth, W. Shi, The R package *Rsubread* is easier, faster, cheaper and better for alignment and quantification of RNA sequencing reads. *Nucleic Acids Res.* **47**, e47 (2019).
105. P. M. Gubser, G. R. Bantug, L. Razik, M. Fischer, S. Dimeloe, G. Hoenger, B. Durovic, A. Jauch, C. Hess, Rapid effector function of memory CD8$^+$ T cells requires an immediate-early glycolytic switch. *Nat. Immunol.* **14**, 1064–1072 (2013).

Acknowledgments: We thank D. Pinschewer for many helpful discussions, sharing reagents, and technical advice; M. Linterman for critical reading of the manuscript; G. Bantug and D. Labes for expertise and discussion; C. Beisel for technical advice; R. Tussiwand and her lab for feedback and support; T. Rezzonico and F. Grassi for technical support, the flow sorting facility, and all the animal caretakers at the DBM University of Basel. scRNA-seq was performed at the Genomics Facility Basel, ETH Zurich. Calculations were performed at sciCORE (http://scicore.unibas.ch/) scientific computing center at the University of Basel.
Funding: Supported by research grants to C.G.K. (SNF PP00P3_157520, Gottfried and Julia Bangerter-Rhyner Stiftung, Olga Mayenfisch Stiftung, and Swiss Life Jubiläumsstiftung).
Author contributions: M.K., D.S., and C.G.K. conceptualized the project. M.K., D.S., and C.G.K. designed the experiments. M.K., T.C.P., C.G.K., J.L., N.S., and L.C.L. performed experiments. Y.I.E. (recombinant NP) and R.P.J. (NICD protector) produced reagents. M.K., D.S., C.G.K., J.R., and F.G. analyzed the data. C.G.K., D.S., and M.K. wrote the manuscript. M.K., D.S., and C.G.K. visualized the data. C.G.K. acquired funding. J.J.T., C.H., and T.M. provided resources. C.G.K. supervised the study. **Competing interests:** The authors declare that they have no competing interests. **Data and materials availability:** The scRNA-seq, bulk RNA-seq, and ATAC-seq data have been deposited in the National Center for Biotechnology Information Gene Expression Omnibus database (accession number: SuperSeries GSE139198). NIP-transgenic mice were generated in the lab of S. Crotty. Requests for this strain should be addressed to S. Crotty (shane@lji.org).

Submitted 30 August 2019
Accepted 16 January 2020
Published 6 March 2020
10.1126/sciimmunol.aay5552

Citation: M. Künzli, D. Schreiner, T. C. Pereboom, N. Swarnalekha, L. C. Litzler, J. Lötscher, Y. I. Ertuna, J. Roux, F. Geier, R. P. Jakob, T. Maier, C. Hess, J. J. Taylor, C. G. King, Long-lived T follicular helper cells retain plasticity and help sustain humoral immunity. *Sci. Immunol.* **5**, eaay5552 (2020).

Science Immunology
AAAS

immunology.sciencemag.org/cgi/content/full/5/45/eaay5552/DC1

Supplementary Materials for

Long-lived T follicular helper cells retain plasticity and help sustain humoral immunity

Marco Künzli, David Schreiner, Tamara C. Pereboom, Nivedya Swarnalekha, Ludivine C. Litzler, Jonas Lötscher, Yusuf I. Ertuna, Julien Roux, Florian Geier, Roman P. Jakob, Timm Maier, Christoph Hess, Justin J. Taylor, Carolyn G. King*

*Corresponding author. Email: carolyn.king@unibas.ch

Published 6 March 2020, *Sci. Immunol.* **5**, eaay5552 (2020)
DOI: 10.1126/sciimmunol.aay5552

The PDF file includes:

Other Supplementary Material for this manuscript includes the following:

(available at immunology.sciencemag.org/cgi/content/full/5/45/eaay5552/DC1)

Methods

Infection

Mice were infected by intraperitoneal (i.p.) injection with $2x10^5$ focus forming units (FFU) of LCMV Armstrong or intravenously (i.v.) with $1x10^7$ colony forming units (CFU) ActA deficient *Listeria monocytogenes* (Lm.ActA). In adoptive transfer studies, recipient mice were infected with LCMV Armstrong by i.p. injection with $2x10^5$ on the day following cell transfer. LCMV was grown on BHK-21 cells and titrated on 3T3-cells as described previously (*93*).

In vivo treatments

Anti-ICOSL (HK5.3, Bioxcell, #BE0028) treatment was performed by i.p. injection. Each mouse received 4 injections of 100µg every 72 hours. 2-Deoxy-D-glucose (Sigma, #D8375) was supplied in the drinking water for 14 days at a concentration of 6mg/ml. Rapamycin or vehicle control (1% DMSO in PBS) was given daily by i.p. injection of 75µg/kg body weight for 14 days. For BrdU labelling experiment, BrdU was provided in the drinking water at 0.8mg/ml for 12 days.

Mixed bone marrow chimeras and adoptive transfers

Wild-type (WT) host CD45.1 mice were lethally irradiated with 2 fractionated doses of 500 cGγ and reconstituted with a 1:1 mixture of bone marrow cells from CD45.1 WT and $P2X7R^{-/-}$ CD45.2 donor mice. The reconstitution ability of T- and B cells was assessed at least 6 weeks after reconstitution and before LCMV infection. Adoptive transfer experiments with $CD4^+$ SMARTA and NIP cells were performed as previously described (*94*).

Quantitative PCR

RNA from sorted cells was isolated with RNAqueous™-Micro Total RNA Isolation Kit (Invitrogen™) and was reverse transcribed to cDNA using either qScript XLT cDNA SuperMix (Quantabio) or iScript™cDNA Synthesis Kit (Bio-Rad). Samples were run on an Applied Biosystems Viia7 Real-time PCR system. Primers used for the indicated genes are listed in the supplementary table.

Isolation of lymphocytes

Single-cell suspensions of cells were prepared from lymph nodes, spleens, blood, liver, and bone marrow. Lymph nodes (inguinal, brachial and axillary) were mashed and filtered through a 100µm strainer. Spleens were either mashed and filtered through a 100µm strainer (for T cell analysis) or digested at 37°C for 1 hour using Collagenase D and DNase I (for B cell analysis). To isolate bone marrow, femur and tibia bones were flushed with a 25G needle followed by filtration through a 100µm strainer. Livers were perfused with PBS and mashed through a 100µm strainer, followed by gradient centrifugation in Percoll. Lymphocytes from the blood were isolated by gradient centrifugation in Ficoll (LSM MP Biomedicals). Erythrocytes were lysed using Ammonium-Chloride-Potassium (ACK) lysis buffer.

Flow cytometry and cell sorting

Isolation of LCMV-specific $CD4^+$ T cells was performed by staining single-cell suspensions for 1 hour at room temperature with IAb:NP309-328 PE or IAb:GP66-77 APC (provided by NIH tetramer core), followed by enrichment and counting (*94*). Anti-CXCR5 BV421 was added at the time of tetramer staining; for p-S6 detection, cells were stained with tetramer for 20 minutes on ice in the presence of 50nM

Dasatinib. For transfer of effector or memory cells, tetramer staining was performed with 50nM Dasatinib for 1 hour at room temperature. LCMV-specific B cells were detected as previously described, using a tetramer for NPΔ340 and a Decoy reagent to discriminate PE-specific B cells (*70*). All other surface staining was performed for 30min on ice in presence of a viability dye. Transcription factor staining was performed by fixation and permeabilization using the eBioscience Foxp3/Transcription Factor staining set. To assess phospho-protein levels, cells were fixed with BD Phosflow Lyse/Fix Buffer for 10 min at 37°C and permeabilized using BD Phosflow Perm/Wash Buffer for 30 min at room temperature. To stain for BrdU incorporation, the FITC BrdU Flow kit (BD) was used. 2-NBDG staining (Thermo Fisher) was performed for 10 min at 37°C in 100μM 2-NBDG. To identify early apoptotic cells, Annexin V staining (PE, BioLegend, #640907) was performed at room temperature for 15min in Annexin V Binding Buffer (BioLegend, #422201). Fortessa LSR II and Sorp Aria cytometers (BD Biosciences) were used for flow cytometry and cell sorting respectively. Data were analyzed with FlowJo X software (TreeStar).

The following antibodies were used for staining: CD4 (BUV496, GK1.5, BD, #564667), CD8a (biotin, 53-6.7, BioLegend, #100704), CD11b (PE-Cy5, M1/70, BioLegend, #101222), CD11c (PE-Cy5, N418, BioLegend, #117316), CD27 (BV510, LG.3A10, BioLegend, #124229), CD38 (BV421, 90, BD, #562768), CD44 (BUV395, IM7, BD, #740215; APC-Cy7, IM7, BioLegend, #103028; PE, IM7, BD, #553134), CD45.1 (PE, A20, BioLegend, #110707; FITC, A20, BD, #553775), CD45.2 (FITC, 104, BD, #553772; APC-eFluor780, 104, eBioscience, #47-0454-82; APC-Fire, 104, BioLegend, #109852), CD62L (APC, MEL-14, BD, #553152; BV711, MEL-14, BioLegend, #104445), CD69 (FITC, H1.2F3, BD, #553236; PE, H1.2F3,

eBioscience, #12-0691-83; APC-Cy7, H1.2F3, BioLegend, #104526; BV785, H1.2F3, BioLegend, #104543), CD73 (APC Fire, TY/11.8, BioLegend, #127221), CD80 (PE-Cy7, 16-10A1, BioLegend, #104734), CD138(BV421, 281-2, BioLegend, #142507; BV711, 281-2, BioLegend, #142519), FAS (PE, 15A7, eBioscience, #12-0951-83; FITC, 15A7, BD, #554257), PSGL-1 (BV605, 2PH1, BD, #740384, BUV395, 2PH1, BD, #740273), CXCR4 (BV711, L276F12, BioLegend, #146517), CCR7 (PE, 4B12, BioLegend, #120106; PE-Cy7, 4B12, BioLegend, #120123), ICOSL (PE, HK5.3, eBioscience, #12-5985-81), ICOS (PE, 7E.17G9, BioLegend, #117406), PD1 (BV785, 29F.1A12, BioLegend, #135225), IgD (BV510, 11-26c.2a, BioLegend, #405723), IgM (BV786, R6-60.2, BD, #564028), Vα2 TCR (FITC, B20.1, eBioscience, #11-5812-82, PE, B20.1, eBioscience, #12-5812-82), Vβ8.3 (FITC, 1B3.3, BD, #553663; PE, 1B3.3, BD, #553664), B220 (PE-Cy5, RA3-6B2, BioLegend, #103210; BV650, RA3-6B2, BioLegend, #103241; PE-Cy7, RA3-6B2, BioLegend, #103222; biotin, RA3-6B2, BD, #553085), CXCR5 (BV421, L138D7, BioLegend, #145512), F4/80 (PE-Cy5, BM8, BioLegend, #123112), FR4 (PE-Cy7, 12A5, BioLegend, #125012, APC-Fire, 12A5, BioLegend, #125013), CD127 (BV711, A7R34, BioLegend, #135035), GL7 (Alexa Fluor 647, GL7, BioLegend, #144606; Alexa Fluor 48, GL7, BioLegend, #144612), GR-1 (PE-Cy5, RB6-8C5, BioLegend, #108410), Ly6C (BV711, HK1.4, BioLegend, #128037; BV510, HK1.4, BioLegend, #128033; FITC, AL-21, BD, #553104), I-Ab (biotin, AF6-120.1, BioLegend, #116404), NK1.1 (biotin, PK136, BioLegend, #553163), P2X7R (PE, 1F11, BioLegend, #148704; PE-Cy7, 1F11, BioLegend, #148707), Bcl6 (PE-Cy7, K112-91, BD, #563582; PE, K112-91, BD, #561522; AF488, K112-91, BD, #561524), FoxP3 (Alexa Fluor 488, 150D, BioLegend, #320012; PE-Cy7, FJK-16s, eBioscience, #25-5773-82), HIF-1a (PE, 241812, R&D Systems, #IC1935P; Alexa

Fluor 700, 241812, R&D Systems, #IC1935N), phospho-AKT S473 (Alexa Fluor 647, D9E, Cell Signaling Technology, #4075S), phospho-S6 S240/244 (Rabbit mAb, , Cell Signaling Technology, #5364S), Goat anti-Rabbit IgG (Alexa Fluor 488, Life technologies, #A11034), TCF1 (PE, S33-966. BD, #564217), Zombie Fixable Viability Dye (Zombie Red, BioLegend, #423110; Zombie Green, BioLegend, #423112).

Enzyme-linked immunosorbent assay

LCMV-specific NP serum antibody titers were determined as previously described (*95*). Briefly, 96-well plates were coated with 100ul of recombinant NP at 3µg/ml in sodium carbonate buffer adjusted to pH 9.6. Plates were blocked with 5% milk in PBS-Tween 0.05% before adding the prediluted sera to the plate (3-fold dilutions starting with 1:100 dilution of serum). ABTS color reaction was used to detect HRP-coupled goat anti-mouse IgG antibody (Jackson, 115-035-062). Optical density was measured with a Synergy H1 reader (BioTek).

Detection of LCMV NP-specific IgG antibody secreting cells by ELISpot

LCMV NP-specific antibody secreting cells (ASC) were detected as previously described (*96*). Briefly, 96-well plates were coated with 100ul of recombinant NP at 3µg/ml in PBS. Plates were blocked with cell culture medium before adding 100µl pre-diluted single-cell suspension from the bone marrow or the spleen (starting at $2*10^6$ cells/ml and $1*10^7$ cells/ml respectively). Cells were incubated for 5h at 37°C before HRP-coupled goat Fcy-specific anti-mouse IgG antibody was added (Jackson, 115-035-008). AEC solution (BD Bioscience) was used to detect ASC. Spots were quantified using an ELISpot reader from AID.

Immunofluorescent microscopy

Spleens were isolated on day 0, 15 or 54 after LCMV infection and frozen in OCT matrix (Tissue-Tek). 7µm sections were fixed in ice cold methanol. Sections were subsequently stained with 5µg/ml mAb anti- CD4 AF647 (BioLegend, #100426), and anti-GL7 AF488 (BioLegend, #144612) and 0.5µg/ml anti-B220 BV421 (Biolegend, #103240). Images were acquired on a Nikon Ti2 microscope equipped with a photometrics 95B camera, using a 20X objective.

scRNA-seq

Sample preparation: 3-10 x 10^3 LCMV-specific $CD4^+$ memory cells ($CD4^+dump^-CD44^+GP66^+$) from either T-bet ZsGreen (1x sample) or wild-type mice (2x biological replicates) day 35 and day 37 post infection were provided for library preparation using the 10x Chromium platform. Each sample represented cells from 1-3 mice. Single-cell capture and cDNA and library preparation were performed with a Single Cell 3' v2 Reagent Kit (10× Genomics) according to manufacturer's instructions. Sequencing was performed on one flow-cell of an Illumina NexSeq 500 at the Genomics Facility Basel of the ETH Zurich. Paired-end reads were obtained and their quality was assessed with the FastQC tool (version 0.11.5). The length of the first read was 26 nt, composed of individual cells barcodes of 16 nt, and unique molecular identifiers (UMIs) of 10 nt. The length of the second read, composed of the transcript sequence, was 58 nt. The samples in the different wells were identified using sample barcodes of 8 nt.

Sample analysis: Sequencing data was processed using 10X Genomics' cellranger software version 2.1.0, modified to report only one alignment (randomly)

for multi-mapped reads (keep only those mapping up to 10 genomic locations). Raw molecule info from cellranger was initially filtered leniently, discarding cells with fewer than 100 genes. The resulting UMI matrix was further filtered to keep only cells with log library size > 2.8, log number of features > 2.6, % mitochondrial reads <= 6, % ribosomal protein reads >= 20. Genes with average counts < .005 were removed. Normalization was done using the R package scran's deconvolution method, where cells are pre-clustered, normalized within each cluster, and normalized between each cluster. Technical noise within gene expression was modeled using scran, and biologically relevant highly variable genes were calculated after separating the technical from biological variance, using FDR < 0.05 and biological variance > 0.1. A PCA was run on the normalized data using the top 500 most variable genes by biological variance, and the PCA was denoised to account for the modelled technical variation. Cells were clustered hierarchically using Ward's method on the distance matrix of the PCA. Default dendrogram cut height using the R package dynamicTreeCut resulted in 3 clusters, which also mapped to the highest average silhouette width. The cut height for a finer clustering (7) was chosen based on the next highest local maximum in a plot of average silhouette width. *t*-distributed stochastic neighbor embedding (tSNE) was executed with a perplexity of 30. GSEA between clusters was performed using camera from the limma R package on standard gene set categories (MSigDB) as well as sets curated from relevant publications (*97*–*99*). Subsequent visualization and analysis such as dropout imputation were performed using version 2.3.4 of the Seurat R package. Single-cell regulatory network inference and clustering (SCENIC) was performed using version 0.9.7 and the published workflow on the pySCENIC github repository (*100*). Pseudotime analysis was performed with Monocle2 version 2.10.1. Normalized data

as above were further filtered to exclude genes found in less than 5% of cells. Dimension reduction was performed using DDRTree and differentially expressed genes calculated with the differentialGeneTest function based on the hierarchical clustering above. The root state of the trajectory was chosen where Tcf7 expression was highest.

In silico pseudo-bulk data was generated from three biological replicates (one without and two with NICD-protector). Biological replicate, percent mitochondrial reads and percent ribosomal reads each explained < 0.1 % of variance in the data. Counts for each gene were summed by cluster, and data re-normalized using Trimmed Mean of M-Values (TMM). Differential expression analysis was performed between the most extreme T_{fh} and T_H1 clusters using edgeR and limma. Ingenuity Pathway Analysis was performed on the resulting list of differentially expressed genes (adj P-value < 0.05).

ATAC-seq

Sample preparation: 6.5-7.5 x 10^3 LCMV-specific T_{fh} cells ($Ly6C^{lo}PSGL1^{lo}$), T_H1 cells ($Ly6C^{hi}PSGL1^{hi}$) were sorted in duplicates from different mice to obtain biologically independent samples 32 days post infection. Naïve $CD4^+$ cells ($CD44^{lo}$ $CD62L^{hi}$) were sorted in duplicates and represent technical replicates. Library preparation for sequencing was performed as described previously with an additional clean up step to reduce reads mapping to mitochondrial DNA (*101*). Briefly, sort-purified cells were lysed and tagmented for 30 min at 37°C. DNA was purified using Zymo DNA Clean and Concentrator Kit and amplified for five cycles. Real-time PCR was used to determine the number of additional PCR cycles. DNA was cleaned up using AMpure XP beads at a 1.2 x ratio twice. Sequencing was performed on an Illumina NexSeq 50 machine using 41-bp paired-end run.

Alignment and basic QC: Reads were aligned to the mouse genome (UCSC version mm10) with bowtie2 (version 2.3.2) using options "--maxins 2000 --no-mixed--no-discordant --local --mm". The output was sorted and indexed with samtools (version 1.7) and duplicated reads were marked with picard (version 2.9.2). The read and alignment quality was evaluated using the qQCReport function of the Bioconductor package QuasR (R version 3.5.2; Bioconductor version 3.8).

Single sample peak calling: For each group of biological replicates, regions of accessible chromation where called with macs2 (version 2.1.1.20160309) using the option '-f BAM -g 2652783500 --nomodel --shift -100 --extsize 200 --broad --keep-dup all --qvalue 0.05'. Since the majority of duplicated reads came from mitochondria, the resulting peak lists were cleaned from peaks called in mitochondria and additionally ENCODE blacklist regions. All peaks also required a log-fold change > 1 and FDR < 0.05. The resulting peak lists, one per population, were merge using the function reduce from the GenomicRanges package, requiring at least 250 bases gap for separate peak calls and a minimum peak width of 100 bases. This merged peak list resulted in 118999 peaks (5.1% genome) across all five populations. The Bioconductor package bamsignals was used to generate a counts matrix for the merged peak list.

Across sample normalization and peak calling: T_{fh} and T_H1 samples differed strongly from naïve samples in the enrichment of reads within accessible chromatin as compared to genomic background (Supplementary Methods Figure A). One possible source of this bias is a differential tagmentation efficiency between samples or cell types as previously observed (*102*). This bias also leads to an artificial regulation when comparing ATAC signals of open versus closed promoters

(Supplementary Methods Figure B). Here we do not expect a difference in the dynamic range between both states across samples/cell types. In order to compare log-fold changes across samples we therefore applied quantile normalization to log-CPM levels of the TMM-scaled peak counts. The resulting peak intensities were converted to a Bioconductor ExpressionSet object and all further differential accessibility analysis was performed with this object. Specifically, the limma package was used for differential accessibility between all pairs of populations using functions lmFit and eBayes

Differential motif analysis using HOMER: Fasta sequences of T_H1 and T_{fh} peaks were extracted using functions from the BSgenome, Biostrings and rtracklayer R/Bioconductor packages. These sequences were stratified according to population specific peaks (=open in only one population) and common peaks (= open in both) based on thresholding the differential accessibility results by logFC > 2 and FDR < 0.05. Homer (version 4.9) was used to predict known TF motifs (motif database: vertebrates/known.motif) within these sequence sets by running the command 'homer2 known -strand both' with additional setting specifying the specific peaks as foreground and the common peaks as background sequence sets. Differential motif occurrence
results were visualized using R.

Ingenuity pathway analysis: Ingenuity pathway analysis (Qiagen, version 01-14) was performed on differentially accessible peak regions (log_2 FC > 0.5 and FDR of 0.05) in T_H1 memory vs long-lived T_{fh} cells with default settings.

Bulk RNA-seq

Sample preparation: 0.5-4.0 x 10^3 GP66-specific T_{fh} cells ($Ly6C^{lo}PSGL1^{lo}$) were sorted in quadruplicates from individual mice to obtain biologically independent samples from control and αICOSL treated mice. Total RNA was isolated with the PicoPure^{TM} RNA Isolation kit (ThermoFisher, # KIT0202). cDNA and library preparation were performed with a SMART-Seq v4 Ultra Low Input RNA Sequencing Kit (Takara Bio) according to manufacturer's instructions. Sequencing was performed on one flow-cell of an Illumina NexSeq 500 using 38-bp paired-end run.

Sample analysis: Single-end RNA-seq reads were mapped to the mouse genome assembly, version mm10 (analysis set, downloaded from UCSC https://genome.ucsc.edu), with STAR (version 2.7.0c, (*103*)), with default parameters except for reporting only one hit for multi-mappers in the final alignment files (outSAMmultNmax=1) and filtering reads without evidence in spliced junction table (outFilterType="BySJout").") (*103*). All subsequent gene expression data analyses were done within the R software (R Foundation for Statistical Computing, Vienna, Austria). Using Ensembl Genes mRNA coordinates from ensembl version 84 (https://www.ensembl.org) and the featureCounts function from Rsubread package, we quantified gene expression as the number of reads that started within any annotated exon of a gene (*104*). Only genes annotated as "protein_coding" were kept for further analysis. Genes that did not show an expression level of at least 0.5 CPM in each of the 8 samples were filtered out and TMM normalization performed. Differential expression analysis was performed with the Bioconductor limma package using the function voomWithQualityWeights and applying a cyclic-loess normalization. We found this methodology to perform best in dealing with the reduced transcriptome complexity in samples with the lowest number of cells used

as input. Although no gene was significantly differentially expressed at an FDR threshold of 5%, the top genes were consistent with protein expression experiments. Gene set enrichment analysis was performed using the cameraPR function from limma on standard gene set categories (MSigDB) as well as sets curated from relevant publications.

Extracellular metabolic flux analysis

A Seahorse XFe96 metabolic extracellular flux analyzer was used to determine the extracellular acidification rate (ECAR) in mpH/min and the oxygen consumption rate (OCR) in pmol/min. In brief, T-cells were sorted in $CD4^{+}CD44^{+}$ T_{fh} cells ($Ly6C^{lo}PSGL1^{lo}$) or T_H1 cells ($Ly6C^{hi}PSGL1^{hi}$) and seeded ($2x10^5$/well at memory time point or 2.5 $x10^5$/well at effector time point in respective experiments) in serum-free unbuffered RPMI 1640 medium (Sigma-Aldrich # R6504) onto Cell-Tak (#354240, Coring, NY, USA) coated cell plates. Mito Stress test was performed by sequential addition of oligomycin (1 µM; Sigma Aldrich 75351), carbonyl cyanide-4-(trifluoromethoxy)phenylhydrazone (FCCP; 2 µM; Sigma Aldrich C2920) and rotenone (1 µM; Sigma Aldrich R8875) at the indicated time points. Metabolic parameters were calculated as described previously (*105*).

Table for qPCR primers

Gene	Forward primer	Reverse primer
Igf1R	GCTTCGTTATCCACGACGATG	GAATGGCGGATCTTCACGTAG
Nav2	CAACCTCAGCACGGATGACATC	TTCCTCTCCACCTGTGAGTGCT
Slc43a1	TTCACATGGTCTGGCCTGG	TGTGGTCCAAGGCTAACCC
Tubb2a	CCTCCACCCCTTCTACAACCA	CCAAAACTTAGCGCCGATCT

Supplementary Figure 1.

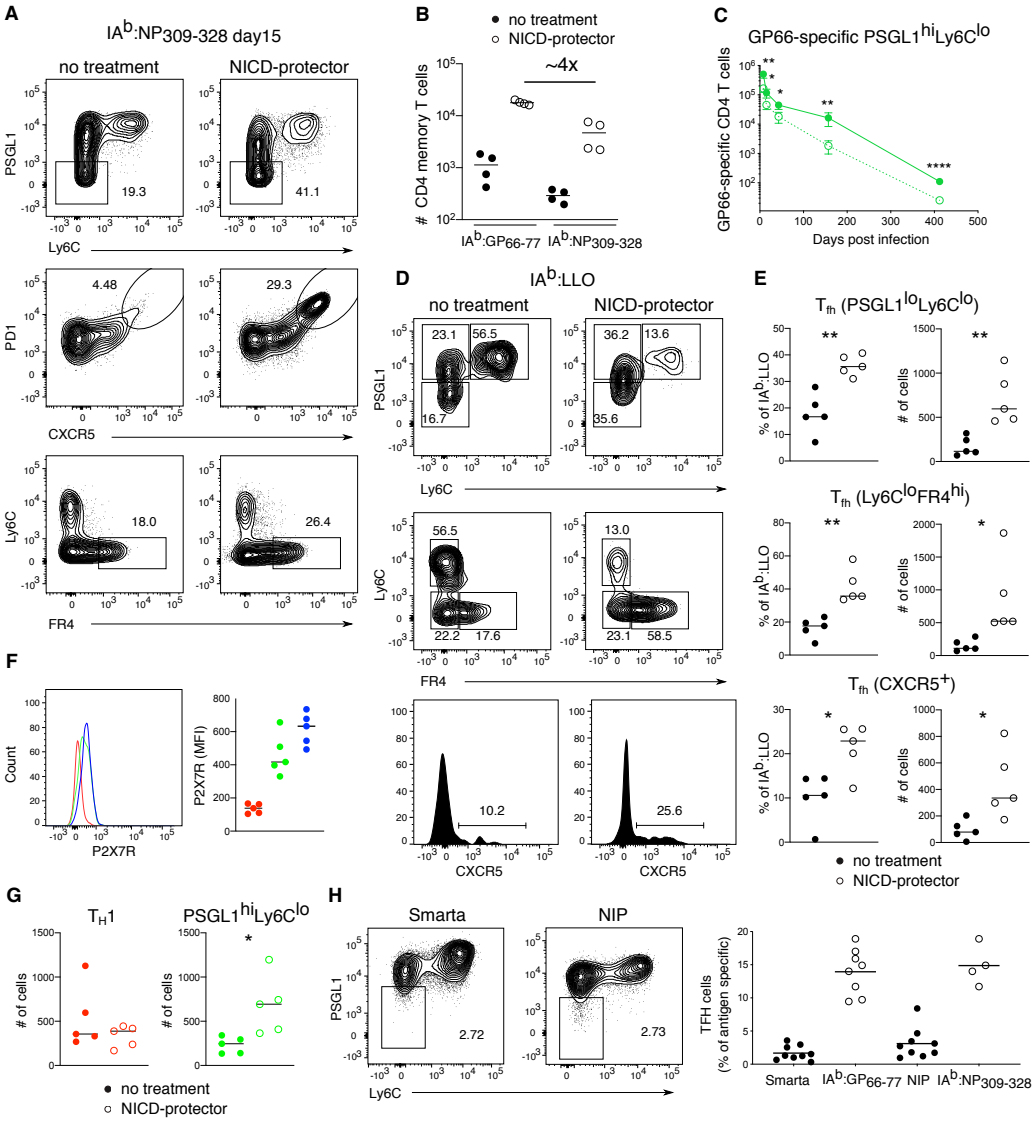

Fig. S1. T_{fh} cells are susceptible to death during isolation.

(**A**) Flow cytometry plots of NP-specific splenic CD4+ T cells isolated at day 15 post infection, with or without NICD-protector with different gating strategies to identify long-lived T_{fh} cells. (**B**) Comparison of epitope-specific CD4+ memory cell numbers in control and NICD-protector treated mice >30 days post infection. (**C**) GP66-

specific Ly6C^{lo}PSGL1^{hi} memory cell numbers (green, gated as in Figure 1**D**) over time with (solid line) or without (dashed line) NICD-protector. (**D** and **E**) Flow cytometry plots (**D**) and quantification (**E**) of splenic LLO-specific T_{fh} cells isolated >30 days post infection with or without NICD-protector after Listeria infection. (**F**) Histogram (left) and MFI (right) of P2X7R in LLO-specific T_H1 (red), Ly6C^{lo}PSGL1^{hi} (green) and long-lived T_{fh} (blue) cells >30 days post infection. (**G**) Quantification of LLO-specific CD4 memory subsets isolated >30 days post infection with or without NICD-protector after Listeria infection. Thin lines represent the mean ~~± s.d~~. (**H**) Flow cytometry plots (left) and proportions of long-lived T_{fh} cells (right) in SMARTA and NIP memory cells compared to polyclonal memory compartments >30 days post infection. Data represent *N* = 2 (**B**, **D**-**H**) independent experiments with *n* = 3-5 mice or summarize *N* = 5 independent experiments (**H**) with *n* = 4- 9 mice per group (dots represent cells from individual mice, and the line represents the mean). Unpaired two-tailed Student's t test was performed for each individual time point (**C**). **P* < 0.05, ***P* < 0.01, ~~****P* < 0.001,~~ **** *P* < 0.0001.

Supplementary Figure 2.

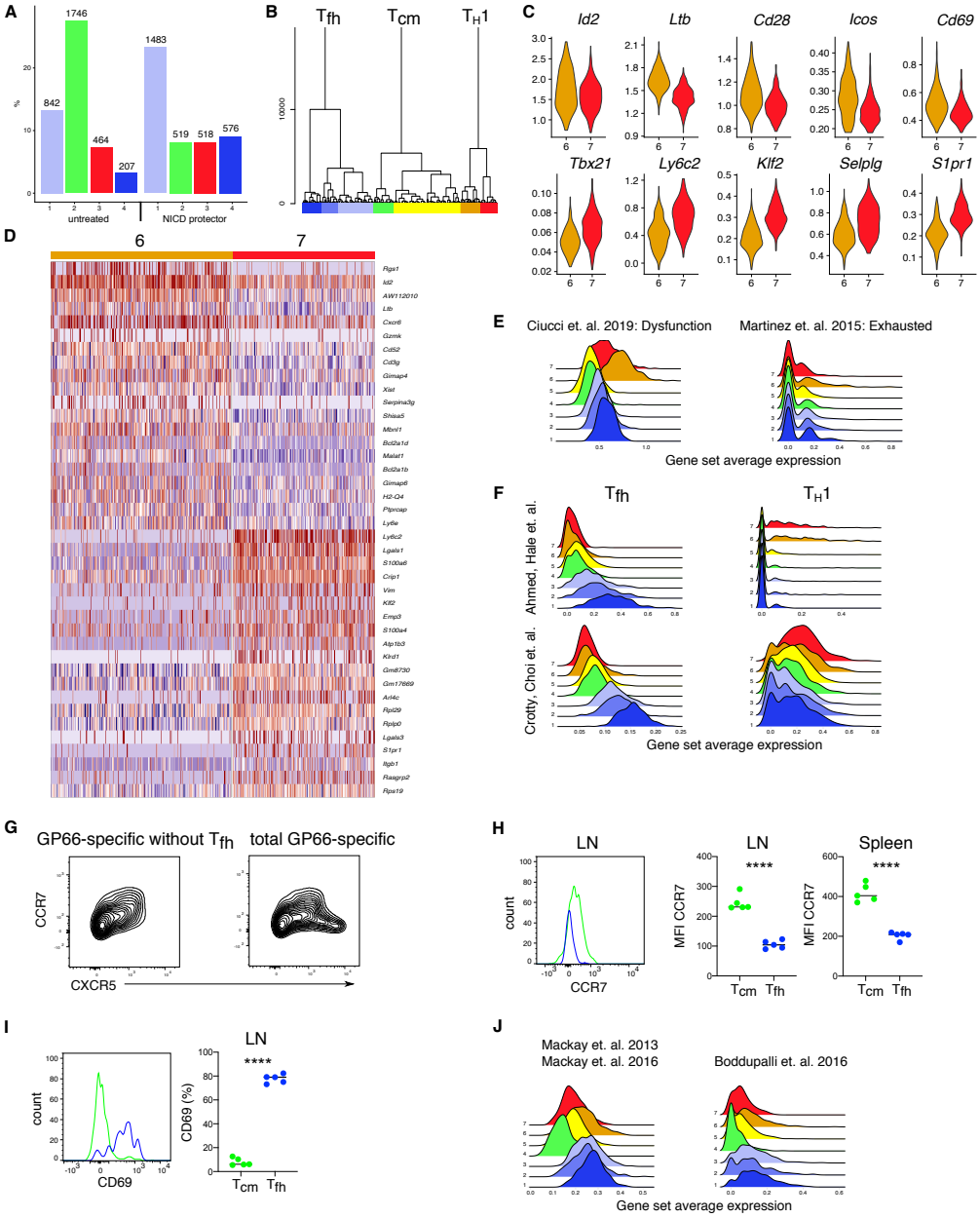

Fig. S2. FR4 discriminates long-lived T_{fh} from transcriptionally distinct T_{cm}.

(**A**) Clustering analysis of combined scRNA-seq datasets. T_{fh}-like clusters in blue (1, 4), T_{cm}-like in green (2) and T_H1-like in red (3). (**B**) Dendrogram showing hierarchical

clustering. Single cells colored by cluster on x axis with tree height on y axis. (**C**) Imputed expression of selected genes differing between two T_H1-like clusters. (**D**) Heatmap showing top 20 genes segregating T_H1-like clusters. (**E**) Log-normalized average expression of dysfunction (left) and exhaustion (right) genes. (**F**) Log-normalized average expression of published gene sets defining subsets. (**G**) Flow cytometry analysis of total GP66-specific CD4 cells with (right) or without (left) T_{fh} ($Ly6C^{lo}PSGL1^{lo}$) >50 days post infection. (**H**-**I**) Representative histograms and quantification of CCR7 (**H**) and proportions of $CD69^+$ cells (**I**) in T_{cm} (green) and long-lived T_{fh} (blue) cells >100 days post infection in lymph nodes and spleen. (**J**) Log-normalized average expression of published T_{rm} signatures. Data represents one of *N* = 2 independent experiments with *n* = 4 (**G**) or 5 (**H, I**) mice. Unpaired two-tailed Student's t test was performed with **** $P < 0.0001$.

Supplementary Figure 3.

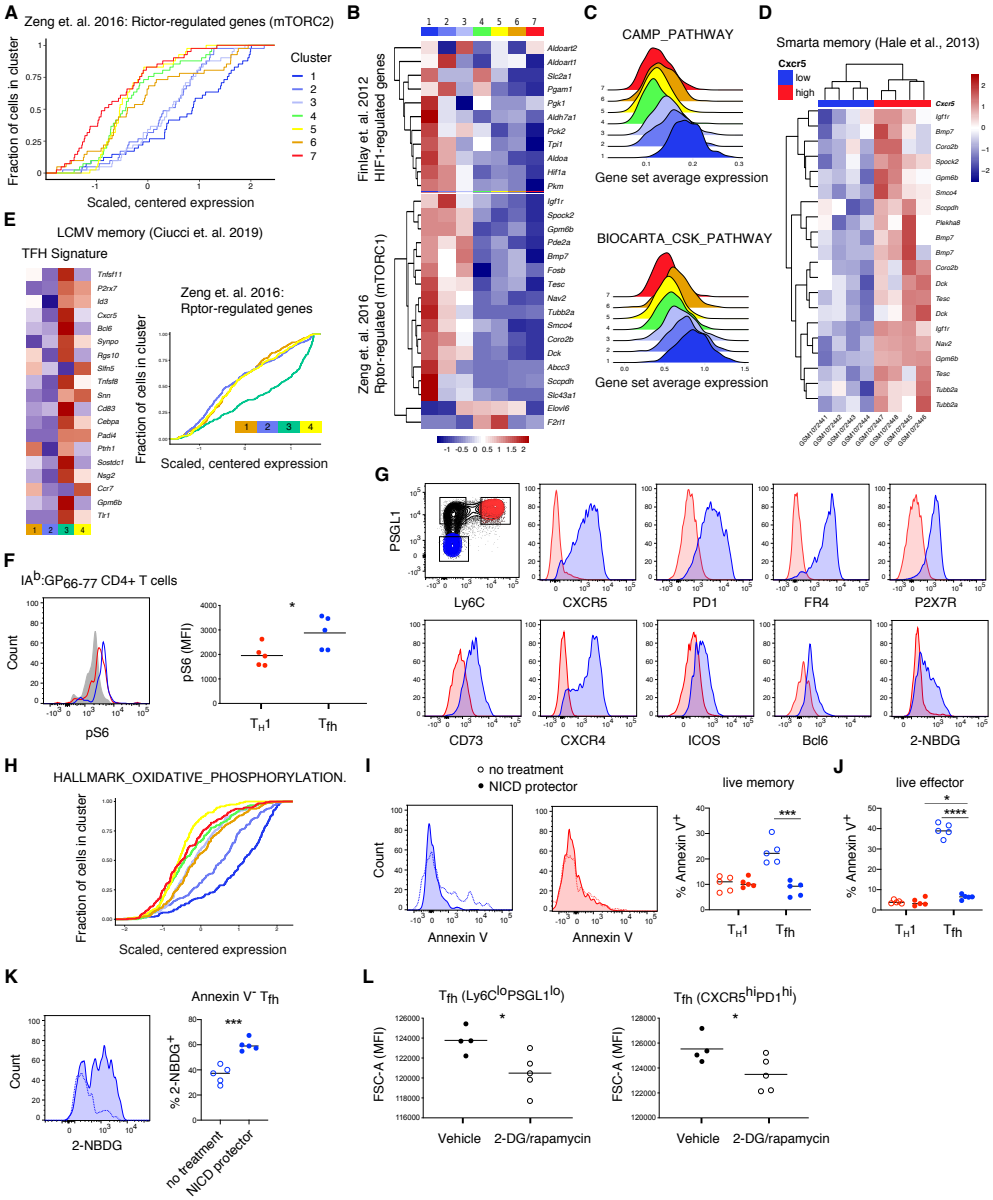

Fig. S3. Long-lived T_{fh} cells are constitutively glycolytic.

(**A**) Cumulative distribution of scaled, centered mRNA expression by cluster of Rictor-regulated genes (mTORC2) (**B**) Heatmap showing scaled, centered, per-

cluster expression of leading edge mTORC1-related genes and HIF1-regulated genes. (**C**) Log-normalized average expression of CAMP_PATHWAY and BIOCARTA_CSK_PATHWAY gene sets. (**D**) Secondary analysis of published data from Cxcr5$^-$ and Cxcr5$^+$ SMARTA CD4$^+$ memory cells showing leading edge Rptor-regulated genes from Zeng et. al (**E**) Analysis of published data from day 30 CD4$^+$ memory to LCMV: heatmap of expression of T_{fh} signature genes and cumulative distribution of Rptor-regulated genes. (**F**) Flow cytometry analysis of phospho-S6 Ser240/244 and MFI in GP66-specific memory T_H1 (red) and long-lived T_{fh} (blue) compared to naive CD4 T cells (grey). (**G**) Flow cytometry analysis of indicated markers in CD44$^+$ T_H1 memory and long-lived T_{fh} cells. (**H**) Cumulative distribution of gene set HALLMARK_OXIDATIVE_PHOSPHORYLATION.
(**I-J**) Representative histograms and quantification of Annexin V on CD44$^+$ memory (**I**) and CD44$^+$ effector cells (**J**). (**K**) Representative histograms and quantification of 2-NBDG uptake on CD44$^+$ Annexin V$^-$ long lived T_{fh} cells. (**L**) MFI of FSC-A in GP66-specific long-lived T_{fh} cells treated with vehicle or 2-DG/rapamycin. *N* = 2 independent experiments with *n* = 5 (**F**, **G**, **I-L**) mice per group. Line depicts the mean and dots cells from individual mice. Unpaired two-tailed Student's t test was performed with *$P < 0.05$, *** $P < 0.001$ and **** $P < 0.0001$.

Supplementary Figure 4.

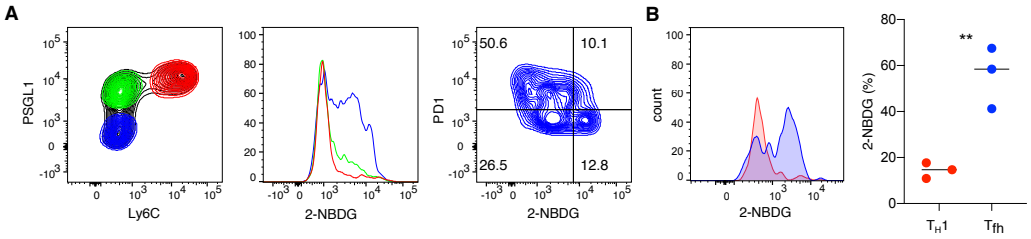

Fig. S4. Antigen is not required for the survival of long-lived T_{fh} cells.

(**A**) Representative flow cytometry plot of 2-NBDG uptake (middle) in ~~the different~~ LCMV GP66-specific CD4 T_H1 memory (red), T_{cm} (green), and long-lived T_{fh} (blue). 2-NBDG uptake versus PD-1 expression in the long-lived T_{fh} compartment (right). (**B**) Representative flow cytometry plot of 2-NBDG uptake (left) and proportion of 2-NBDG$^+$ GP66-specific T_H1 (red) or T_{fh} (blue) memory cells (right) 412 days post infection. The line represents the mean and each dot represents cells from individual mice. Data are representative of *N* = 1 independent experiments with *n* = 3 (**B**) or *N* = 2 with 5 mice (**A**). Unpaired two-tailed Student's t test was performed with $^{**}P < 0.01$.

Supplementary Figure 5.

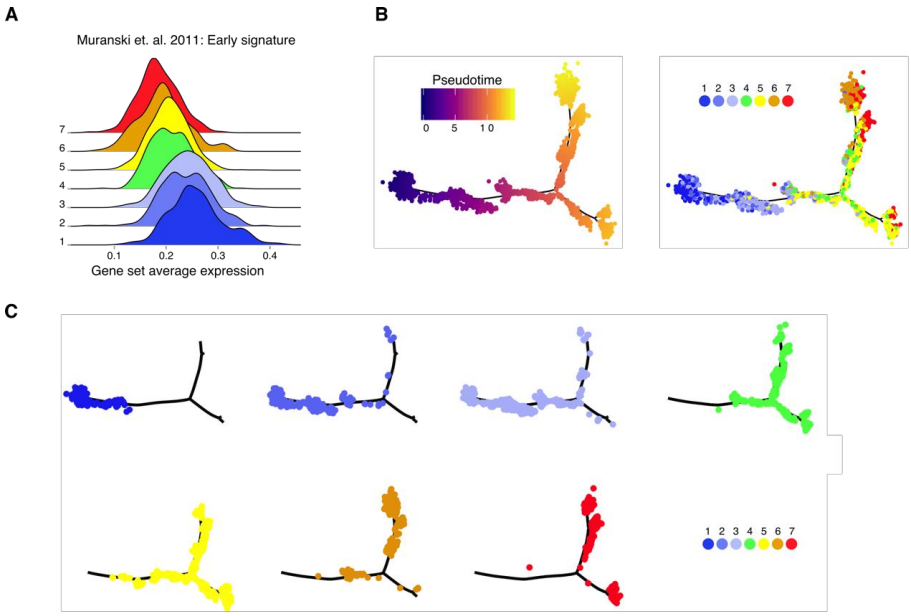

Fig. S5. T_{fh} cells generate multiple cell fates upon recall.

(**A**) Normalized average scRNA-seq expression of early memory signature. (**B**) Monocle2 analysis showing trajectory in pseudotime (left) and with cluster assignment (right). (**C**) Monocle2 trajectory with clusters separated.

Supplementary Figure 6.

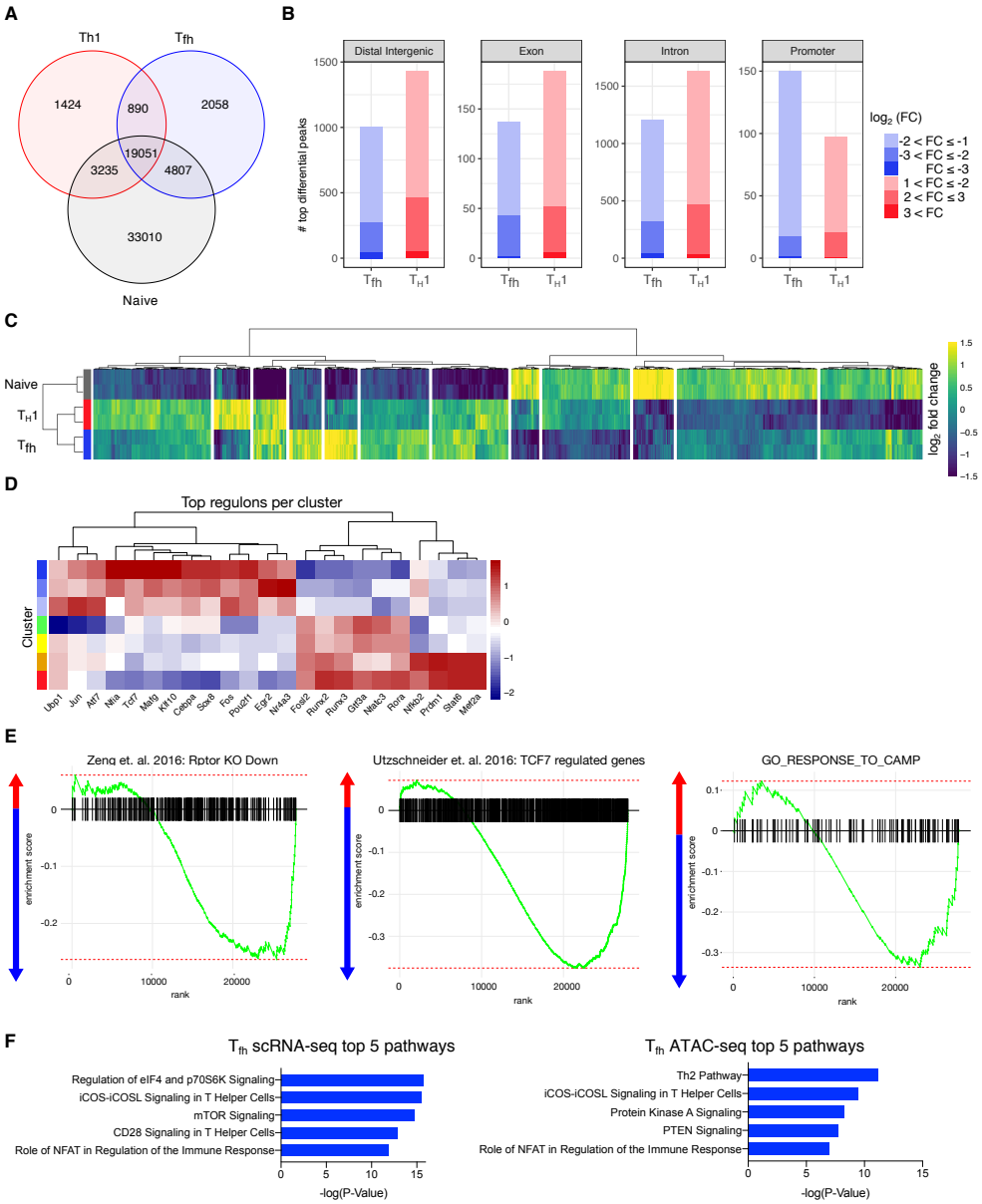

Fig. S6. Epigenetic regulation of long-lived T_{fh} cells.

(**A**) Venn diagram of all called peaks in Assay for Transposase-Accessible Chromatin using sequencing (ATAC-seq) data depicting the overlap of peaks in the subsets. (**B**) Number of differentially accessible regions for each genomic feature.

(**C**) Heatmap of hierarchically clustered promoter regions with absolute value (log_2FC) > 1 in at least one comparison and FDR < 0.1. (**D**) Heatmap depicting top transcriptional network regulators (regulons) on scRNA-seq data found by pySCENIC (Single-Cell rEgulatory Network Inference and Clustering) algorithm. (**E**) GSEA analysis of Rptor (left) and Tcf7 (middle) and cAMP (right) regulated genes with negative enrichment score indicating enrichment in long-lived T_{fh} (blue) and positive score indicating enrichment in T_H1 memory (red). (**F**) Top 5 pathways enriched in long-lived T_{fh} cells determined by Ingenuity Pathway Analysis in combined scRNA-seq data (with and without NICD-protector) comparing T_{fh} cluster to T_H1 cluster from 3-cluster version (left) and ATAC-seq peaks mapped to nearest TSS within TAD (right).

Supplementary Figure 7.

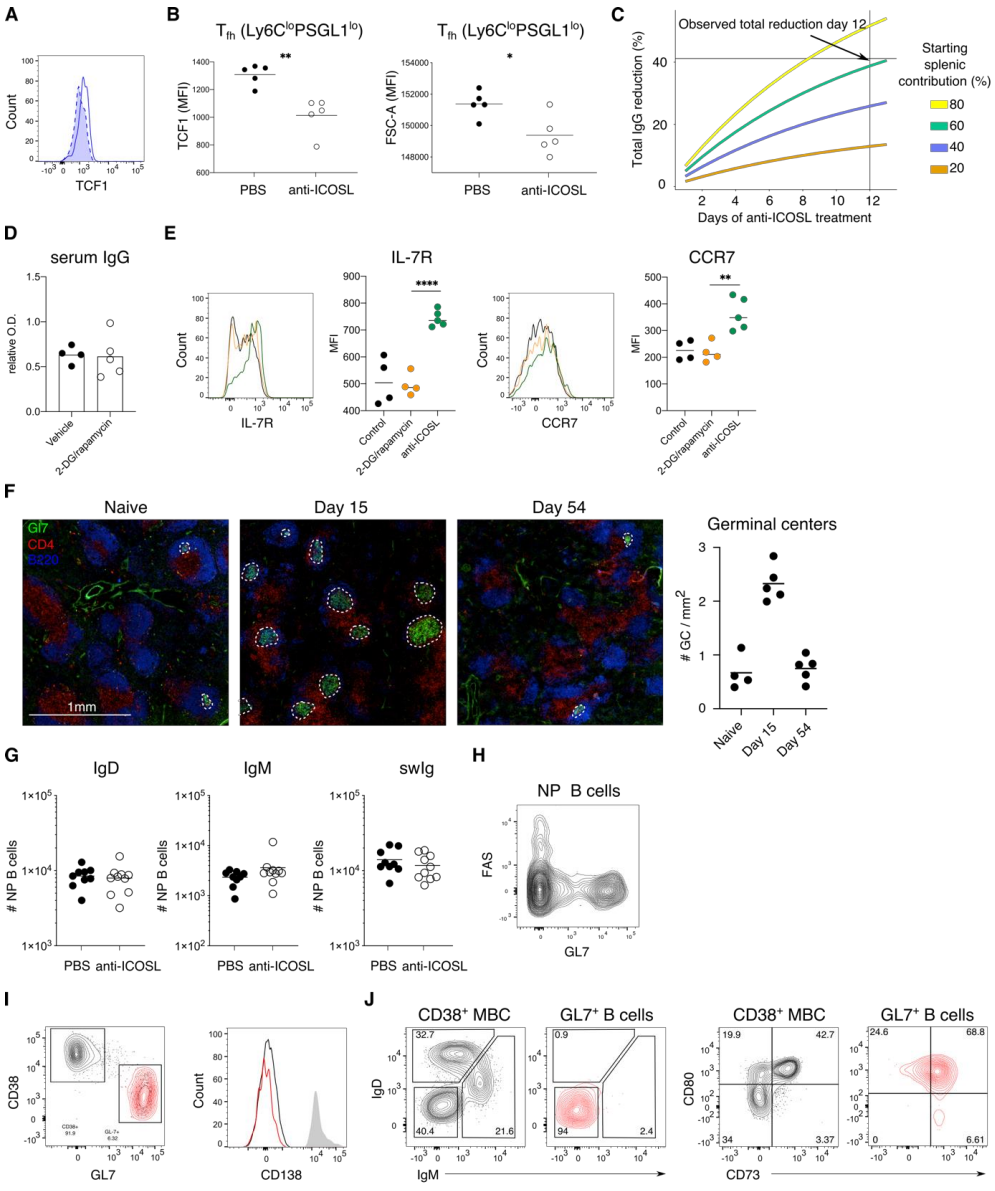

Fig. S7. ICOS signaling maintains T_{fh} cell identity at late time points.

(**A**) Flow cytometry analysis (left) and MFI of TCF1 expression in GP66-specific long-lived T_{fh} cells comparing PBS (solid line) and anti-ICOSL treated mice (dashed line

with filled histogram). (**B**) MFI of FSC-A in GP66-specific long-lived T_{fh} cells comparing PBS vs anti-ICOSL treated mice. The thin line represents the mean and each dot represents cells from an individual mouse. (**C**) Exponential decay model showing IgG reduction after 12 days of anti-ICOSL treatment at various starting splenic contributions and assuming 100% abrogation of splenic contribution. (**D**) NP-specific IgG serum titer at 1:8100 dilution comparing vehicle to 2-DG/rapamycin treated mice. (**E**) Representative histograms and quantification of IL-7R (left) and CCR7 (right) expression in gp66-specific long-lived T_{fh} comparing vehicle, 2-DG/rapamycin and anti-ICOSL treated mice. (**F**) Splenic sections stained for B220 (blue), CD4 (red) and GL7 (green) to identify (left) and quantify (right) germinal centers in naïve, day 15 or day 54 post infected mice. (**G**) Cell numbers of IgD, IgM or swIg NP-specific memory B cells comparing PBS and anti-ICOSL treated mice. (**H**) Flow cytometry analysis of NP-specific B cells. (**I**-**J**) Flow cytometry analysis of NP-specific $GL7^+$ B cells (red) in comparison to $CD38^+$ memory B cells (MBC, black). Data is representative of $N = 2$ independent experiments with $n = 4$-5 mice per group (**A**-**B, D-E, H-J**) or summarizes $N = 2$ independent experiments with $n = 9$-10 mice per group (**G**). (**F**) Dots represent individual nonconsecutive sections. The thin line represents the mean and each dot represents cells from an individual mouse. Unpaired two-tailed Student's t test was performed with $*P < 0.05$, $**P < 0.01$ and **** $P < 0.0001$.

Supplementary Methods Figure.

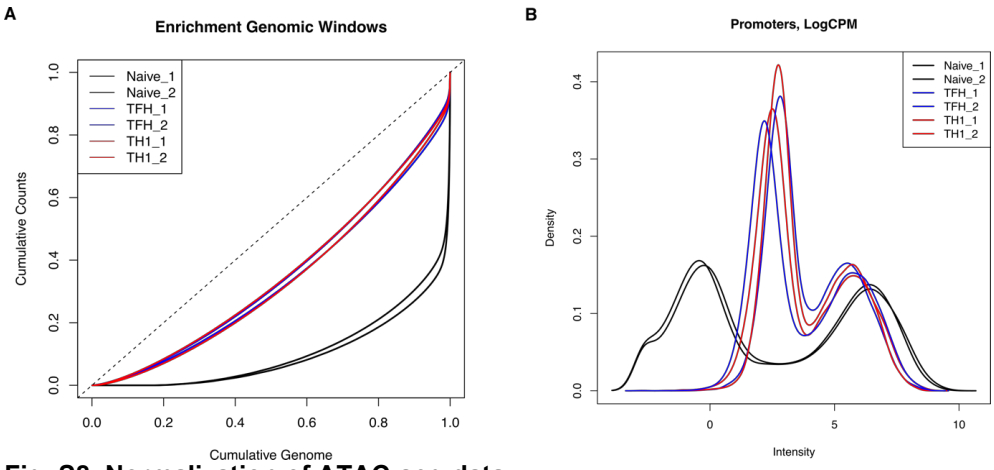

Fig. S8. Normalization of ATAC-seq data.

(**A**) Enrichment of genomic windows in the different ATAC-seq samples. (**B**) Density of logCPM values for the different ATAC-seq samples in promoter regions.

3.2. Project #2: The Impact of TCR signal strength on CD4 T cell differentiation in acute and chronic viral infection

Title: Opposing effects of T cell receptor signal strength on CD4 T cells responding to acute versus chronic viral infection

Authors: Marco Künzli[1], Peter Reuther[2], Daniel D. Pinschewer[2], Carolyn G. King[1,3,*]

Affiliations:

[1]Immune Cell Biology Laboratory, Department of Biomedicine, University of Basel, University Hospital Basel CH-4031 Basel, Switzerland.

[2]Division of Experimental Virology, Department of Biomedicine – Haus Petersplatz, University of Basel, CH-4031 Basel, Switzerland.

[3]Lead contact

*Correspondence: carolyn.king@unibas.ch

To whom correspondence should be addressed:

Carolyn King
Department of Biomedicine
University of Basel
University Hospital Basel
Hebelstrasse 20
CH-4031 Basel, Switzerland
Email: carolyn.king@unibas.ch
Tel: +41 61 907 15 68

Abstract

A hallmark of the adaptive immune response is the ability of CD4 T cells to differentiate into a variety of pathogen appropriate and specialized effector subsets. A long-standing question in CD4 T cell biology is whether the strength of TCR signals can instruct one Th cell fate over another. The contribution of TCR signal strength to the development of Th1 and T follicular helper (Tfh) cells has been particularly difficult to resolve, with conflicting results reported in a variety of models. Although cumulative TCR signal strength can be modulated by the infection specific environment, whether or not TCR signal strength plays a dominant role in Th1 versus Tfh cell fate decisions across distinct infectious contexts is not known. Here we characterized the differentiation of CD4 TCR transgenic T cells responding to a panel of recombinant wild type or altered peptide ligand lymphocytic choriomeningitis viruses (LCMV) derived from acute and chronic parental strains. We found that while TCR signal strength positively regulates T cell expansion in both infection settings, it exerts opposite and hierarchical effects on the balance of Th1 and Tfh cells generated in response to acute versus persistent infection. The observation that weakly activated T cells, which comprise up to fifty percent of an endogenous CD4 T cell response, support the development of Th1 effectors highlights the possibility that they may resist functional inactivation during chronic infection. We anticipate that the panel of variant ligands and recombinant viruses described herein will be a valuable tool for immunologists investigating a wide range of CD4 T cell responses.

Keywords

T cell receptor signal, T cell receptor, T helper 1 cell, T follicular helper cell, infection, chronic infection, T cell exhaustion, T cell differentiation, CD4 T cell

Graphical abstract

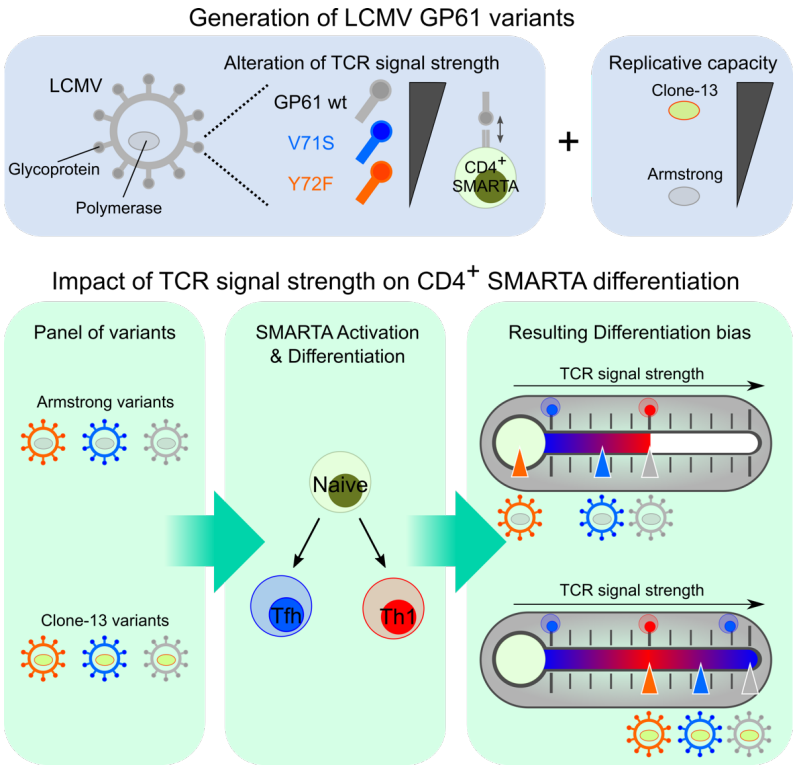

Highlights

- Identification of a wide panel of altered peptide ligands for the LCMV-derived GP61 peptide
- Generation of LCMV variant strains to examine the impact of TCR signal strength on CD4 T cells responding during acute and chronic viral infection
- The relationship between TCR signal strength and Th1 differentiation shifts according to the infection context: TCR signal strength correlates positively with Th1 generation during acute infection but negatively during chronic infection.

Introduction

Following infection or vaccination, antigen specific T cells undergo clonal expansion and differentiation into effector cells with specialized functions. This process begins with T cell receptor (TCR) recognition of peptide/MHC (pMHC) on antigen presenting cells (APCs) and is further modulated by cytokines and costimulatory molecules(*1, 2*). Viral infection induces the early bifurcation of CD4 T cells into Th1 and T follicular helper (Tfh) cells. Th1 cells potentiate CD8 T cell and macrophage cytotoxicity, whereas Tfh cells support antibody production by providing survival and proliferation signals to B cells(*1, 3*).

Although the cumulative strength of interaction between TCR and pMHC has a clear impact on T cell expansion and fitness, its influence on the acquisition of Th1 and Tfh cell fates is controversial(*4-12*). An essential role for TCR signal was implicated in a study assessing the phenotype of progeny derived from individual, TCR transgenic (tg) T cells responding during infection(*9*). The authors observed that distinct TCRs induced reproducible and biased patterns of Th1 and Tfh phenotypes. Although earlier reports suggested that Tfh cell differentiation requires high TCR signal strength, recent work supports the idea that Tfh cells develop across a wide range of signal strengths, while increasing TCR signal intensity favors Th1 generation(*4-11*). A central difficulty in reconciling these findings is the use of different TCR tg systems as well as immunization and infection models that may induce distinct levels of costimulatory and inflammatory signals known to influence T cell differentiation. Although existing reports suggest that persistent TCR signaling drives a shift towards Tfh differentiation during chronic infection, whether this outcome can be modulated by TCR signal strength has not been examined(*13-15*).

The impact of TCR signal strength on CD4 T cell differentiation *in vivo* has been historically challenging to address. The use of MHC-II tetramers to track endogenous polyclonal T cell responses does not adequately detect low affinity T cells that can comprise up to fifty percent of an effector response in autoimmune or viral infection settings(*16*). TCR tg models paired with a panel of ligands with varying TCR potency have been informative, but only a handful of MHC-II restricted systems exist(*17, 18*). To bypass these limitations, the generation of novel transgenic/retrogenic TCR strains or recombinant pathogen strains is required(*4, 12, 19, 20*). To our knowledge, this approach has not yet been used to modify a naturally occurring CD4 T cell epitope of an infectious agent. To test the impact of TCR signal strength across different types of infectious contexts, we generated a series of lympocytic choriomeningitis virus (LCMV) variants by introducing single amino acid mutations into the GP61 envelope glycoprotein sequence and expressing them from both acute and chronic parent strains. These strains were used to assess the dynamics and differentiation of SMARTA T cells, a widely used TCR tg mouse line that mirrors the endogenous, immunodominant CD4 T cell response to LCMV(*13*). We observed that depending on the infection setting, TCR signal strength has opposing effects on the balance between Th1 and Tfh cell differentiation. In an acute infection, strong TCR signals preferentially induce Th1 effectors, whereas weak TCR signals shift the balance toward Tfh effectors. In contrast, strong T cell activation during chronic infection induces Tfh cell differentiation while more weakly activated T cells are biased to differentiate into Th1 cells. Based on these findings we propose a Goldilocks model for the generation of Th1 effectors during viral infection, where too little or too much TCR signaling skews the CD4 T cell response toward Tfh differentiation.

Results

Generation and viral fitness of GP61 LCMV variants

To generate recombinant LCMV variants, we first screened a panel of altered peptide ligands (APLs) with single amino acid mutations in the LCMV derived GP61 peptide. Using the early activation marker CD69 as a proxy for TCR signal strength we identified 75 APLs for the SMARTA TCR transgenic line (Figure S1A, Figure 1A, B, Table 1). We selected twelve of these APLs, covering a wide range of T cell activation potential, to generate recombinant variant viruses, using site-directed PCR mutagenesis (*21*). Five APL-encoding sequences were successfully introduced into the genomes of both LCMV Armstrong (Armstrong variants) and Clone-13 (Clone-13 variants), the latter of which contains a mutation in the polymerase gene L that enhances the replicative capacity of the virus, enabling viral persistence(*22, 23*). To exclude a potential impact of differential glycoprotein-mediated viral tropism on CD4 T cell differentiation, we equipped both the Armstrong- and Clone-13-based viruses with the identical glycoprotein of the WE strain and introduced the epitope mutations therein (resulting viruses referred to as rLCMV Armstrong and rLCMV Clone-13, respectively)(*24*). Of these viruses, two variants, V71S and V72F (EC50 ~ 0.1 μM and 1μM, respectively) demonstrated comparable viral fitness *in vitro* and *in vivo* (Figure 1C, D). We further performed an out-competition assay with invariant chain knockout splenocytes to ensure comparable presentation of these APLs by MHC-II (Figure 1E)(*25*). Taken together, these data demonstrate the development of a novel tool to examine the impact of TCR signal strength on SMARTA T cells activated by either acute or chronic viral infection.

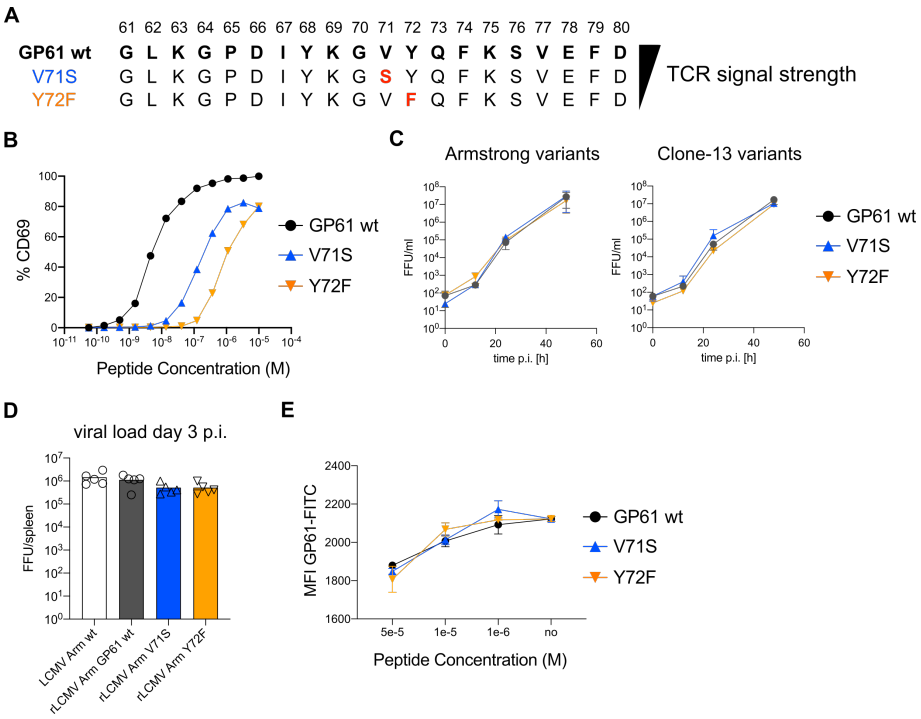

Figure 1: Generation and viral fitness of GP61 LCMV variants

(A) Scheme of GP61 wt and APL sequences with mutations highlighted in red ordered hierarchically according to TCR signal strength.

(B) Peptide dose – activation curves of overnight cultured SMARTA cells with peptide pulsed splenocytes using the percentage of $CD69^+$ SMARTA cells as a readout for activation. EC_{50} values are ~ 5 nM for GP61 wt, ~ 0.1 µM for V71S and ~ 1µM for Y72F.

(C) *In vitro* growth kinetics depicting the viral load in the culture medium (FFU/ml, focus forming units) of GP61 wt or V71S and Y72F variants of Armstrong (left) and Clone-13 (right) variant infection on BHK21 cells over time. Data are displayed as mean ± SD.

(D) Early splenic viral load day 3 post infection (p.i.) in Armstrong variants. Bars represent the mean and symbols represent individual mice.

(E) Peptide dose – response curves depicting the out-competition of the GP61 FITC signal by unlabeled GP61 wt or variants on $B220^+$ B cells. Data are displayed as mean ± SD of 2-3 technical replicates.

Data represent one of n = 2 independent experiments (B, D-,E) or pooled data from n = 2 independent experiments (C).

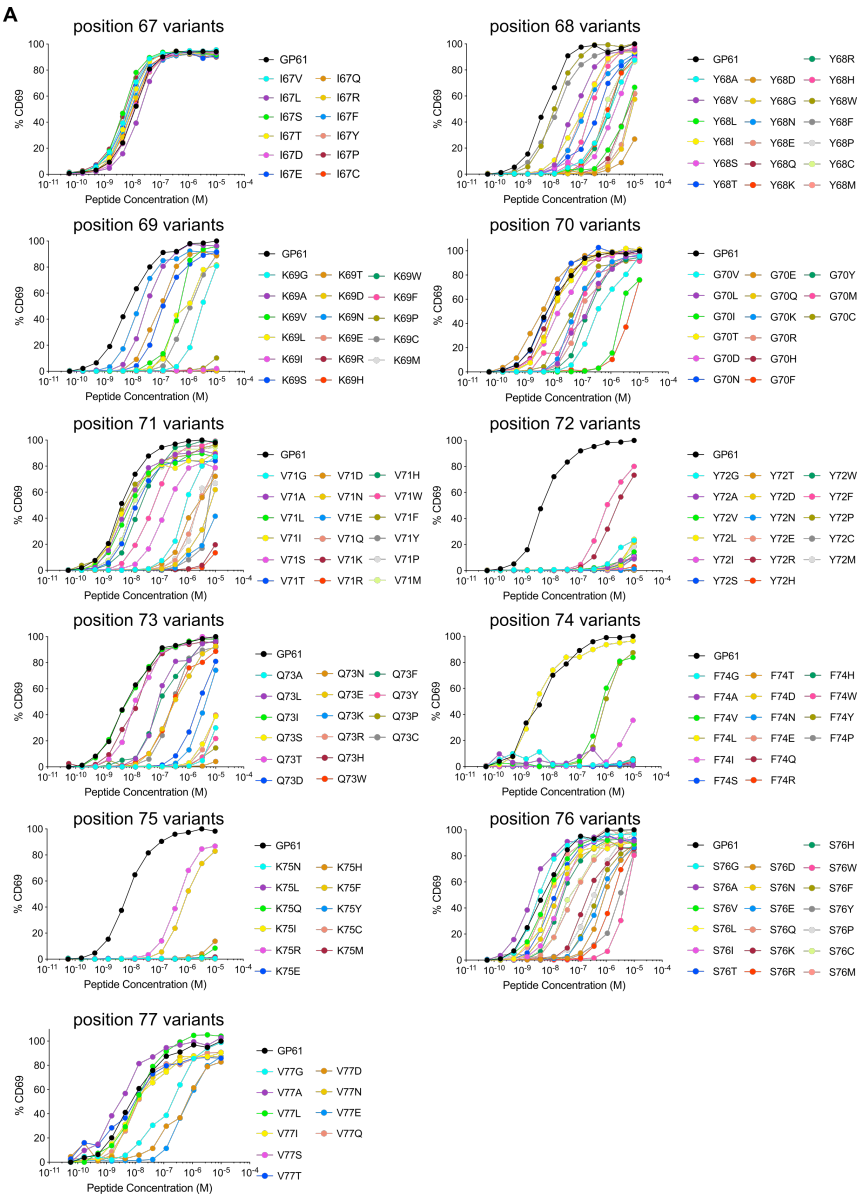

Figure S1: Generation and viral fitness of GP61 LCMV variants
(A) Peptide dose – activation curves of overnight cultured SMARTA cells with peptide pulsed splenocytes using the percentage of $CD69^{+}$ SMARTA cells as a readout for activation.
Data represent one of n = 2 independent experiments.

APL	EC50 [M]
GP61wt	5.2E-09
Y68 A	1.3E-06
Y68 V	7.2E-08
Y68 L	6.5E-06
Y68 I	1.3E-07
Y68 S	2.6E-06
Y68 T	4.8E-07
Y68 N	1.6E-07
Y68 E	7.0E-05
Y68 Q	6.7E-06
Y68 K	1.1E-06
Y68 R	1.5E-06
Y68 H	3.1E-07
Y68 W	1.4E-08
Y68 P	1.1E-05
Y68 C	1.0E-06
Y68 M	1.6E-07
K69 G	5.2E-06
K69 A	3.2E-08
K69 V	5.0E-07
K69 L	5.5E-07
K69 S	1.2E-07
K69 T	8.1E-08
G70 V	3.5E-07
G70 L	1.2E-07
G70 I	3.5E-06
G70 K	5.8E-08
G70 R	1.1E-07
G70 F	1.4E-05
G70 Y	1.7E-07
G70 M	6.2E-08
V71 G	9.3E-07
V71 S	1.4E-07
V71 D	1.4E-06
V71 N	8.4E-06
V71 E	9.5E-06
V71 Q	2.9E-06
V71 H	2.2E-08

APL	EC50 [M]
V71 W	5.9E-08
V71 P	2.2E-06
V71 M	1.2E-08
V71 C	2.1E-07
Y72 S	4.2E-05
Y72 T	1.7E-05
Y72 E	2.1E-07
Y72 R	2.1E-06
Y72 F	9.6E-07
Y72 P	6.3E-08
Y72 M	5.6E-05
Q73 L	8.7E-08
Q73 S	2.5E-05
Q73 D	3.2E-06
Q73 E	3.1E-07
Q73 K	8.3E-06
Q73 W	2.6E-07
Q73 F	1.1E-07
Q73 C	2.9E-07
F74 V	8.7E-07
F74 I	1.9E-05
F74 Y	1.3E-06
K75 R	5.1E-07
S76 D	1.0E-06
S76 E	5.7E-07
S76 Q	5.9E-08
S76 K	2.0E-07
S76 R	2.2E-06
S76 W	7.9E-05
S76 F	4.5E-07
S76 Y	5.3E-06
S76 P	3.8E-07
S76 C	5.9E-08
V77 G	1.8E-07
V77 S	3.6E-08
V77 D	4.8E-07
V77 E	6.5E-07
V77 P	4.0E-08

Table 1: APLs with altered potential to activate SMARTA and corresponding EC_{50} values.

TCR signal strength positively correlates with Th1 cell differentiation during LCMV Armstrong variant infection

To assess the impact of TCR signal strength during acute viral infection, SMARTA T cells were transferred into congenic recipients followed by infection with rLCMV Armstrong GP61 wt, V71S or Y72F. All LCMV variants were capable of inducing SMARTA T cell expansion at day 10 post infection (p.i.) and a direct correlation between TCR signal strength and the number of SMARTA T cells recovered was observed (Figure 2A). In contrast, expansion of endogenous LCMV nucleoprotein (NP)-specific as well as antigen-experienced $CD44^+$ T cells was similar across all three viral strains (Figure 2A). The expansion hierarchy among the viruses was maintained >30 days after LCMV infection (Figure 2A).

We next examined the phenotype of SMARTA T cells, focusing our analyses on effector cells due to the impaired generation of Tfh memory by SMARTA T cells(*26*). As the Y72F variant induced very few effector cells, we excluded this strain from further investigation. Consistent with earlier reports, strong T cell stimulation induced a larger proportion of $Ly6c^+$ Th1 effectors, whereas the proportion of Tfh effectors was decreased (Figure 2B-D)(*4, 8-10*). In contrast, the ratio of Th1 and Tfh effector cells generated by host NP-specific T cells was consistent across all viral strains, providing an internal control for the comparable ability of these viruses to induce endogenous T cell responses (Figure 2D, Figure S2A). Expression of folate receptor 4 (FR4), an alternative marker for Tfh cell identification, was additionally used in combination with PD1 to discriminate the Tfh cell compartment, and demonstrated a decreased proportion of Tfh cells activatd by strong compared to weak TCR stimulation (Fig. S2B)(*26, 27*). Accordingly, the expression of Bcl6 and T-bet, lineage defining transcription factors for Tfh and Th1 cells, respectively, revealed a mild but

119 significant trend toward increased Tbet and decreased Bcl6 in response to strong
120 stimulation (Fig. 2E). Importantly, Bcl6 expression was higher on Tfh compared to
121 Th1 effectors, with no differences observed between strong and weak stimulation
122 (Figure 2F, S2C). These data indicate that TCR signal strength is unlikely to exert a
123 qualitative impact on these subsets. Notably, we did not observe any impact of TCR
124 signal strength on the development of PSGL1^{hi}Ly6c^{lo} T cells, previously reported to be
125 a less differentiated population of Th1 effectors (Figure S2D)(*26*). In sum, consistent
126 with earlier reports (references?), TCR signal strength positively correlates with an
127 increased ratio of Th1 to Tfh effectors during acute LCMV infection.

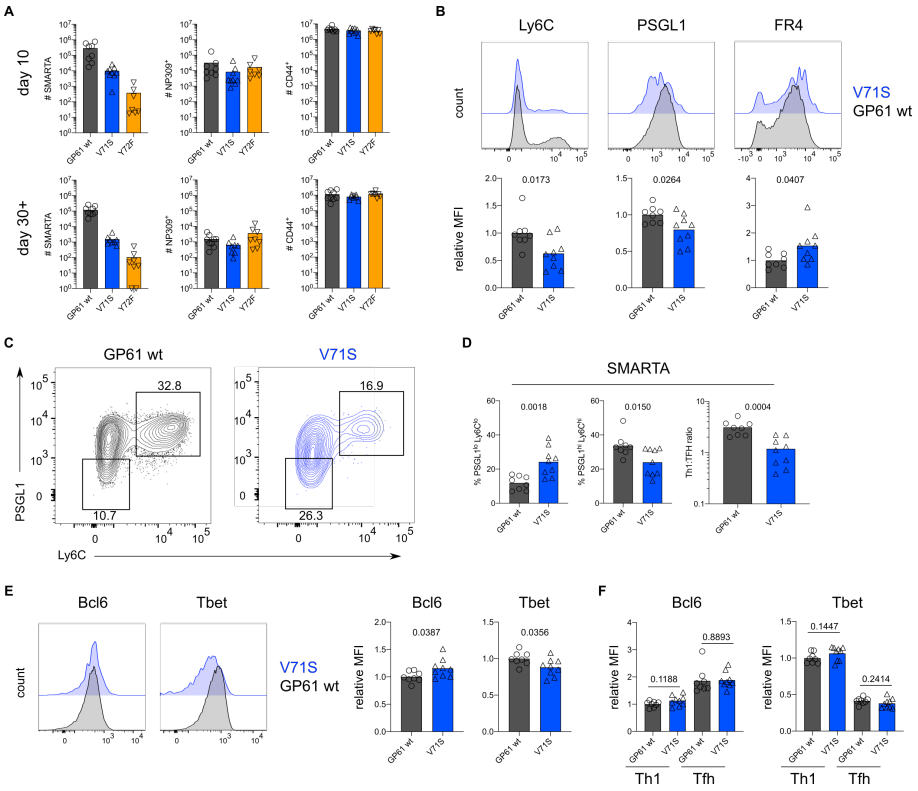

Figure 2: TCR signal strength positively correlates with Th1 cell differentiation during LCMV Armstrong variant infection

(A) Number of SMARTA (left), NP309^{+} (middle) and CD44^{+} cells (right) 10 days (top) or >30 days (bottom) p.i.

(B) Histograms (top) and relative MFI (bottom) of indicated phenotypic markers in the SMARTA compartment 10 days p.i.

(C) Identification of Th1 (Ly6C^{hi}PSGL1^{hi}) and Tfh (Ly6C^{lo}PSGL1^{lo}) subset in the SMARTA compartment by flow cytometry 10 days p.i.

(D) Proportion of Tfh (left), Th1 cells (middle) and the Th1:Tfh ratio (right) of the SMARTA compartment 10 days p.i.

(E) Histograms (left) and relative MFI (right) of Bcl6 and Tbet expression in the SMARTA compartment 10 days p.i

(F) Bcl6 and Tbet MFI in SMARTA Th1 and Tfh subsets.

Data are pooled from n = 2 independent experiments with 7-9 samples per group. Bars represent the mean and symbols represent individual mice. Significance was determined by unpaired two-tailed Student's t-tests.

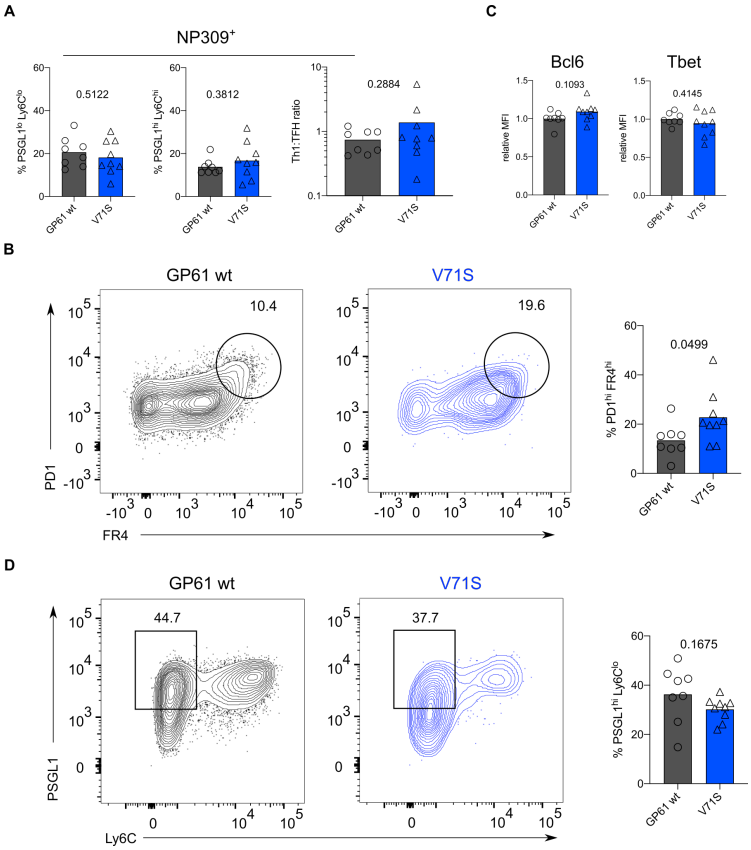

Figure S2: TCR signal strength positively correlates with Th1 cell differentiation during LCMV Armstrong variant infection

(A) Proportion of Tfh (left), Th1 cells (middle) and the Th1:Tfh ratio (right) of the NP309^{+} compartment 10 days p.i.

(B) Identification and proportion of PD1^{hi} FR4^{hi} Tfh cells in the SMARTA compartment by flow cytometry.

(C) Relative MFI of Bcl6 and Tbet expression in the Ly6C^{lo} Th1 SMARTA compartment.

(D) Identification and proportion of Ly6C^{lo} Th1 (Ly6C^{lo}PSGL1^{hi}) in the SMARTA compartment by flow cytometry.

Data are pooled from n = 2 independent experiments with 8-9 samples per group. Bars represent the mean and symbols represent individual mice. Significance was determined by unpaired two-tailed Student's t-tests.

TCR signal strength positively correlates with Tfh cell differentiation during LCMV Clone-13 variant infection

In contrast to acute LCMV infection, SMARTA T cells responding to chronic LCMV preferentially adopt a Tfh effector phenotype(*14, 15*). The impact of TCR signal strength within this context has not been determined, although affinity diversity among endogenous T cells is reportedly similar between acute and chronic LCMV infection(*28*). To directly assess the impact of TCR signal strength during chronic infection we transferred SMARTA T cells into congenic recipients followed by infection with rLCMV Clone-13 expressing either GP61 wt, V71S or Y72F. As an additional control we infected mice with rLCMV Armstrong which induced a similar expansion of SMARTA, NP-specific and $CD4^+CD44^+$ T cells as its Clone-13 counterpart (Fig S3A). Consistent with the results from acute infection, SMARTA T cell numbers at day 7 p.i. positively correlated with TCR signal strength, while the expansion of NP-specific and $CD4^+CD44^+$ T cells was similar in response to all three Clone-13 variants (Figure 3A). Importantly, infection with rLCMV Clone-13 Y72F induced approximately 2-fold more SMARTA T cell effectors compared to acute infection, allowing for a thorough investigation of T cells responding to this very weak potency variant (Figure 3A, Figure 2A).

With respect to T cell phenotype, strong TCR stimulation during rLCMV Clone-13 GP61 wt infection shifted the balance toward Tfh effector cell differentiation when compared to strong TCR stimulation in the context of acute infection (Figure S3B-C). Unexpectedly, and in contrast to the Armstrong variants, weaker TCR signaling during Clone-13 variant infection resulted in increased proportions of both $PSGL1^{hi}Ly6c^{hi}$ and $PSGL1^{hi}Ly6c^{lo}$ Th1 cells with the weakest variant, Y72F, generating the highest proportion of Th1 effectors (Figure 3B-D, S3D). The shift toward Th1 effectors in

153 response to lower TCR signal strength is unlikely due to differences in antigen load as
154 all variants sustained high viral titers in the kidneys at day 7 p.i (Figure S3E). In
155 addition, although the viral titer of intermediate potency variant V71S was slightly
156 decreased compared to GP61 wt and Y72F infection, NP-specific CD4 T cells
157 exhibited a similar ratio of Th1 to Tfh effectors across all three infections (Figure S3F).
158 Taken together, these reveal that TCR signal strength differentially modulates T cell
159 fate acquisition according to the infectious context.

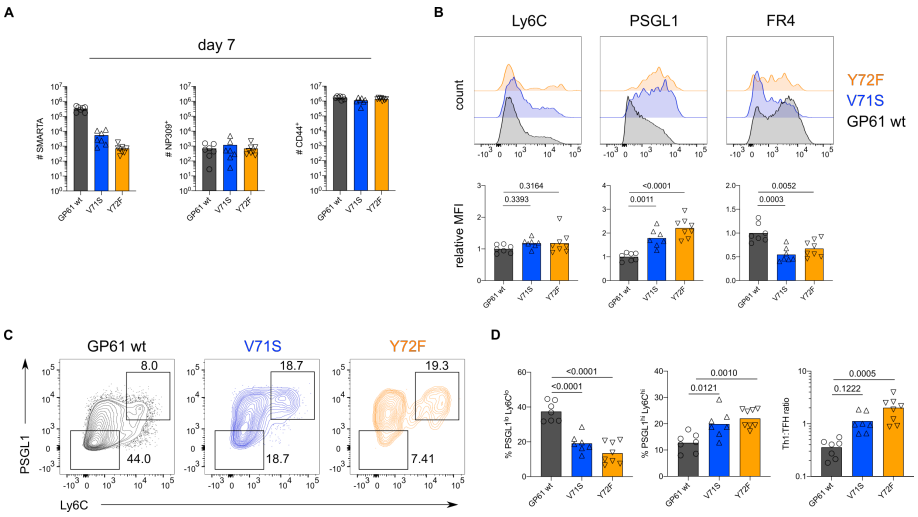

Figure 3: TCR signal strength positively correlates with Tfh cell differentiation during LCMV Clone-13 variant infection

Spleens were harvested 7 days after infection with LCMV Clone-13 variants.

(A) Number of SMARTA (left), NP309^{+} (middle) and CD44^{+} cells (right).

(B) Histograms (top) and relative MFI (bottom) of indicated phenotypic markers in the SMARTA compartment.

(C) Identification of Th1 (Ly6C^{hi}PSGL1^{hi}) and Tfh (Ly6C^{lo}PSGL1^{lo}) subset in the SMARTA compartment by flow cytometry.

(D) Proportion of Tfh (left), Th1 cells (middle) and the Th1:Tfh ratio (right) of the SMARTA compartment.

Data are pooled from n = 2 independent experiments with 7-8 samples per group. Bars represent the mean and symbols represent individual mice. Significance was determined by one-way analysis of variance (ANOVA) followed by Tukey's post-test.

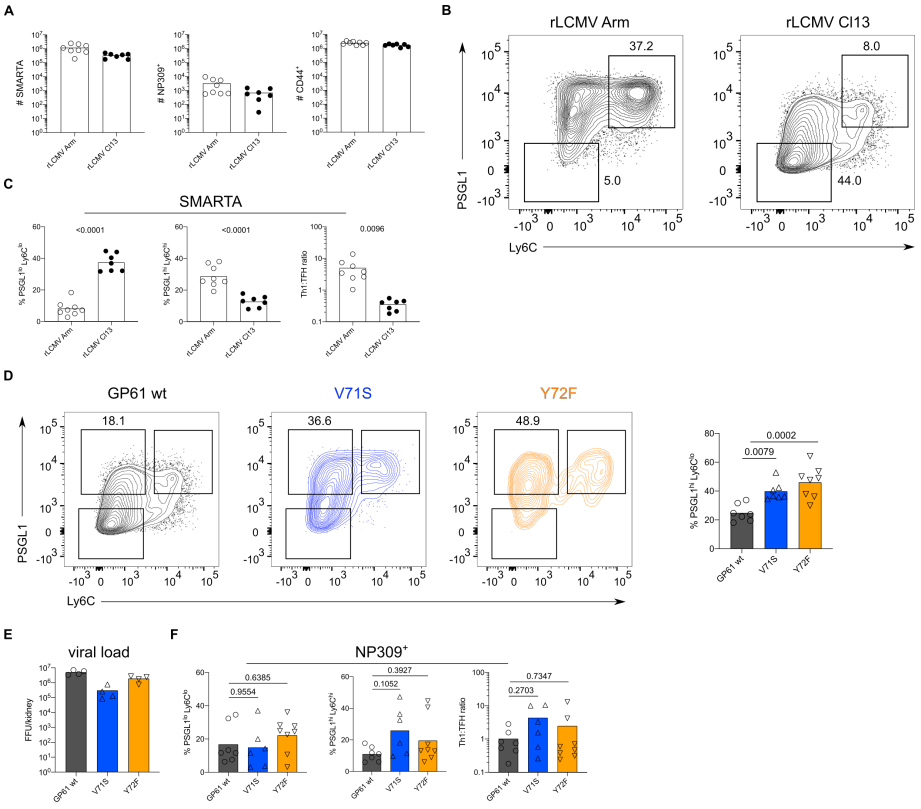

Figure S3: TCR signal strength positively correlates with Tfh cell differentiation during LCMV Clone-13 variant infection

Spleens were harvested 7 days after infection with LCMV Clone-13 variants.

(A) Number of SMARTA (left), NP309^{+} (middle) and CD44^{+} cells (right).

(B) Identification of Th1 (Ly6C^{hi}PSGL1^{hi}) and Tfh (Ly6C^{lo}PSGL1^{lo}) subset in the SMARTA compartment by flow cytometry.

(C) Proportion of Tfh (left), Th1 cells (middle) and the Th1:Tfh ratio (right) of the SMARTA compartment.

(D) Identification and proportion of Ly6C^{lo} Th1 (Ly6C^{lo}PSGL1^{hi}) in the SMARTA compartment by flow cytometry.

(E) Viral load in kidneys.

(F) Proportion of Tfh (left), Th1 cells (middle) and the Th1:Tfh ratio (right) of the NP309^{+} compartment.

Data are pooled from n = 2 independent experiments with 7-8 samples per group except for (E) where one representative experiment of n = 2 independent experiments is shown with 4 samples per group. Bars represent the mean and symbols represent individual mice. Significance was determined by one-way analysis of variance (ANOVA) followed by Tukey's post-test.

Increasing TCR signal strength promotes the expression of markers associated with chronic T cell stimulation

During Clone-13 infection, T cells start to upregulate inhibitory surface markers associated with chronic activation, a state often referred to as "exhaustion"(*15, 29-31*). To understand if TCR signal strength impacts the expression of these markers we analyzed SMARTA T cells responding to Clone-13 GP61 wt and variant viruses at day 14. T cells responding to strong TCR signals expressed the highest levels of both PD1 and Lag3, two well characterized co-inhibitory receptors (Figure 4A-B) (*15, 29*). SMARTA T cells co-expressing both PD1 and Lag3 were most abundant following Clone-13 GP61 wt infection and decreased in response to Clone-13 variant infection (Figure 4C-D). Although the viral load was decreased in Clone-13 variant infections at this time point, the basal activation of $CD4^+CD44^+$ T cells was equivalent across all three strains and clearly above the recombinant LCMV Armstrong control (Figure S4A-B). Next, we examined the expression of TOX, a transcription factor involved in the adaptation of CD8 T cells to chronic infection(*32-36*). In response to acute infection, SMARTA Tfh cells expressed higher levels of TOX compared to Th1 cells, consistent with an earlier study highlighting the importance of TOX for Tfh cell development (Figure S4C)(*37*). In contrast, TOX expression during rLCMV Clone-13 wt infection was most highly upregulated by Th1 effectors (Figure S4C). In line with the expression of PD1 and Lag3, TOX was decreased on SMARTA T cells responding to rLCMV Clone-13 variant viruses, despite being comparably induced on $CD4^+CD44^+$ T cells (Figure 4E, Figure S4D). TOX was recently demonstrated to be important for the survival of stem-like $TCF1^+$ CD8 T cells that accumulate during chronic LCMV(*34, 38, 39*). Given the transcriptional similarities of $TCF1^+$ CD8 T cells and Tfh cells, we wondered if TCF1 would be similarly regulated by TCR signal strength following Clone-

13 variant infection(*40*). Here we observed that unlike TOX expression, TCF1 is similarly expressed by T cells responding to all three rLCMV Clone-13 variants (Figure 4F, S4E), indicating that TCF1 expression is likely to be maintained independently of TCR signals.

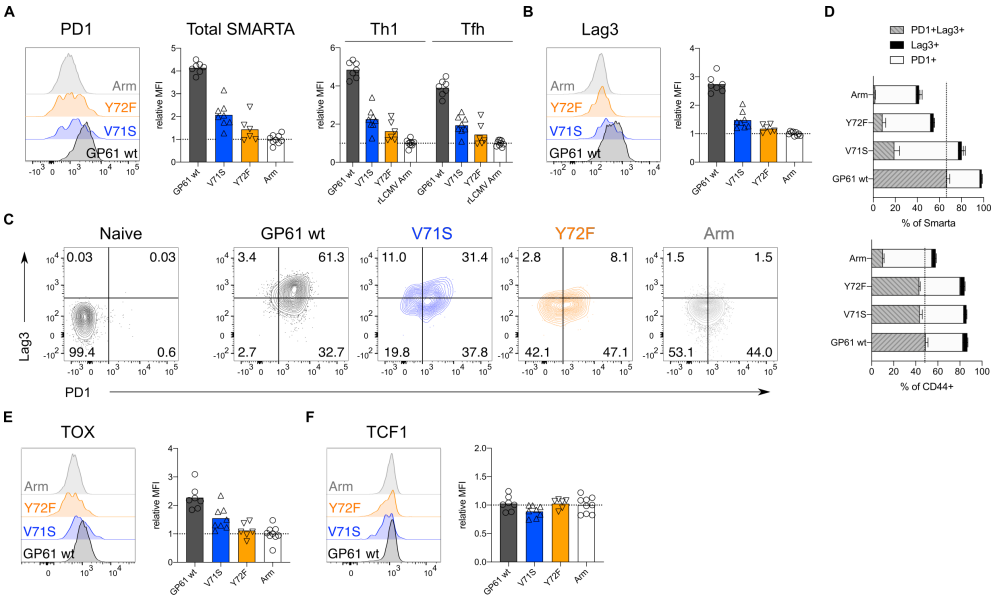

Figure 4: Increased TCR signal strength induces expression of markers associated with chronic T cell stimulation
Spleens were harvested 14 days after infection with LCMV Clone-13 based variants.
(A) Histograms (left) and relative MFI (right) of PD1 in the total SMARTA compartment (left) or SMARTA Th1 and Tfh subsets (right).
(B) Histograms (left) and relative MFI (right) of Lag3 in the SMARTA compartment.
(C) Identification of $PD1^{+}Lag3^{+}$ SMARTA cells by flow cytometry compared to naïve $CD62L^{+}$ $CD44^{-}$ CD4 T cells from an uninfected mouse.
(D) Quantification of $PD1^{+}Lag3^{+}$ SMARTA cells in the SMARTA (top) or $CD44^{+}$ (bottom) compartment.
(E) Histogram (left) and relative MFI (right) of TOX in the SMARTA compartment.
(F) Histogram (left) and relative MFI (right) of TCF1 in the SMARTA compartment.
Data are pooled from n = 2 independent experiments with 6-9 samples per group. Bars represent the mean and symbols represent individual mice. Significance was determined by one-way analysis of variance (ANOVA) followed by Tukey's post-test.

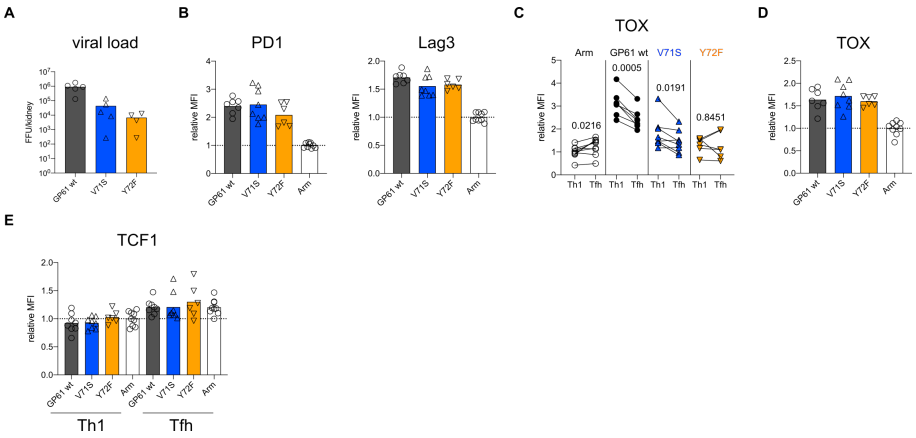

Figure S4: Increased TCR signal strength induces expression of markers associated with chronic T cell stimulation

Spleens were harvested 14 days after infection with LCMV Clone-13 based variants.
(A) Viral load in kidneys.
(B) Relative MFI (right) of PD1 and Lag3 in the $CD44^+$ compartment.
(C) Relative MFI of TOX in SMARTA Th1 and Tfh.
(D) Relative MFI (right) of TOX in the $CD44^+$ compartment.
(E) Relative MFI of TCF1 in the SMARTA Th1 and Tfh subsets.
Data are pooled from n = 2 independent experiments with 6-9 samples per group except for (A) where one representative experiment of n = 2 independent experiments is shown with 4-5 samples per group. Bars represent the mean and symbols represent individual mice. Significance was determined by one-way analysis of variance (ANOVA) followed by Tukey's post-test (B,D) or by paired two-tailed Student's t-tests (C).

Discussion

The results of this study highlight the differential impact of TCR signal strength in shaping CD4 T cell fate according to the infection context. By systematically comparing the differentiation of TCR transgenic T cells responding to variant ligands in two distinct infection models, we demonstrate that the impact of TCR signal strength is heavily dependent on the infection specific parameters such as antigen load and inflammation.

The observation that TCR signal intensity correlates with Th1 generation during acute infection is consistent with accumulating evidence that higher potency ligands increase T cell sensitivity to IL-2, which likely drives the survival and expansion of Th1 effectors (*4, 8, 41-45*). This is similar to the paradigm described for Th1/Th2 cell differentiation, where stronger signals induce Th1 cells and weaker signals induce Th2 cells(*46*). Nevertheless, at very high antigen doses, T cells revert to Th2 differentiation, potentially due to the susceptibility of Th1 cells to activation induced cell death (AICD)(*47, 48*). AICD of Th1 cells might also contribute to biased Tfh generation at the higher end of TCR signal strength during Clone-13 infection(*49, 50*).

The shift of relatively high affinity CD4 T cells toward a Tfh cell phenotype during Clone-13 infection is well documented(*14, 40, 51*). In addition to antigen persistence, however, Clone-13 presents an altered inflammatory environment which contributes to an interferon stimulated gene signature and IL-10 production by chronically activated CD4 T cells(*15, 52*). It is possible that the unique cytokine milieu present during Clone-13 infection cooperates with strong TCR signals to fine tune T cell fate. For example, activation of T cells in the presence of IFNα induces T cell secretion of IL-10 which is positively regulated by TCR signal strength(*53, 54*). While this may ultimately serve to limit host pathology, it may also prevent the accumulation

of Th1 effectors. Consistent with this idea, blocking IFNα or IL-10 during Clone-13 infection rescues the Th1 effector compartment and improves viral control, although this likely depends on the rate of viral replication(*55-57*). Within the same inflammatory context, weaker TCR signals might induce less T cell derived IL-10 which has been shown to impair Th1 effector cell differentiation(*52*). Of particular interest, T cell production of IL-10 during chronic infection depends on sustained, but ERK-independent TCR signals, suggesting that inflammatory versus suppressive cytokine secretion may have distinct TCR signaling requirements(*52*). Future experiments should address this by determining whether TCR signal strength contributes to cytokine production as well as cytokine susceptibility (i.e. induction of cytokine receptors) of effector cells responding during acute and chronic viral infection.

Finally, the ability of weakly activated T cells to maintain a higher proportion of Th1 effectors might ultimately contribute to viral control. The observation that the weakest Clone-13 variant, Y72F, elicited significantly more expansion than its Armstrong counterpart demonstrates that prolonged antigen presentation supports the accumulation of relatively low affinity T cells. Importantly, our study only follows the differentiation of T cells specific for a single epitope, while low affinity T cells are demonstrated to comprise up to half of the endogenous effector T cell response(*58*). Going forward, it will be interesting to determine whether targeting the expansion of lower affinity T cells with the potential to resist functional inactivation and maintain proliferative potential will improve control of viral infection.

Acknowledgments

We thank all members of the Pinschewer lab for helpful discussion and David Schreiner for editing of the manuscript. Research was supported by the Swiss

National Science Foundation (SNF, grants number PP00P3_157520 to CGK and number 310030_173132 to DDP), Gottfried and Julia Bangerter-Rhyner Stiftung, Olga Mayenfisch Stiftung, the Nikolaus and Bertha Burckhardt-Bürgin Stiftung (NBB), and the Freiwillige Akademische Gesellschaft (FAG) Basel.

Author contributions

C.G.K. conceptualized the project. M.K. and C.G.K. designed the experiments, analyzed the data, wrote the manuscript and acquired funding. M.K. and P.R. performed experiments. D.P. acquired funding, provided advice on experimental design and revised the manuscript.

Declaration of Interests

The authors declare no competing interests.

References

1. J. Zhu, H. Yamane, W. E. Paul, Differentiation of effector CD4 T cell populations (*). *Annu Rev Immunol* **28**, 445-489 (2010).
2. M. M. Davis *et al.*, Ligand recognition by alpha beta T cell receptors. *Annu Rev Immunol* **16**, 523-544 (1998).
3. S. Crotty, Follicular Helper CD4 T Cells (TFH). *Annual Review of Immunology* **29**, 621-663 (2011).
4. S. Keck *et al.*, Antigen affinity and antigen dose exert distinct influences on CD4 T-cell differentiation. *Proc Natl Acad Sci U S A* **111**, 14852-14857 (2014).
5. D. I. Kotov *et al.*, TCR Affinity Biases Th Cell Differentiation by Regulating CD25, Eef1e1, and Gbp2. *J Immunol* **202**, 2535-2545 (2019).
6. J. P. Snook, C. Kim, M. A. Williams, TCR signal strength controls the differentiation of CD4(+) effector and memory T cells. *Sci Immunol* **3**, (2018).
7. D. DiToro *et al.*, Differential IL-2 expression defines developmental fates of follicular versus nonfollicular helper T cells. *Science* **361**, (2018).
8. V. Krishnamoorthy *et al.*, The IRF4 Gene Regulatory Module Functions as a Read-Write Integrator to Dynamically Coordinate T Helper Cell Fate. *Immunity* **47**, 481-497 e487 (2017).
9. N. J. Tubo *et al.*, Single naive CD4+ T cells from a diverse repertoire produce different effector cell types during infection. *Cell* **153**, 785-796 (2013).
10. M. J. Ploquin, U. Eksmond, G. Kassiotis, B cells and TCR avidity determine distinct functions of CD4+ T cells in retroviral infection. *J Immunol* **187**, 3321-3330 (2011).
11. N. Fazilleau, L. J. McHeyzer-Williams, H. Rosen, M. G. McHeyzer-Williams, The function of follicular helper T cells is regulated by the strength of T cell antigen receptor binding. *Nat Immunol* **10**, 375-384 (2009).
12. V. Vanguri, C. C. Govern, R. Smith, E. S. Huseby, Viral antigen density and confinement time regulate the reactivity pattern of CD4 T-cell responses to vaccinia virus infection. *Proc Natl Acad Sci U S A* **110**, 288-293 (2013).
13. A. Oxenius, M. F. Bachmann, R. M. Zinkernagel, H. Hengartner, Virus-specific MHC-class II-restricted TCR-transgenic mice: effects on humoral and cellular immune responses after viral infection. *Eur J Immunol* **28**, 390-400 (1998).
14. L. M. Fahey *et al.*, Viral persistence redirects CD4 T cell differentiation toward T follicular helper cells. *J Exp Med* **208**, 987-999 (2011).
15. A. Crawford *et al.*, Molecular and transcriptional basis of CD4(+) T cell dysfunction during chronic infection. *Immunity* **40**, 289-302 (2014).
16. J. J. Sabatino, Jr., J. Huang, C. Zhu, B. D. Evavold, High prevalence of low affinity peptide-MHC II tetramer-negative effectors during polyclonal CD4+ T cell responses. *J Exp Med* **208**, 81-90 (2011).
17. E. Corse, R. A. Gottschalk, M. Krogsgaard, J. P. Allison, Attenuated T cell responses to a high-potency ligand in vivo. *PLoS Biol* **8**, (2010).
18. E. S. Huseby, F. Crawford, J. White, P. Marrack, J. W. Kappler, Interface-disrupting amino acids establish specificity between T cell receptors and complexes of major histocompatibility complex and peptide. *Nat Immunol* **7**, 1191-1199 (2006).
19. A. M. Gallegos *et al.*, Control of T cell antigen reactivity via programmed TCR downregulation. *Nat Immunol* **17**, 379-386 (2016).

20. C. Kim, T. Wilson, K. F. Fischer, M. A. Williams, Sustained interactions between T cell receptors and antigens promote the differentiation of CD4(+) memory T cells. *Immunity* **39**, 508-520 (2013).
21. L. Flatz, A. Bergthaler, J. C. de la Torre, D. D. Pinschewer, Recovery of an arenavirus entirely from RNA polymerase I/II-driven cDNA. *Proc Natl Acad Sci U S A* **103**, 4663-4668 (2006).
22. A. Bergthaler *et al.*, Viral replicative capacity is the primary determinant of lymphocytic choriomeningitis virus persistence and immunosuppression. *Proc Natl Acad Sci U S A* **107**, 21641-21646 (2010).
23. B. M. Sullivan *et al.*, Point mutation in the glycoprotein of lymphocytic choriomeningitis virus is necessary for receptor binding, dendritic cell infection, and long-term persistence. *Proc Natl Acad Sci U S A* **108**, 2969-2974 (2011).
24. A. Bergthaler, D. Merkler, E. Horvath, L. Bestmann, D. D. Pinschewer, Contributions of the lymphocytic choriomeningitis virus glycoprotein and polymerase to strain-specific differences in murine liver pathogenicity. *J Gen Virol* **88**, 592-603 (2007).
25. X. Liu *et al.*, Alternate interactions define the binding of peptides to the MHC molecule IA(b). *Proc Natl Acad Sci U S A* **99**, 8820-8825 (2002).
26. M. Kunzli *et al.*, Long-lived T follicular helper cells retain plasticity and help sustain humoral immunity. *Sci Immunol* **5**, (2020).
27. S. S. Iyer *et al.*, Identification of novel markers for mouse CD4(+) T follicular helper cells. *Eur J Immunol* **43**, 3219-3232 (2013).
28. R. Andargachew, R. J. Martinez, E. M. Kolawole, B. D. Evavold, CD4 T Cell Affinity Diversity Is Equally Maintained during Acute and Chronic Infection. *J Immunol* **201**, 19-30 (2018).
29. Y. Dong *et al.*, CD4(+) T cell exhaustion revealed by high PD-1 and LAG-3 expression and the loss of helper T cell function in chronic hepatitis B. *BMC Immunol* **20**, 27 (2019).
30. Z. Mou *et al.*, Parasite-derived arginase influences secondary anti-Leishmania immunity by regulating programmed cell death-1-mediated CD4+ T cell exhaustion. *J Immunol* **190**, 3380-3389 (2013).
31. M. Jean Bosco *et al.*, The exhausted CD4(+)CXCR5(+) T cells involve the pathogenesis of human tuberculosis disease. *Int J Infect Dis* **74**, 1-9 (2018).
32. C. Yao *et al.*, Single-cell RNA-seq reveals TOX as a key regulator of CD8(+) T cell persistence in chronic infection. *Nat Immunol* **20**, 890-901 (2019).
33. F. Alfei *et al.*, TOX reinforces the phenotype and longevity of exhausted T cells in chronic viral infection. *Nature* **571**, 265-269 (2019).
34. O. Khan *et al.*, TOX transcriptionally and epigenetically programs CD8(+) T cell exhaustion. *Nature* **571**, 211-218 (2019).
35. A. C. Scott *et al.*, TOX is a critical regulator of tumour-specific T cell differentiation. *Nature* **571**, 270-274 (2019).
36. H. Seo *et al.*, TOX and TOX2 transcription factors cooperate with NR4A transcription factors to impose CD8(+) T cell exhaustion. *Proc Natl Acad Sci U S A* **116**, 12410-12415 (2019).
37. W. Xu *et al.*, The Transcription Factor Tox2 Drives T Follicular Helper Cell Development via Regulating Chromatin Accessibility. *Immunity* **51**, 826-839 e825 (2019).

38. S. J. Im *et al.*, Defining CD8+ T cells that provide the proliferative burst after PD-1 therapy. *Nature* **537**, 417-421 (2016).
39. D. T. Utzschneider *et al.*, T Cell Factor 1-Expressing Memory-like CD8(+) T Cells Sustain the Immune Response to Chronic Viral Infections. *Immunity* **45**, 415-427 (2016).
40. L. A. Vella, R. S. Herati, E. J. Wherry, CD4(+) T Cell Differentiation in Chronic Viral Infections: The Tfh Perspective. *Trends Mol Med* **23**, 1072-1087 (2017).
41. N. J. Tubo *et al.*, Single Naive CD4(+) T Cells from a Diverse Repertoire Produce Different Effector Cell Types during Infection. *Cell* **153**, 785-796 (2013).
42. N. Fazilleau, L. J. McHeyzer-Williams, H. Rosen, M. G. McHeyzer-Williams, The function of follicular helper T cells is regulated by the strength of T cell antigen receptor binding. *Nat Immunol* **10**, 375-384 (2009).
43. R. A. Gottschalk *et al.*, Distinct influences of peptide-MHC quality and quantity on in vivo T-cell responses. *Proc Natl Acad Sci U S A* **109**, 881-886 (2012).
44. M. J. Ploquin, U. Eksmond, G. Kassiotis, B cells and TCR avidity determine distinct functions of CD4+ T cells in retroviral infection. *J Immunol* **187**, 3321-3330 (2011).
45. K. A. Allison *et al.*, Affinity and dose of TCR engagement yield proportional enhancer and gene activity in CD4+ T cells. *Elife* **5**, (2016).
46. X. Tao, S. Constant, P. Jorritsma, K. Bottomly, Strength of TCR signal determines the costimulatory requirements for Th1 and Th2 CD4+ T cell differentiation. *J Immunol* **159**, 5956-5963 (1997).
47. N. A. Hosken, K. Shibuya, A. W. Heath, K. M. Murphy, A. O'Garra, The effect of antigen dose on CD4+ T helper cell phenotype development in a T cell receptor-alpha beta-transgenic model. *J Exp Med* **182**, 1579-1584 (1995).
48. P. A. Bretscher, G. Wei, J. N. Menon, H. Bielefeldt-Ohmann, Establishment of stable, cell-mediated immunity that makes "susceptible" mice resistant to Leishmania major. *Science* **257**, 539-542 (1992).
49. B. L. Lohman, R. M. Welsh, Apoptotic regulation of T cells and absence of immune deficiency in virus-infected gamma interferon receptor knockout mice. *J Virol* **72**, 7815-7821 (1998).
50. M. Schorer *et al.*, TIGIT limits immune pathology during viral infections. *Nat Commun* **11**, 1288 (2020).
51. L. M. Snell *et al.*, Overcoming CD4 Th1 Cell Fate Restrictions to Sustain Antiviral CD8 T Cells and Control Persistent Virus Infection. *Cell Rep* **16**, 3286-3296 (2016).
52. I. A. Parish *et al.*, Chronic viral infection promotes sustained Th1-derived immunoregulatory IL-10 via BLIMP-1. *J Clin Invest* **124**, 3455-3468 (2014).
53. B. Corre *et al.*, Type I interferon potentiates T-cell receptor mediated induction of IL-10-producing CD4(+) T cells. *Eur J Immunol* **43**, 2730-2740 (2013).
54. M. Saraiva *et al.*, Interleukin-10 production by Th1 cells requires interleukin-12-induced STAT4 transcription factor and ERK MAP kinase activation by high antigen dose. *Immunity* **31**, 209-219 (2009).
55. J. R. Teijaro *et al.*, Persistent LCMV infection is controlled by blockade of type I interferon signaling. *Science* **340**, 207-211 (2013).
56. E. B. Wilson *et al.*, Blockade of chronic type I interferon signaling to control persistent LCMV infection. *Science* **340**, 202-207 (2013).
57. K. Richter, G. Perriard, A. Oxenius, Reversal of chronic to resolved infection by IL-10 blockade is LCMV strain dependent. *Eur J Immunol* **43**, 649-654 (2013).

389 58. R. J. Martinez, R. Andargachew, H. A. Martinez, B. D. Evavold, Low-affinity CD4+ T
390 cells are major responders in the primary immune response. *Nat Commun* **7**, 13848
391 (2016).
392 59. M. Battegay, [Quantification of lymphocytic choriomeningitis virus with an
393 immunological focus assay in 24 well plates]. *ALTEX* **10**, 6-14 (1993).
394 60. J. J. Moon *et al.*, Tracking epitope-specific T cells. *Nat Protoc* **4**, 565-581 (2009).
395

Material & Methods

Viruses

Virus rescue was performed as described previously using the pol-I/pol-II-driven reverse genetic system for LCMV (*21*). Single amino acids changes of the GP61-epitope were introduced by site directed mutagenesis of the previously described pI-S-WE-GP rescue plasmid (*21*). This plasmid encodes the nucleoprotein (NP) of the LCMV Armstrong strain *on cis* with the glycoprotein (GP) of LCMV WE. Additionally, the LCMV Armstrong specific D63K mutation was introduced into the GP61-coding sequence of the WE-GP gene matching the LCMV Armstrong / Clone-13 amino acid sequence of the GP61 peptides employed in the T cell activation assay. The resulting S-rescue plasmids were combined either a plasmid expressing either the Armstrong or the Clone-13 L segment in order to generate acute and chronic variants respectively. The presence of the desired mutations in the viral genomes was verified by sanger sequencing of RT-PCR amplicons generated with the OneStep RT-PCR-kit (Qiagen) using LCMV WE GP-specific primers (GATTGCGCTTTCCTCTAGATC and TCAGCGTCTTTTCCAGATAG). Viral RNA was extracted from cell culture supernatants using the Direct-zol RNA MicroPrep kit (Zymo Research). Virus titer were determined by immunofocus assay as described on NIH/3T3 cells (*59*).

Viral growth kinetics

To determine viral replication capacities, BHK21 cells were seeded 24 hours prior to infection with a MOI of 0.01. Supernatant was collected at indicated time points and replaced with fresh culture medium.

Mice and Animal experiments

Mice were bred and housed under specific pathogen-free conditions at the University Hospital of Basel according to the animal protection law in Switzerland. For all experiments, male or female sex-matched mice were used that were at least 6 weeks old at the time point of infection. The following mouse strains were used: C57BL/6 CD45.2, SMARTA Ly5.1, $CD74^{-/-}$. Mice were injected with intraperitoneal injection of $2x10^5$ FFU for Armstrong variants or via intravenous injection of $2x10^6$ FFU for Clone-13 variants.

NICD-protector

Mice were intravenously (i.v.) injected with 12.5µg homemade ARTC2.2-blocking nanobody s+16 (NICD-protector) at least 15 minutes prior to organ harvest.

Adoptive cell transfer

Single-cell suspensions of cells were prepared from lymph nodes by mashing and filtering through a 100µm strainer. Naïve Smarta cells were enriched using Naïve CD4 T cell isolation kit (StemCell). $1x10^4$ SMARTA Ly5.1 cells were adoptively transferred into Ly5.2 recipients via intravenous injection as previously described (*60*).

Flow Cytometry

Spleens were removed and single-cell suspensions were generated by mashing and filtering the spleens through a 100µm strainer followed by erythrocytes lysing using Ammonium-Chloride-Potassium (ACK) lysis buffer. SMARTA and endogenous LCMV-specific CD4 T cells were analyzed using IAb:NP309-328 (PE) or IAb:GP66-77 (APC) (provided by NIH tetramer core) tetramer. Following staining for 1 hour at room

446 temperature in the presence of 50nM Dasatinib, tetramer-binding cells were enriched
447 using magnetic beads and counted as previously published (*60*). Surface combined
448 with viability staining was performed for 30min on ice. For transcription factor staining,
449 fixation and permeabilization was performed according to the Foxp3/Transcription
450 Factor staining kit (eBioscience). Samples were analyzed on Fortessa LSR II or Canto
451 II cytometers (BD Biosciences) followed by data analysis with FlowJo X software
452 (TreeStar). $CD4^+$ T cells were pre-gated on lymphocytes in FSC/SSC, dump-, live
453 $CD4^+$ cells and then further gated on $CD44^+$ $Tetramer^-$ to assess the $CD44^+$
454 compartment, $CD44^+$ $CD45.1^+$ $GP66^+$ for SMARTA and $CD44^+$ $NP309^+$ for NP-specific
455 cells.
456 The following antibodies were used: CD4 (BUV496, GK1.5, BD, #564667; APC
457 eFluor780, GK1.5, eBioscience, #47-0041-82), CD11b (PE-Cy5, M1/70, BioLegend,
458 #101222), B220 (PE-Cy5, RA3-6B2, BioLegend, #103210, PE-Cy7, RA3-6B2,
459 BioLegend, #103222), CD11c (PE-Cy5, N418, BioLegend, #117316; AF647, N418,
460 BioLegend, #117312), CD44 (BUV395, IM7, BD), CD45.1 (FITC, A20, BD, #553775;
461 APC, A20, eBioscience, #17-0453-82), CD45.2 (APC-Fire, 104, BioLegend,
462 #109852), CD69 (PE, H1.2F3, eBioscience), CD62L (APC, MEL-14, BD, #553152),
463 PSGL-1 (BV605, 2PH1, BD, #740384), PD1 (BV785, 29F.1A12, BioLegend,
464 #135225), Vα2 TCR (PE, B20.1, eBioscience, #12-5812-82; FITC, B20.1,
465 eBioscience, #11-5812-82), Vβ8.3 TCR (FITC, 1B3.3, BD, #553663), F4/80 (PE-Cy5,
466 BM8, BioLegend, #123112), I-Ab (PE, AF6-120.1, BD, #553552), FR4 (PE-Cy7, 12A5,
467 BioLegend, #125012), Ly6C (BV510, HK1.4, BioLegend, #128033), Bcl6 (BV421,
468 K112-91, BD, #563363), T-bet (BV711, 4B10, BioLegend, #644820), TOX (PE,
469 TXRX10, eBioscience, #12-6502-82), Lag3 (BV421, C9B7W, BioLegend, #125221),

TCF1 (AF700, 812145, R&D Systems, #FAB8224N), Zombie Fixable Viability Dye (Zombie Red, BioLegend, #423110).

CD69 SMARTA activation assays

Serial dilutions of the GP61-wt peptide or APLs were plated. $5x10^5$ Ly5.2 Splenocytes and $1x10^5$ Ly5.1 SMARTA cells per well were added to the dilution series, stimulated overnight at 37°C, and subsequently stained and analyzed at the flow cytometer.

MHC-II out-competition assays

$CD74^{-/-}$ splenocytes were cultured with a custom made GP61-FITC at a fixed concentration of $1x10^{-6}$ M and various serial dilutions of GP61-wt or APLs for 4 hours at 37°C. After stimulation, the cells were stained and analyzed at the flow cytometer. The FITC-labelled GP61 peptide was custom made by Eurogentec.

Statistical analysis

Geometric mean was used to determine the mean fluorescence intensity (MFI) and values were normalized to the mean of the control group from each experiment before data was pooled. Pooled and normalized MFIs are referred to as relative MFI. EC_{50} values were calculated using a sigmoidal dose-response fit in GraphPad Prism (version 8). For statistical analysis of one parameter between two groups, unpaired two-tailed Student's t-tests were used to determine statistical significance. To compare one parameter between more than two groups, one-way analysis of variance (ANOVA) was used followed by Turkey's post-test for multiple comparisons. P values are indicated on the graphs. Data was analyzed using GraphPad Prism software (version 8).

4. DISCUSSION

4.1. Project #1: Long-lived Tfh cells

Tfh memory & NAD induced cell death

We and others found that Tfh cells in contrast to other CD4 T cell subsets express high levels of the stimulatory, ATP-gated ion channel P2X7R (*216, 265, 266*). Besides the classical pathway via ATP, P2X7R can be activated in an alternative way: NAD can trigger the enzyme ARTC2.2 to ADP-ribosylate P2X7R, which leads to the continuous activation of P2X7R and ultimately to cell death (*266*). Cell populations that have previously been reported to be susceptible to NICD are splenic CD4 Tregs, and non-SLO resident CD8 T cells and NK T cells (*267-270*). This finding can at least partially be attributed to the isolation techniques of cells from different organs. Cell preparation at 37°C but not at 4°C leads to externalization of phosphatidylserine due to P2X7R activation (*271*). The common procedure to isolate CD8 T cells from the spleen is to mash the organ through a cell strainer to generate a single cell suspension followed by surface or tetramer staining at 4°C. However, most T cell isolation techniques from non-SLO tissues rely on a digestion reaction carried out at 37°C. Tissue destruction inducing NAD release combined with the incubation temperature during digestion facilitates NICD.

In comparison to CD8 T cells, CD4 T cells are more difficult to stain with tetramer due to lower affinity of TCR/pMHC interactions in class II vs class I restricted T cells (*272*). Thus, in order to increase the signal, tetramer staining of CD4 T cells is usually performed at room temperature or 37°C for at least 1 hour. This renders splenic CD4 T cells but not splenic CD8 T cells potentially susceptible to NICD. We found that in line with the high levels of P2X7R expression, splenic Tfh cells are long-lived but compared to other CD4 subsets extremely susceptible to NICD during tissue isolation. NICD occurs at memory time points (>30 days p.i.) but also at the late effector response (day 15 p.i.). However, since Tfh cells are abundant at the late effector time point, some proportion of Tfh cells can still be recovered. In contrast,

>30 days p.i. Tfh cells are basically absent and therefore have previously been overlooked. Notably, TCR stimulation leads to the downregulation of P2X7R and might provide an additional reason why NICD is more pronounced at memory time points due to decreased antigen signaling after clearance of the pathogen (*266*). By inhibiting NICD through intravenous administration of NICD-protector 15 minutes prior to sacrificing the mouse we were able to increase the recovery of Tfh cells at all time points thereby enabling the study of a previously invisible Tfh memory population with increased CXCR5 and PD1 expression. NICD previously prevented the characterization of bona fide Tfh memory cells which at least partially explains the controversial results from previous studies on Tfh persistence. From an evolutionary point of view, the fact that TCR engagement leads to P2X7R down-regulation might indicate that NICD in Tfh exists to limit bystander Tfh activation which could obscure the antigen-specific humoral response or induce autoimmune diseases (*273*).

Interestingly, when looking at TCR transgenic cells specific for the glycoprotein (SMARTA) or nucleoprotein (NIP) of LCMV, we saw an impairment in Tfh memory generation in both TCR-transgenic but not in the polyclonal compartment from the same mouse. Why TCR-transgenic T cells fail to efficiently generate Tfh memory cells but show no defect in generating Tfh effectors requires further investigation. We speculate that there is a cell-intrinsic defect preventing SMARTA and NIP cells from generating Tfh memory cells as transfer of high and low numbers of naïve transgenic CD4 T cells, which could potentially skew the immune response more to one or another subset, didn't improve the Tfh memory recovery. Additionally, the fact that the polyclonal compartment from the same mouse shows no impairment in Tfh memory generation excludes a role of the environment on impairment of Tfh memory. In agreement with this, a study has previously shown that TCR transgenic cells don't reflect the full breadth of a polyclonal CD4 T cell response and instead stick to a certain differentiation pattern (*54*). Furthermore, a recent publication indicates that the TCR of Tfh and non-Tfh cells clonally diverges and that Tfh cells preferentially react to slightly different epitopes than non Tfh cells (*57*). Therefore, one way to overcome the limitation of Tfh memory generation in TCR transgenic systems would be to reverse engineer a TCR by sorting Tfh

memory cells from a polyclonal compartment, sequence the TCR and then use the sequenced TCR to generate a new transgenic mouse.

Tfh memory survival requirements

Due to the fact that Tfh memory cells have previously been overlooked, very little is known about their survival requirements. Quiescent T memory cells have been described to mainly rely on OXPHOS for energy production, whereas effector cells additionally engage extensive glycolysis to meet their energetic demand (*274*). Within the memory compartment, despite decreased energetic needs Tem cells seem to be more closely related to effector T cells than to Tcm in regard to their metabolic state. Surprisingly, we found that Tfh memory cells in comparison to Th1 memory cells (also referred to as Tem in viral infection models) rely on increased glucose uptake even >400 days after infection, which correlates with increased ECAR in metabolic flux analysis and increased mTORc1 activity. Blocking glycolysis/mTOR using 2-DG/rapamycin treatment resulted in a decreased Tfh memory survival, while other compartments were unaffected.

This finding opens up several questions: What triggers mTORc1 activity? Is the requirement for glucose an adaptation to the nutrient poor or hypoxic environment the cells are localized in? What is glucose used for in Tfh memory cells? Glucose can be used in several ways, as a source for OXPHOS, fueling the pentose phosphate pathway (PPP) crucial for NADPH and nucleotide production, or as a source of acetyl groups used for epigenetic modifications. These questions could theoretically be addressed with ^{13}C-glucose tracing experiments. However, this assay requires a high number of cells that cannot be reached with Tfh memory cells isolated from mice without using an unethical number of mice. Nevertheless, recent advances in the Crispr/Cas9 methodology potentially allow for specific deletion of certain key enzymes at specific checkpoints in metabolic pathways thereby allowing the investigation of resource use in a more precise way (*275*). The use of Crispr/Cas9 additionally allows one to circumvent the limitations of metabolic assays performed in this project which are relying on *ex vivo* studies under unphysiological conditions (e.g. increased oxygen

tension) which could induce changes in the metabolic state. Isolation of the cells from organs can also impact their metabolic fitness as exemplified by the glucose uptake in Tfh memory cells: Tfh memory cells only take up glucose if previously treated with NICD protector (*265*). Additionally, blocking of glycolysis and mTOR using 2-DG and Rapamycin is rather unspecific and likely has off target effects. For example, 2-DG can be taken up into the cells but its degradation into 2DG-6-phosphate, which is the first step in glycolysis and important to feed the PPP, is inhibited by its structure and thereby not only leads to blockade of ATP generation but also prevents PPP activity or acetyl-CoA synthesis for epigenetic modifications (*276*). However, specifically targeting the enzyme Pgi which is downstream of Glucose-6-phosphate would allow the assessment of the impact of glycolysis on cell survival without affecting the PPP activity. Ideally, the Crispr/Cas9 approach should be paired with an imaging technique like fluorescent microscopy of whole organs or intravital imaging in order to circumvent tissue isolation of the target population. Thereby, the metabolic requirements could be determined without any mayor flaw in the experimental setup, all assuming a new TCR transgenic mouse becomes available that efficiently generates Tfh memory cells.

Another important question that has not been fully addressed in this project is whether Tfh memory cells need cognate antigenic stimulation for survival. Long-term T cell survival in the absence of cognate antigen has been defined as a hallmark feature of memory T cells (*277*). Adoptive transfer experiments into infection matched or naïve mice paired with the weak correlation of PD-1 and Nur77 expression (both readouts for TCR activity) indicate that Tfh memory cells are able to survive in the absence of cognate antigen, but do better in its presence. Furthermore, TCR signaling could be one (of many) possible triggers of mTORc1. However, it's possible that Nur77 expression can be induced by other stimuli than TCR signaling and adoptive transfer experiments are very unphysiological. Therefore, a better approach to tackle antigen requirement would be to assess survival upon inducible deletion of MHCII on antigen presenting cells or the TCRα/β chain on T cells. This approach would allow one to address antigen dependence over a prolonged time period without having to

transfer memory T cells thereby circumventing a poor take rate in recipient mice and the potential alteration of their survival capacity by the transfer procedure.

Tfh memory function

Our data revealed a surprising role for Tfh memory cells in sustaining the late humoral response (> day 50 p.i.) which is at least partially mediated through ICOS-ICOSL interactions. When inhibiting ICOS signaling, we found a 50% reduction of LCMV NP-specific IgG antibody titers in the serum and a reduction in splenic but not bone marrow derived antibody producing cells. One possibility is that at this time point, there is still an ongoing differentiation of GL7+ GC or ex-GC B cells into SLPC fueled by persisting antigen consistent with an older hypothesis (*278*). In line with this, we noted a decrease in GL7+ NP-specific B cells upon blockade of ICOS-ICOSL signaling. However, the GL7+ cells displayed an unusual GC B cell phenotype lacking Fas expression, another hallmark marker for GC B cells, indicating that they might have undergone germinal center reaction but recently emigrated. This hypothesis is challenged by the fact that we were not able to detect germinal centers 50 days after infection by histology, indicating that the ongoing germinal center response had already decayed which makes it unlikely that ongoing differentiation at a very low level is responsible for 50% of the total NP specific IgG antibodies in the serum. Yet, it remains open whether NP-specific antibody levels decrease to the same extent when ICOS signaling is blocked at very late time points, e.g. 300 days after infection. If a similar observation could be made at day 300 p.i., this would further decrease the likelihood that ongoing differentiation of B cells into plasma cells is occurring since it's unlikely that antigen from an acute infection would persist up to that time point. The observation that germinal centers are absent at day 50 p.i. opens up an alternative possibility in which Tfh cells might play a role in maintaining LLPCs in the spleen. It was previously reported that the splenic compartment contains LLPCs, however, the bone marrow was identified as the major reservoir (roughly 80-90%) (*279*). Since the splenic compartment contributes approximately 50% of the NP-specific IgG titers suggests that either

a) splenic LLPC numbers have been previously underestimated or b) splenic LLPCs have a higher antibody output. Plasma cell numbers from the bone marrow were traditionally estimated based on ^{59}Fe labeling studies which indicated that the femur contains approximately 6% of total bone marrow cells (*280-282*). Subsequently, this value was used as a conversion factor to estimate total bone marrow cell numbers based on the cells recovered from femurs. Isolation and identification of plasma cells from the bone marrow compartments femur, tibia, humerus, rib and sternum revealed no difference in ASC activity and lead to the assumption that all compartments have equivalent ASC activity with the caveat that some bones were precluded from the analysis due to their small size. In contrast, a more recent study in macaques showed that ASC tend to accumulate in femur, tibia and humerus while other bone marrow sites like radius, vertebrae or iliac crest show decreased ASC activity thereby challenging the current conversion factor used to estimate ASC numbers in mice from the femur (*283*). Unfortunately, technical limitations make it challenging to identify antigen-specific plasma cells, discriminate SLPCs from LLPCs and quantify their antibody output since plasma cells express few surface proteins. However, one could investigate the localization of long-lived Tfh cells by histology within the spleen to assess whether Tfh memory cells are in close proximity to the red pulp and therefore co-localize with splenic plasma cells previously identified in this area (*284*).

How can Tfh memory cells facilitate help to antibody secreting cells (ASC) mechanistically? Not much is known about the survival requirements of LLPCs, yet certain factors like IL-6, IL-21, or B-cell activating factor (BAFF) have been linked to contributing to plasma cell maintenance and simultaneously can be produced by the CD4 compartment (*285, 286*). Another possibility is that CD4 Tfh cells support plasma cell survival indirectly by maintaining the structural organization within the spleen. Consequently, anti-ICOSL treatment resulting in impaired Tfh memory survival could lead to the destruction of the structural organization and dissolve the plasma cell niche.

Tfh memory classification & plasticity

Since the discovery of the two distinct circulating memory subsets Tem and Tcm the field has been interested in what the functional differences and relations of these subsets are to each other (*214*). The current dogma states that Tem can instantly produce inflammatory cytokines upon reencountering the pathogen but show limited proliferation potential, whereas Tcm are thought to represent a less differentiated "stem-like" compartment, having limited effector functions but secreting large amounts of IL-2 and maintaining high proliferative potential. Since it was controversial whether long-lived Tfh cells exist, it was unclear how these cells would fit into the current CD4 memory model. Using scRNA Seq, we identified folate receptor 4 (FR4) as a marker to clearly discriminate Tcm from Tfh memory cells. Surprisingly, we found that 400 days after infection the Tcm compartment was absent whereas the Tem compartment, in our infection model also referred to as Th1 memory, and the Tfh memory compartment persisted, thereby challenging the current dogma that Tcm cells represent the stem compartment. The data further indicates that the Tcm compartment might not represent the best target to generate an efficient vaccine. Tem and Tcm cells have been discriminated by the expression of CD62L and CCR7: Tem cells are $CCR7^{-}CD62L^{-}$, whereas Tcm are $CCR7^{+}CD62L^{+}$ (*214*). Despite the vast overlap of surface marker and transcription factors between Tcm and Tfh memory and their high proliferation potential, Tfh memory cells can be considered as Tem by their CCR7 and CD62L expression. However, Tfh cells are stingy cytokine producers and therefore miss a hallmark feature of Tem, the immediate ability to secrete inflammatory cytokines upon reactivation. Additionally, Tfh cells show an enrichment in genes associated with tissue residency, indicating that they might be spleen resident thereby differing in their migration pattern from both Tem and Tcm. In summary, this indicates that the current CD4 memory model is oversimplified as Tfh memory cells don't fit in any of the currently widely accepted memory subsets Tem, Tcm or Trm. However, out of the three, Tfh memory cells might fit best into the SLO Trm compartment also shown to exist in CD8 T cells (*287*).

We also identified a TCF1/Wnt pathway signature in Tfh cells associated with stem-like properties and subsequent transfer experiments revealed full plasticity: only the Tfh memory compartment could generate all 3 effector subsets. In contrast, cell fates of Tcm and Th1 memory cells were more fixed. These data suggest that Tfh memory cells might serve as a stem-like reservoir capable of replenishing other CD4 memory subsets like Tcm and Tem. Due to the pluripotent potential, Tfh memory cells could be seen as a less differentiated cell type or as the default differentiation pathway of a naive CD4 T cell. However, a recent publication indicates that Tfh cell differentiation is not the default pathway, as CD4 cells deficient in Bcl6 and Blimp-1 (important for Th1 differentiation) don't generate Tfh cells (*288*). Why Tfh but not Th1 memory cells maintain plasticity and are able to undergo transcriptional reprogramming requires further investigation. However, one major limitation of our approach is the unphysiological setting of the transfer experiment, where cells are removed from their tissue microenvironment which might lead to a forced adaptation to the conditions in the circulation. Further studies will be required to investigate whether Tfh cells can also trans-differentiate into Tcm or Tem *in vivo*. Additionally, stronger evidence of Tfh memory flexibility could be provided by showing plasticity on single cell level, e.g. with time lapse microscopy or intravital imaging of transcription factor reporter mice.

Tfh memory as a vaccine target

To date, vaccine approaches inducing a potent Tfh response scarcely exist. However, based on our data, Tfh memory cells provide an attractive vaccine target because of a) their important role in shaping and potentiating the humoral response and b) their developmental plasticity which potentially allows trans-differentiation into Th1 cells thereby supporting the cell mediated response. Work by the Linterman lab has shown that stimulating human germinal center responses by using an adjuvant that acts on TLR-4 signaling called "GLA-SE" can increase long-lived antibody production (while maintaining the BCR mutation frequency) specific to Malaria and correlates with an increased proportion of circulating Tfh cells (*289*). Circulating Tfh cells are a proxy for the size of germinal center reactions in SLOs and have

been shown to be transcriptionally and clonally similar to GC Tfh cells in this particular infection model (*289*). Mechanistically, further investigations are required to understand how GLA-SE potentiates germinal center reactions, but it is likely indirectly by creating a different environment as TLR4 stimulation on naïve CD4 T cells was found to be irrelevant for T helper differentiation (*290*) . The Tfh memory response can likely be further potentiated by combining the adjuvant GLA-SE to the ideal epitope that preferentially induces the differentiation of naïve CD4 T cells into Tfh cells (and B cell epitopes against which the antibodies should be formed) (Figure 4). A recent study revealed that there is little TCR sequence overlap between Tfh and non-Tfh cells (*57*). Surprisingly, there was also a very small overlap between Tfh and non-Tfh cells in terms of binding capacity of different peptides from Influenza hemagglutinin (HA) (*57*). Therefore, the pMHCII/TCR interaction between APCs and T cells is likely impacting the differentiation of naïve CD4 T cells, nudging them to become a Tfh or a non-Tfh cell. Identifying the epitope generating the strongest skew towards Tfh would therefore help to maximize the Tfh pool.

In which scenarios could targeting Tfh cells be beneficial over classical vaccine approaches? In the case of influenza, we predict the dominant virus strain of the upcoming season and generate a vaccine based on the prediction. We have to undergo this yearly routine because influenza viruses are highly mutative and the antibody response is directed against non-conserved regions that fail to facilitate cross-protection to upcoming strains. In contrast, CD4 T cells can react to conserved epitopes and therefore might enable a more flexible humoral response facilitating universal influenza protection (*291*). Therefore, Tfh memory could be beneficial in a scenario where viruses are slightly mutated from the parent strain. Another example might be Tuberculosis (Tb): CD4 T cells, especially Th1 cells that secrete IFN-γ are crucial for control as mice and human with a genetic deficiency are unable to control Tb (*292-294*). Recently, the vaccine candidate MVA85A targeting the CD4 response was developed and tested in humans. Unfortunately, despite stimulating a potent Th1 response, the results were disappointing, showing no statistical improvement in protection compared to the low efficacy BCG vaccine (*295*). A potential explanation for the lack of

protection is that the vaccine-induced Th1 cells were found to efficiently produce IFN-γ but are short lived and therefore decrease in numbers over time (*296*). However, in mice a Tfh-like population can be found upon Tb infection in the lung (*296*). Since we observed that Tfh memory cells retain plasticity, generating a vaccine that induces a more balanced response might provide a pool of “stem-like” Tfh cells that are able to replenish the Th1 effector pool and thereby contribute to protection.

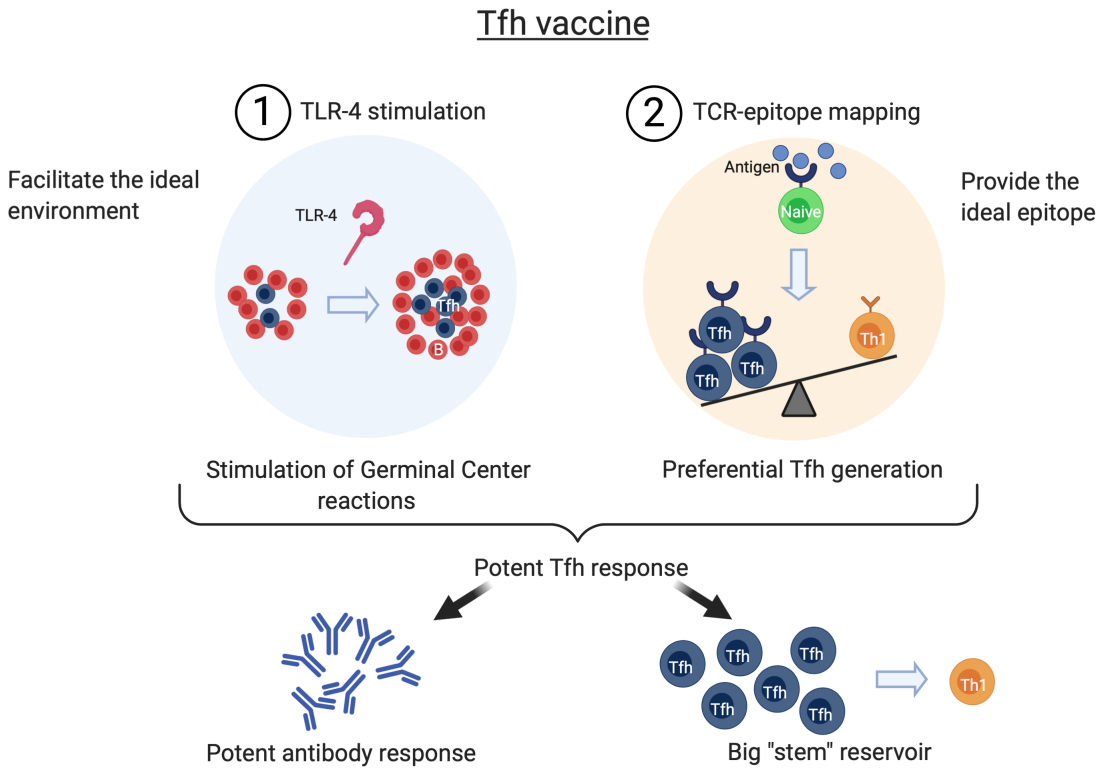

Figure 4: Schematic to induce a potent Tfh response. To maximize the Tfh response, one could combine the adjuvant GLA-SE which facilitates a beneficial environment for GC responses, with an antigen preferentially stimulating Tfh differentiation. The resulting Tfh pool could potentially sustain high levels of antigen-specific antibodies while still maintaining the potential to generate inflammatory Th1 effectors to stimulate the cell-mediated response if necessary.

4.2. Project #2: GP61 variants

A novel tool to study weakly stimulated CD4 T cells

Due to technical limitations, the impact of TCR signal strength on CD4 T cell differentiation has been difficult to study. One major limitation is that tetramer staining for CD4 T cells mostly captures T cells bearing high affinity receptors. However, weakly stimulated T cells that cannot be stained with tetramer but produce cytokines upon peptide stimulation can make up a high proportion of responding cells (*56*). Therefore, to study TCR signal strength researchers have mainly relied on TCR transgenic systems combined with altered peptide ligands (APL) to model different levels of stimulation through the TCR (*41, 47*). However, in contrast to CD8 T cells, only few APL systems are available for the CD4 compartment, and none have been incorporated into viral infection models. The disadvantage of our model is that mutating the glycoprotein of the virus comes at a cost of decreased viral fitness/persistence within 2 weeks. Combined with the impaired Tfh memory generation in SMARTA cells, it might not be possible to adequately study late T cell exhaustion in this setup (*265*). However, the observed effect on the early exhaustion phenotype cannot be explained solely by the lack of viral fitness, as the antigen experienced $CD44^+$ compartment showed similar levels of chronically activated $PD1^+$ $Lag3^+$ double-positive T cells in all Clone-13 strains, indicating that this tool is suitable to study early processes inducing T cell exhaustion in the CD4 compartment. Furthermore, it can be used to study various other immunological contexts, e.g. how TCR signal strength impacts tissue resident memory generation, recall responses, Treg differentiation or tumor-restricted effectors. Therefore, this tool fills an important research gap and is a contribution to the field of CD4 T cell immunology.

TCR signal strength exerts opposite effects on CD4 T cells

The impact of TCR signal strength on the CD4 response in the acute Armstrong variants confirms what has previously been shown in bacterial infection models: Th1 induction positively correlated with TCR affinity at the expense of Tfh generation (*41, 54*). In contrast,

peptide and sheep red blood cell immunization demonstrated a requirement for high affinity antigen to efficiently generate Tfh cells (*48, 50*). However, antigen presentation is likely not sustained in these models, and additional factors like different infection-induced inflammatory environments, antigen localization or using a polyclonal vs monoclonal approach might explain the opposing results.

The expansion of SMARTA T cells correlated with the TCR signal strength in both Armstrong and Clone-13 variants which is in line with previous reports (*41*). However, prolonged TCR signaling in Clone-13 variants can at least partially compensate the expansion deficit of cells receiving weak TCR signal in the acute setting as exemplified by the Y72F variant. The increase in recovered SMARTA cells is roughly two-fold, with the caveat that the mice were harvested at slightly different time points. In contrast, the GP61 wt Armstrong variant yielded approximately four-fold more SMARTA cells than its Clone-13 counterpart. These observations suggest that continuous TCR signal can have different effects on the clonal expansion depending on whether the TCR signal is weak or strong.

In terms of CD4 differentiation in Clone-13 variants, we observed the opposite effect of the acute setting: TCR signal strength positively correlated with Tfh induction at the expense of Th1 cells. How can the opposite effect be explained? One possibility is that prolonged antigen presentation limits the Th1 response a) by increased susceptibility of Th1 cells to activation induced cell death and/or b) increased susceptibility to T cell exhaustion suggested by the elevated expression of the exhaustion regulator TOX in the Th1 compartment in our data (*297*). Why strongly stimulated Th1 cells appear to be more susceptible to TOX upregulation requires further investigation. One possibility is that the different localization of Th1 and Tfh cells within the spleen plays a role. Tfh cells might sit in a more “protected” environment after reaching the B cell follicle. In contrast, Th1 cells situated in the red pulp, which functions as an antigen filter from the blood, might be exposed to higher levels of antigen. Due to the inability to quantify antigen levels *in vivo*, this hypothesis cannot be addressed adequately. Notably, weakly stimulated Th1 cells showed decreased acquisition of chronic activation markers, suggesting that these cells might be more resistant to exhaustion.

Another possibility is that the altered inflammatory environment in Clone-13 infection compared to Armstrong infection contributes to the opposing effects of TCR signal strength. It has previously been shown that TCR signal strength positively correlates with IL-10 induction in T cells in the presence of IFNα and therefore might limit Th1 differentiation to ultimately protect the host from an excessive inflammatory response (*298-300*). It will be important to assess how TCR signal strength in the distinct infection contexts influences cytokine production as well as expression of cytokine receptors.

In summary, our data are in favor of a goldilocks model, where the right amount of cumulative TCR signal favors a Th1 skewed response. This also indicates that TCR signal strength exerts different effects on CD4 differentiation bias based on the immunological context. From an evolutionary point of view, the limitation of the Th1 response might be beneficial to prevent excessive inflammation and thereby limit immunopathology. It remains open how weakly stimulated T cells can be specifically targeted for robust expansion and whether these cells are beneficial in the treatment of chronic diseases like HIV or cancer due to their increased resistance to the acquisition of chronic activation and exhaustion markers.

5. REFERENCES

1. R. Ahmed, D. Gray, Immunological memory and protective immunity: understanding their relation. *Science* **272**, 54-60 (1996).
2. F. E. Andre *et al.*, Vaccination greatly reduces disease, disability, death and inequity worldwide. *Bull World Health Organ* **86**, 140-146 (2008).
3. B. Greenwood, The contribution of vaccination to global health: past, present and future. *Philos Trans R Soc Lond B Biol Sci* **369**, 20130433 (2014).
4. M. Doherty, P. Buchy, B. Standaert, C. Giaquinto, D. Prado-Cohrs, Vaccine impact: Benefits for human health. *Vaccine* **34**, 6707-6714 (2016).
5. S. Riedel, Edward Jenner and the history of smallpox and vaccination. *Proc (Bayl Univ Med Cent)* **18**, 21-25 (2005).
6. P. E. Fine, U. K. Griffiths, Global poliomyelitis eradication: status and implications. *Lancet* **369**, 1321-1322 (2007).
7. C. P. Muller *et al.*, Reducing global disease burden of measles and rubella: Report of the WHO Steering Committee on research related to measles and rubella vaccines and vaccination, 2005. *Vaccine* **25**, 1-9 (2007).
8. I. Delany, R. Rappuoli, E. De Gregorio, Vaccines for the 21st century. *EMBO Mol Med* **6**, 708-720 (2014).
9. H. I. Nakaya, B. Pulendran, Vaccinology in the era of high-throughput biology. *Philos Trans R Soc Lond B Biol Sci* **370**, (2015).
10. S. H. Kaufmann, The contribution of immunology to the rational design of novel antibacterial vaccines. *Nat Rev Microbiol* **5**, 491-504 (2007).
11. B. Pulendran, Immunology taught by vaccines. *Science* **366**, 1074-1075 (2019).
12. M. M. Davis *et al.*, Ligand recognition by alpha beta T cell receptors. *Annu Rev Immunol* **16**, 523-544 (1998).
13. S. Crotty, Follicular helper CD4 T cells (TFH). *Annu Rev Immunol* **29**, 621-663 (2011).
14. I. Raphael, S. Nalawade, T. N. Eagar, T. G. Forsthuber, T cell subsets and their signature cytokines in autoimmune and inflammatory diseases. *Cytokine* **74**, 5-17 (2015).
15. V. T. Marchesi, J. L. Gowans, The Migration of Lymphocytes through the Endothelium of Venules in Lymph Nodes: An Electron Microscope Study. *Proc R Soc Lond B Biol Sci* **159**, 283-290 (1964).
16. J. L. Gowans, E. J. Knight, The Route of Re-Circulation of Lymphocytes in the Rat. *Proc R Soc Lond B Biol Sci* **159**, 257-282 (1964).
17. A. Pandit, R. J. De Boer, Stochastic Inheritance of Division and Death Times Determines the Size and Phenotype of CD8(+) T Cell Families. *Front Immunol* **10**, 436 (2019).
18. J. A. Maciolek, J. A. Pasternak, H. L. Wilson, Metabolism of activated T lymphocytes. *Curr Opin Immunol* **27**, 60-74 (2014).
19. J. C. Rathmell, Metabolism and autophagy in the immune system: immunometabolism comes of age. *Immunol Rev* **249**, 5-13 (2012).
20. E. A. Newsholme, B. Crabtree, M. S. Ardawi, The role of high rates of glycolysis and glutamine utilization in rapidly dividing cells. *Biosci Rep* **5**, 393-400 (1985).
21. S. Dimeloe, A. V. Burgener, J. Grahlert, C. Hess, T-cell metabolism governing activation, proliferation and differentiation; a modular view. *Immunology* **150**, 35-44 (2017).
22. J. Geginat *et al.*, Plasticity of human CD4 T cell subsets. *Front Immunol* **5**, 630 (2014).
23. M. S. Krangel, Mechanics of T cell receptor gene rearrangement. *Curr Opin Immunol* **21**, 133-139 (2009).

24. A. K. Sewell, Why must T cells be cross-reactive? *Nat Rev Immunol* **12**, 669-677 (2012).
25. D. Mason, A very high level of crossreactivity is an essential feature of the T-cell receptor. *Immunol Today* **19**, 395-404 (1998).
26. G. J. Kersh, P. M. Allen, Structural basis for T cell recognition of altered peptide ligands: a single T cell receptor can productively recognize a large continuum of related ligands. *J Exp Med* **184**, 1259-1268 (1996).
27. C. Viret, F. S. Wong, C. A. Janeway, Jr., Designing and maintaining the mature TCR repertoire: the continuum of self-peptide:self-MHC complex recognition. *Immunity* **10**, 559-568 (1999).
28. A. W. Goldrath, M. J. Bevan, Low-affinity ligands for the TCR drive proliferation of mature CD8+ T cells in lymphopenic hosts. *Immunity* **11**, 183-190 (1999).
29. B. Ernst, D. S. Lee, J. M. Chang, J. Sprent, C. D. Surh, The peptide ligands mediating positive selection in the thymus control T cell survival and homeostatic proliferation in the periphery. *Immunity* **11**, 173-181 (1999).
30. W. C. Kieper, J. T. Burghardt, C. D. Surh, A role for TCR affinity in regulating naive T cell homeostasis. *J Immunol* **172**, 40-44 (2004).
31. K. Hochweller *et al.*, Dendritic cells control T cell tonic signaling required for responsiveness to foreign antigen. *Proc Natl Acad Sci U S A* **107**, 5931-5936 (2010).
32. J. Juang *et al.*, Peptide-MHC heterodimers show that thymic positive selection requires a more restricted set of self-peptides than negative selection. *J Exp Med* **207**, 1223-1234 (2010).
33. A. H. Courtney, W. L. Lo, A. Weiss, TCR Signaling: Mechanisms of Initiation and Propagation. *Trends Biochem Sci* **43**, 108-123 (2018).
34. A. Weiss, D. R. Littman, Signal transduction by lymphocyte antigen receptors. *Cell* **76**, 263-274 (1994).
35. G. Furlan, T. Minowa, N. Hanagata, C. Kataoka-Hamai, Y. Kaizuka, Phosphatase CD45 both positively and negatively regulates T cell receptor phosphorylation in reconstituted membrane protein clusters. *J Biol Chem* **289**, 28514-28525 (2014).
36. G. Gaud, R. Lesourne, P. E. Love, Regulatory mechanisms in T cell receptor signalling. *Nat Rev Immunol* **18**, 485-497 (2018).
37. P. A. Thill, A. Weiss, A. K. Chakraborty, Phosphorylation of a Tyrosine Residue on Zap70 by Lck and Its Subsequent Binding via an SH2 Domain May Be a Key Gatekeeper of T Cell Receptor Signaling In Vivo. *Mol Cell Biol* **36**, 2396-2402 (2016).
38. L. Balagopalan, N. P. Coussens, E. Sherman, L. E. Samelson, C. L. Sommers, The LAT story: a tale of cooperativity, coordination, and choreography. *Cold Spring Harb Perspect Biol* **2**, a005512 (2010).
39. J. P. Snook, C. Kim, M. A. Williams, TCR signal strength controls the differentiation of CD4(+) effector and memory T cells. *Sci Immunol* **3**, (2018).
40. D. Zehn, S. Y. Lee, M. J. Bevan, Complete but curtailed T-cell response to very low-affinity antigen. *Nature* **458**, 211-214 (2009).
41. S. Keck *et al.*, Antigen affinity and antigen dose exert distinct influences on CD4 T-cell differentiation. *Proc Natl Acad Sci U S A* **111**, 14852-14857 (2014).
42. C. C. Govern, M. K. Paczosa, A. K. Chakraborty, E. S. Huseby, Fast on-rates allow short dwell time ligands to activate T cells. *Proc Natl Acad Sci U S A* **107**, 8724-8729 (2010).
43. R. A. Gottschalk *et al.*, Distinct influences of peptide-MHC quality and quantity on in vivo T-cell responses. *Proc Natl Acad Sci U S A* **109**, 881-886 (2012).
44. E. Corse, R. A. Gottschalk, J. P. Allison, Strength of TCR-peptide/MHC interactions and in vivo T cell responses. *J Immunol* **186**, 5039-5045 (2011).
45. H. A. Purvis *et al.*, Low-strength T-cell activation promotes Th17 responses. *Blood* **116**, 4829-4837 (2010).
46. E. L. Frost, A. E. Kersh, B. D. Evavold, A. E. Lukacher, Cutting Edge: Resident Memory CD8 T Cells Express High-Affinity TCRs. *J Immunol* **195**, 3520-3524 (2015).

47. V. Krishnamoorthy *et al.*, The IRF4 Gene Regulatory Module Functions as a Read-Write Integrator to Dynamically Coordinate T Helper Cell Fate. *Immunity* **47**, 481-497 e487 (2017).
48. N. Fazilleau, L. J. McHeyzer-Williams, H. Rosen, M. G. McHeyzer-Williams, The function of follicular helper T cells is regulated by the strength of T cell antigen receptor binding. *Nat Immunol* **10**, 375-384 (2009).
49. N. A. Hosken, K. Shibuya, A. W. Heath, K. M. Murphy, A. O'Garra, The effect of antigen dose on CD4+ T helper cell phenotype development in a T cell receptor-alpha beta-transgenic model. *J Exp Med* **182**, 1579-1584 (1995).
50. S. Hwang *et al.*, TCR ITAM multiplicity is required for the generation of follicular helper T-cells. *Nat Commun* **6**, 6982 (2015).
51. D. I. Kotov *et al.*, TCR Affinity Biases Th Cell Differentiation by Regulating CD25, Eef1e1, and Gbp2. *J Immunol* **202**, 2535-2545 (2019).
52. M. J. Ploquin, U. Eksmond, G. Kassiotis, B cells and TCR avidity determine distinct functions of CD4+ T cells in retroviral infection. *J Immunol* **187**, 3321-3330 (2011).
53. X. Tao, S. Constant, P. Jorritsma, K. Bottomly, Strength of TCR signal determines the costimulatory requirements for Th1 and Th2 CD4+ T cell differentiation. *J Immunol* **159**, 5956-5963 (1997).
54. N. J. Tubo *et al.*, Single naive CD4+ T cells from a diverse repertoire produce different effector cell types during infection. *Cell* **153**, 785-796 (2013).
55. D. DiToro *et al.*, Differential IL-2 expression defines developmental fates of follicular versus nonfollicular helper T cells. *Science* **361**, (2018).
56. R. J. Martinez, R. Andargachew, H. A. Martinez, B. D. Evavold, Low-affinity CD4+ T cells are major responders in the primary immune response. *Nat Commun* **7**, 13848 (2016).
57. E. Brenna *et al.*, CD4(+) T Follicular Helper Cells in Human Tonsils and Blood Are Clonally Convergent but Divergent from Non-Tfh CD4(+) Cells. *Cell Rep* **30**, 137-152 e135 (2020).
58. K. J. Lafferty, S. J. Prowse, C. J. Simeonovic, H. S. Warren, Immunobiology of tissue transplantation: a return to the passenger leukocyte concept. *Annu Rev Immunol* **1**, 143-173 (1983).
59. K. J. Lafferty, J. Woolnough, The origin and mechanism of the allograft reaction. *Immunol Rev* **35**, 231-262 (1977).
60. M. K. Jenkins, J. D. Ashwell, R. H. Schwartz, Allogeneic non-T spleen cells restore the responsiveness of normal T cell clones stimulated with antigen and chemically modified antigen-presenting cells. *J Immunol* **140**, 3324-3330 (1988).
61. P. Bretscher, M. Cohn, A theory of self-nonself discrimination. *Science* **169**, 1042-1049 (1970).
62. M. K. Jenkins, P. S. Taylor, S. D. Norton, K. B. Urdahl, CD28 delivers a costimulatory signal involved in antigen-specific IL-2 production by human T cells. *J Immunol* **147**, 2461-2466 (1991).
63. C. H. June, J. A. Ledbetter, M. M. Gillespie, T. Lindsten, C. B. Thompson, T-cell proliferation involving the CD28 pathway is associated with cyclosporine-resistant interleukin 2 gene expression. *Mol Cell Biol* **7**, 4472-4481 (1987).
64. P. S. Linsley, E. A. Clark, J. A. Ledbetter, T-cell antigen CD28 mediates adhesion with B cells by interacting with activation antigen B7/BB-1. *Proc Natl Acad Sci U S A* **87**, 5031-5035 (1990).
65. G. J. Freeman *et al.*, Murine B7-2, an alternative CTLA4 counter-receptor that costimulates T cell proliferation and interleukin 2 production. *J Exp Med* **178**, 2185-2192 (1993).
66. G. J. Freeman *et al.*, Cloning of B7-2: a CTLA-4 counter-receptor that costimulates human T cell proliferation. *Science* **262**, 909-911 (1993).
67. M. Azuma *et al.*, B70 antigen is a second ligand for CTLA-4 and CD28. *Nature* **366**, 76-79 (1993).

68. M. Karin, Y. Ben-Neriah, Phosphorylation meets ubiquitination: the control of NF-[kappa]B activity. *Annu Rev Immunol* **18**, 621-663 (2000).
69. M. Rincon, R. A. Flavell, AP-1 transcriptional activity requires both T-cell receptor-mediated and co-stimulatory signals in primary T lymphocytes. *EMBO J* **13**, 4370-4381 (1994).
70. K. Kalli, C. Huntoon, M. Bell, D. J. McKean, Mechanism responsible for T-cell antigen receptor- and CD28- or interleukin 1 (IL-1) receptor-initiated regulation of IL-2 gene expression by NF-kappaB. *Mol Cell Biol* **18**, 3140-3148 (1998).
71. C. E. Rudd, A. Taylor, H. Schneider, CD28 and CTLA-4 coreceptor expression and signal transduction. *Immunol Rev* **229**, 12-26 (2009).
72. K. V. Prasad *et al.*, T-cell antigen CD28 interacts with the lipid kinase phosphatidylinositol 3-kinase by a cytoplasmic Tyr(P)-Met-Xaa-Met motif. *Proc Natl Acad Sci U S A* **91**, 2834-2838 (1994).
73. A. August, B. Dupont, CD28 of T lymphocytes associates with phosphatidylinositol 3-kinase. *Int Immunol* **6**, 769-774 (1994).
74. F. Pages *et al.*, Binding of phosphatidylinositol-3-OH kinase to CD28 is required for T-cell signalling. *Nature* **369**, 327-329 (1994).
75. A. K. Stark, S. Sriskantharajah, E. M. Hessel, K. Okkenhaug, PI3K inhibitors in inflammation, autoimmunity and cancer. *Curr Opin Pharmacol* **23**, 82-91 (2015).
76. K. Okkenhaug, Signaling by the phosphoinositide 3-kinase family in immune cells. *Annu Rev Immunol* **31**, 675-704 (2013).
77. R. G. Jones *et al.*, CD28-dependent activation of protein kinase B/Akt blocks Fas-mediated apoptosis by preventing death-inducing signaling complex assembly. *J Exp Med* **196**, 335-348 (2002).
78. K. A. Frauwirth *et al.*, The CD28 signaling pathway regulates glucose metabolism. *Immunity* **16**, 769-777 (2002).
79. L. P. Kane, P. G. Andres, K. C. Howland, A. K. Abbas, A. Weiss, Akt provides the CD28 costimulatory signal for up-regulation of IL-2 and IFN-gamma but not TH2 cytokines. *Nat Immunol* **2**, 37-44 (2001).
80. W. Ouyang, M. O. Li, Foxo: in command of T lymphocyte homeostasis and tolerance. *Trends Immunol* **32**, 26-33 (2011).
81. C. E. Rudd, H. Schneider, Unifying concepts in CD28, ICOS and CTLA4 co-receptor signalling. *Nat Rev Immunol* **3**, 544-556 (2003).
82. K. S. Hathcock *et al.*, Identification of an alternative CTLA-4 ligand costimulatory for T cell activation. *Science* **262**, 905-907 (1993).
83. P. S. Linsley *et al.*, CTLA-4 is a second receptor for the B cell activation antigen B7. *J Exp Med* **174**, 561-569 (1991).
84. A. H. Sharpe, G. J. Freeman, The B7-CD28 superfamily. *Nat Rev Immunol* **2**, 116-126 (2002).
85. P. S. Linsley *et al.*, Intracellular trafficking of CTLA-4 and focal localization towards sites of TCR engagement. *Immunity* **4**, 535-543 (1996).
86. A. Hutloff *et al.*, ICOS is an inducible T-cell co-stimulator structurally and functionally related to CD28. *Nature* **397**, 263-266 (1999).
87. A. J. McAdam *et al.*, Mouse inducible costimulatory molecule (ICOS) expression is enhanced by CD28 costimulation and regulates differentiation of CD4+ T cells. *J Immunol* **165**, 5035-5040 (2000).
88. S. K. Yoshinaga *et al.*, T-cell co-stimulation through B7RP-1 and ICOS. *Nature* **402**, 827-832 (1999).
89. M. M. Swallow, J. J. Wallin, W. C. Sha, B7h, a novel costimulatory homolog of B7.1 and B7.2, is induced by TNFalpha. *Immunity* **11**, 423-432 (1999).
90. C. Fos *et al.*, ICOS ligation recruits the p50alpha PI3K regulatory subunit to the immunological synapse. *J Immunol* **181**, 1969-1977 (2008).
91. Y. Harada *et al.*, A single amino acid alteration in cytoplasmic domain determines IL-2 promoter activation by ligation of CD28 but not inducible costimulator (ICOS). *J Exp Med* **197**, 257-262 (2003).

92. D. J. Wikenheiser, J. S. Stumhofer, ICOS Co-Stimulation: Friend or Foe? *Front Immunol* **7**, 304 (2016).
93. J. Rolf *et al.*, Phosphoinositide 3-kinase activity in T cells regulates the magnitude of the germinal center reaction. *J Immunol* **185**, 4042-4052 (2010).
94. J. Li *et al.*, Phosphatidylinositol 3-kinase-independent signaling pathways contribute to ICOS-mediated T cell costimulation in acute graft-versus-host disease in mice. *J Immunol* **191**, 200-207 (2013).
95. C. Pedros *et al.*, A TRAF-like motif of the inducible costimulator ICOS controls development of germinal center TFH cells via the kinase TBK1. *Nat Immunol* **17**, 825-833 (2016).
96. D. R. Withers, Innate lymphoid cell regulation of adaptive immunity. *Immunology* **149**, 123-130 (2016).
97. M. H. Kaplan, Y. L. Sun, T. Hoey, M. J. Grusby, Impaired IL-12 responses and enhanced development of Th2 cells in Stat4-deficient mice. *Nature* **382**, 174-177 (1996).
98. M. Afkarian *et al.*, T-bet is a STAT1-induced regulator of IL-12R expression in naive CD4+ T cells. *Nat Immunol* **3**, 549-557 (2002).
99. V. T. Thieu *et al.*, Signal Transducer and Activator of Transcription 4 Is Required for the Transcription Factor T-bet to Promote T Helper 1 Cell-Fate Determination. *Immunity* **29**, 679-690 (2008).
100. S. J. Szabo *et al.*, A novel transcription factor, T-bet, directs Th1 lineage commitment. *Cell* **100**, 655-669 (2000).
101. J. Saravia, N. M. Chapman, H. Chi, Helper T cell differentiation. *Cell Mol Immunol* **16**, 634-643 (2019).
102. M. L. Robinette *et al.*, Transcriptional programs define molecular characteristics of innate lymphoid cell classes and subsets. *Nat Immunol* **16**, 306-317 (2015).
103. M. H. Kaplan, U. Schindler, S. T. Smiley, M. J. Grusby, Stat6 is required for mediating responses to IL-4 and for development of Th2 cells. *Immunity* **4**, 313-319 (1996).
104. K. Takeda *et al.*, Essential role of Stat6 in IL-4 signalling. *Nature* **380**, 627-630 (1996).
105. K. Shimoda *et al.*, Lack of IL-4-induced Th2 response and IgE class switching in mice with disrupted Stat6 gene. *Nature* **380**, 630-633 (1996).
106. W. Zheng, R. A. Flavell, The transcription factor GATA-3 is necessary and sufficient for Th2 cytokine gene expression in CD4 T cells. *Cell* **89**, 587-596 (1997).
107. D. H. Zhang, L. Cohn, P. Ray, K. Bottomly, A. Ray, Transcription factor GATA-3 is differentially expressed in murine Th1 and Th2 cells and controls Th2-specific expression of the interleukin-5 gene. *J Biol Chem* **272**, 21597-21603 (1997).
108. L. Zhou *et al.*, IL-6 programs T(H)-17 cell differentiation by promoting sequential engagement of the IL-21 and IL-23 pathways. *Nat Immunol* **8**, 967-974 (2007).
109. Ivanov, II *et al.*, The orphan nuclear receptor RORgammat directs the differentiation program of proinflammatory IL-17+ T helper cells. *Cell* **126**, 1121-1133 (2006).
110. R. I. Nurieva *et al.*, Generation of T follicular helper cells is mediated by interleukin-21 but independent of T helper 1, 2, or 17 cell lineages. *Immunity* **29**, 138-149 (2008).
111. R. Nurieva *et al.*, Essential autocrine regulation by IL-21 in the generation of inflammatory T cells. *Nature* **448**, 480-483 (2007).
112. T. Chtanova *et al.*, T follicular helper cells express a distinctive transcriptional profile, reflecting their role as non-Th1/Th2 effector cells that provide help for B cells. *J Immunol* **173**, 68-78 (2004).
113. C. H. Kim *et al.*, Unique gene expression program of human germinal center T helper cells. *Blood* **104**, 1952-1960 (2004).
114. R. I. Nurieva *et al.*, Bcl6 mediates the development of T follicular helper cells. *Science* **325**, 1001-1005 (2009).

115. R. J. Johnston *et al.*, Bcl6 and Blimp-1 are reciprocal and antagonistic regulators of T follicular helper cell differentiation. *Science* **325**, 1006-1010 (2009).
116. D. Yu *et al.*, The transcriptional repressor Bcl-6 directs T follicular helper cell lineage commitment. *Immunity* **31**, 457-468 (2009).
117. T. S. Davidson, R. J. DiPaolo, J. Andersson, E. M. Shevach, Cutting Edge: IL-2 is essential for TGF-beta-mediated induction of Foxp3+ T regulatory cells. *J Immunol* **178**, 4022-4026 (2007).
118. M. A. Burchill, J. Yang, C. Vogtenhuber, B. R. Blazar, M. A. Farrar, IL-2 receptor beta-dependent STAT5 activation is required for the development of Foxp3+ regulatory T cells. *J Immunol* **178**, 280-290 (2007).
119. J. D. Fontenot, M. A. Gavin, A. Y. Rudensky, Foxp3 programs the development and function of CD4+CD25+ regulatory T cells. *Nat Immunol* **4**, 330-336 (2003).
120. S. Hori, T. Nomura, S. Sakaguchi, Control of regulatory T cell development by the transcription factor Foxp3. *Science* **299**, 1057-1061 (2003).
121. K. K. McKinstry, T. M. Strutt, S. L. Swain, The potential of CD4 T-cell memory. *Immunology* **130**, 1-9 (2010).
122. K. J. Oestreich, S. E. Mohn, A. S. Weinmann, Molecular mechanisms that control the expression and activity of Bcl-6 in TH1 cells to regulate flexibility with a TFH-like gene profile. *Nat Immunol* **13**, 405-411 (2012).
123. L. M. Fahey *et al.*, Viral persistence redirects CD4 T cell differentiation toward T follicular helper cells. *J Exp Med* **208**, 987-999 (2011).
124. S. Nakayamada *et al.*, Early Th1 cell differentiation is marked by a Tfh cell-like transition. *Immunity* **35**, 919-931 (2011).
125. D. Fang *et al.*, Transient T-bet expression functionally specifies a distinct T follicular helper subset. *J Exp Med* **215**, 2705-2714 (2018).
126. I. M. Djuretic *et al.*, Transcription factors T-bet and Runx3 cooperate to activate Ifng and silence Il4 in T helper type 1 cells. *Nat Immunol* **8**, 145-153 (2007).
127. E. S. Hwang, S. J. Szabo, P. L. Schwartzberg, L. H. Glimcher, T helper cell fate specified by kinase-mediated interaction of T-bet with GATA-3. *Science* **307**, 430-433 (2005).
128. V. Lazarevic *et al.*, T-bet represses T(H)17 differentiation by preventing Runx1-mediated activation of the gene encoding RORgammat. *Nat Immunol* **12**, 96-104 (2011).
129. K. Kohu *et al.*, The Runx3 transcription factor augments Th1 and down-modulates Th2 phenotypes by interacting with and attenuating GATA3. *J Immunol* **183**, 7817-7824 (2009).
130. O. Komine *et al.*, The Runx1 transcription factor inhibits the differentiation of naive CD4+ T cells into the Th2 lineage by repressing GATA3 expression. *J Exp Med* **198**, 51-61 (2003).
131. B. J. Laidlaw, J. E. Craft, S. M. Kaech, The multifaceted role of CD4(+) T cells in CD8(+) T cell memory. *Nat Rev Immunol* **16**, 102-111 (2016).
132. S. R. Bennett, F. R. Carbone, F. Karamalis, J. F. Miller, W. R. Heath, Induction of a CD8+ cytotoxic T lymphocyte response by cross-priming requires cognate CD4+ T cell help. *J Exp Med* **186**, 65-70 (1997).
133. J. P. Ridge, F. Di Rosa, P. Matzinger, A conditioned dendritic cell can be a temporal bridge between a CD4+ T-helper and a T-killer cell. *Nature* **393**, 474-478 (1998).
134. F. Castellino *et al.*, Chemokines enhance immunity by guiding naive CD8+ T cells to sites of CD4+ T cell-dendritic cell interaction. *Nature* **440**, 890-895 (2006).
135. S. R. Bennett *et al.*, Help for cytotoxic-T-cell responses is mediated by CD40 signalling. *Nature* **393**, 478-480 (1998).
136. S. P. Schoenberger, R. E. Toes, E. I. van der Voort, R. Offringa, C. J. Melief, T-cell help for cytotoxic T lymphocytes is mediated by CD40-CD40L interactions. *Nature* **393**, 480-483 (1998).

137. J. L. Hor *et al.*, Spatiotemporally Distinct Interactions with Dendritic Cell Subsets Facilitates CD4+ and CD8+ T Cell Activation to Localized Viral Infection. *Immunity* **43**, 554-565 (2015).
138. C. Bourgeois, B. Rocha, C. Tanchot, A role for CD40 expression on CD8+ T cells in the generation of CD8+ T cell memory. *Science* **297**, 2060-2063 (2002).
139. E. B. Wilson, A. M. Livingstone, Cutting edge: CD4+ T cell-derived IL-2 is essential for help-dependent primary CD8+ T cell responses. *J Immunol* **181**, 7445-7448 (2008).
140. C. Sokke Umeshappa *et al.*, CD154 and IL-2 signaling of CD4+ T cells play a critical role in multiple phases of CD8+ CTL responses following adenovirus vaccination. *PLoS One* **7**, e47004 (2012).
141. M. Wiesel *et al.*, Th cells act via two synergistic pathways to promote antiviral CD8+ T cell responses. *J Immunol* **185**, 5188-5197 (2010).
142. M. F. Bachmann, P. Wolint, S. Walton, K. Schwarz, A. Oxenius, Differential role of IL-2R signaling for CD8+ T cell responses in acute and chronic viral infections. *Eur J Immunol* **37**, 1502-1512 (2007).
143. M. A. Williams, A. J. Tyznik, M. J. Bevan, Interleukin-2 signals during priming are required for secondary expansion of CD8+ memory T cells. *Nature* **441**, 890-893 (2006).
144. M. G. de Goer de Herve, S. Jaafoura, M. Vallee, Y. Taoufik, FoxP3(+) regulatory CD4 T cells control the generation of functional CD8 memory. *Nat Commun* **3**, 986 (2012).
145. V. Kalia *et al.*, Prolonged interleukin-2Ralpha expression on virus-specific CD8+ T cells favors terminal-effector differentiation in vivo. *Immunity* **32**, 91-103 (2010).
146. M. E. Pipkin *et al.*, Interleukin-2 and inflammation induce distinct transcriptional programs that promote the differentiation of effector cytolytic T cells. *Immunity* **32**, 79-90 (2010).
147. A. McNally, G. R. Hill, T. Sparwasser, R. Thomas, R. J. Steptoe, CD4+CD25+ regulatory T cells control CD8+ T-cell effector differentiation by modulating IL-2 homeostasis. *Proc Natl Acad Sci U S A* **108**, 7529-7534 (2011).
148. C. S. Hsieh *et al.*, Development of TH1 CD4+ T cells through IL-12 produced by Listeria-induced macrophages. *Science* **260**, 547-549 (1993).
149. M. A. Munoz-Fernandez, M. A. Fernandez, M. Fresno, Synergism between tumor necrosis factor-alpha and interferon-gamma on macrophage activation for the killing of intracellular Trypanosoma cruzi through a nitric oxide-dependent mechanism. *Eur J Immunol* **22**, 301-307 (1992).
150. P. J. Murray, T. A. Wynn, Protective and pathogenic functions of macrophage subsets. *Nat Rev Immunol* **11**, 723-737 (2011).
151. R. D. Stout, J. Suttles, J. Xu, I. S. Grewal, R. A. Flavell, Impaired T cell-mediated macrophage activation in CD40 ligand-deficient mice. *J Immunol* **156**, 8-11 (1996).
152. N. W. Lukacs, Migration of helper T-lymphocyte subsets into inflamed tissues. *J Allergy Clin Immunol* **106**, S264-269 (2000).
153. J. W. Griffith, C. L. Sokol, A. D. Luster, Chemokines and chemokine receptors: positioning cells for host defense and immunity. *Annu Rev Immunol* **32**, 659-702 (2014).
154. F. Sallusto *et al.*, Switch in chemokine receptor expression upon TCR stimulation reveals novel homing potential for recently activated T cells. *Eur J Immunol* **29**, 2037-2045 (1999).
155. C. R. Mackay, W. Marston, L. Dudler, Altered patterns of T cell migration through lymph nodes and skin following antigen challenge. *Eur J Immunol* **22**, 2205-2210 (1992).
156. D. Breitfeld *et al.*, Follicular B helper T cells express CXC chemokine receptor 5, localize to B cell follicles, and support immunoglobulin production. *J Exp Med* **192**, 1545-1552 (2000).

157. P. Schaerli *et al.*, CXC chemokine receptor 5 expression defines follicular homing T cells with B cell helper function. *J Exp Med* **192**, 1553-1562 (2000).
158. S. Crotty, T Follicular Helper Cell Differentiation, Function, and Roles in Disease. *Immunity* **41**, 529-542 (2014).
159. E. N. Arroyo, M. Pepper, B cells are sufficient to prime the dominant CD4+ Tfh response to Plasmodium infection. *J Exp Med* **217**, (2020).
160. Y. S. Choi *et al.*, ICOS receptor instructs T follicular helper cell versus effector cell differentiation via induction of the transcriptional repressor Bcl6. *Immunity* **34**, 932-946 (2011).
161. R. Goenka *et al.*, Cutting edge: dendritic cell-restricted antigen presentation initiates the follicular helper T cell program but cannot complete ultimate effector differentiation. *J Immunol* **187**, 1091-1095 (2011).
162. Y. S. Choi *et al.*, Bcl6 expressing follicular helper CD4 T cells are fate committed early and have the capacity to form memory. *J Immunol* **190**, 4014-4026 (2013).
163. M. Pepper, A. J. Pagan, B. Z. Igyarto, J. J. Taylor, M. K. Jenkins, Opposing signals from the Bcl6 transcription factor and the interleukin-2 receptor generate T helper 1 central and effector memory cells. *Immunity* **35**, 583-595 (2011).
164. Y. S. Choi, D. Eto, J. A. Yang, C. Lao, S. Crotty, Cutting edge: STAT1 is required for IL-6-mediated Bcl6 induction for early follicular helper cell differentiation. *J Immunol* **190**, 3049-3053 (2013).
165. X. Liu *et al.*, Transcription factor achaete-scute homologue 2 initiates follicular T-helper-cell development. *Nature* **507**, 513-518 (2014).
166. J. Y. Lee *et al.*, The transcription factor KLF2 restrains CD4(+) T follicular helper cell differentiation. *Immunity* **42**, 252-264 (2015).
167. J. P. Weber *et al.*, ICOS maintains the T follicular helper cell phenotype by down-regulating Kruppel-like factor 2. *J Exp Med* **212**, 217-233 (2015).
168. K. Hatzi *et al.*, BCL6 orchestrates Tfh cell differentiation via multiple distinct mechanisms. *J Exp Med* **212**, 539-553 (2015).
169. D. Paus *et al.*, Antigen recognition strength regulates the choice between extrafollicular plasma cell and germinal center B cell differentiation. *J Exp Med* **203**, 1081-1091 (2006).
170. J. J. Taylor, K. A. Pape, M. K. Jenkins, A germinal center-independent pathway generates unswitched memory B cells early in the primary response. *J Exp Med* **209**, 597-606 (2012).
171. I. C. MacLennan *et al.*, Extrafollicular antibody responses. *Immunol Rev* **194**, 8-18 (2003).
172. B. P. O'Connor *et al.*, Imprinting the fate of antigen-reactive B cells through the affinity of the B cell receptor. *J Immunol* **177**, 7723-7732 (2006).
173. G. D. Victora, M. C. Nussenzweig, Germinal centers. *Annu Rev Immunol* **30**, 429-457 (2012).
174. M. Muramatsu *et al.*, Specific expression of activation-induced cytidine deaminase (AID), a novel member of the RNA-editing deaminase family in germinal center B cells. *J Biol Chem* **274**, 18470-18476 (1999).
175. G. D. Victora *et al.*, Germinal center dynamics revealed by multiphoton microscopy with a photoactivatable fluorescent reporter. *Cell* **143**, 592-605 (2010).
176. A. D. Gitlin, Z. Shulman, M. C. Nussenzweig, Clonal selection in the germinal centre by regulated proliferation and hypermutation. *Nature* **509**, 637-640 (2014).
177. S. Crotty, T Follicular Helper Cell Biology: A Decade of Discovery and Diseases. *Immunity* **50**, 1132-1148 (2019).
178. C. G. Vinuesa, M. A. Linterman, D. Yu, I. C. MacLennan, Follicular Helper T Cells. *Annu Rev Immunol* **34**, 335-368 (2016).
179. T. G. Phan *et al.*, High affinity germinal center B cells are actively selected into the plasma cell compartment. *J Exp Med* **203**, 2419-2424 (2006).
180. R. Shinnakasu *et al.*, Regulated selection of germinal-center cells into the memory B cell compartment. *Nat Immunol* **17**, 861-869 (2016).

181. F. J. Weisel, G. V. Zuccarino-Catania, M. Chikina, M. J. Shlomchik, A Temporal Switch in the Germinal Center Determines Differential Output of Memory B and Plasma Cells. *Immunity* **44**, 116-130 (2016).
182. Y. Zhang *et al.*, Plasma cell output from germinal centers is regulated by signals from Tfh and stromal cells. *J Exp Med* **215**, 1227-1243 (2018).
183. W. Ise *et al.*, T Follicular Helper Cell-Germinal Center B Cell Interaction Strength Regulates Entry into Plasma Cell or Recycling Germinal Center Cell Fate. *Immunity* **48**, 702-715 e704 (2018).
184. N. J. Krautler *et al.*, Differentiation of germinal center B cells into plasma cells is initiated by high-affinity antigen and completed by Tfh cells. *J Exp Med* **214**, 1259-1267 (2017).
185. D. Suan *et al.*, CCR6 Defines Memory B Cell Precursors in Mouse and Human Germinal Centers, Revealing Light-Zone Location and Predominant Low Antigen Affinity. *Immunity* **47**, 1142-1153 e1144 (2017).
186. T. Yoshino *et al.*, Inverse expression of bcl-2 protein and Fas antigen in lymphoblasts in peripheral lymph nodes and activated peripheral blood T and B lymphocytes. *Blood* **83**, 1856-1861 (1994).
187. T. A. Schwickert *et al.*, A dynamic T cell-limited checkpoint regulates affinity-dependent B cell entry into the germinal center. *J Exp Med* **208**, 1243-1252 (2011).
188. E. Hams *et al.*, Blockade of B7-H1 (programmed death ligand 1) enhances humoral immunity by positively regulating the generation of T follicular helper cells. *J Immunol* **186**, 5648-5655 (2011).
189. N. Wittenbrink, A. Klein, A. A. Weiser, J. Schuchhardt, M. Or-Guil, Is there a typical germinal center? A large-scale immunohistological study on the cellular composition of germinal centers during the hapten-carrier-driven primary immune response in mice. *J Immunol* **187**, 6185-6196 (2011).
190. G. D. Victora *et al.*, Identification of human germinal center light and dark zone cells and their relationship to human B-cell lymphomas. *Blood* **120**, 2240-2248 (2012).
191. I. Yusuf *et al.*, Germinal center T follicular helper cell IL-4 production is dependent on signaling lymphocytic activation molecule receptor (CD150). *J Immunol* **185**, 190-202 (2010).
192. H. Qi, J. L. Cannons, F. Klauschen, P. L. Schwartzberg, R. N. Germain, SAP-controlled T-B cell interactions underlie germinal centre formation. *Nature* **455**, 764-769 (2008).
193. S. Crotty, E. N. Kersh, J. Cannons, P. L. Schwartzberg, R. Ahmed, SAP is required for generating long-term humoral immunity. *Nature* **421**, 282-287 (2003).
194. R. Morita *et al.*, Human blood CXCR5(+)CD4(+) T cells are counterparts of T follicular cells and contain specific subsets that differentially support antibody secretion. *Immunity* **34**, 108-121 (2011).
195. S. Crotty, Follicular Helper CD4 T Cells (TFH). *Annual Review of Immunology* **29**, 621-663 (2011).
196. D. T. Avery, V. L. Bryant, C. S. Ma, R. de Waal Malefyt, S. G. Tangye, IL-21-induced isotype switching to IgG and IgA by human naive B cells is differentially regulated by IL-4. *J Immunol* **181**, 1767-1779 (2008).
197. E. K. Deenick, C. S. Ma, The regulation and role of T follicular helper cells in immunity. *Immunology* **134**, 361-367 (2011).
198. R. Elgueta *et al.*, Molecular mechanism and function of CD40/CD40L engagement in the immune system. *Immunol Rev* **229**, 152-172 (2009).
199. R. J. Armitage *et al.*, Molecular and biological characterization of a murine ligand for CD40. *Nature* **357**, 80-82 (1992).
200. R. J. Noelle *et al.*, A 39-kDa protein on activated helper T cells binds CD40 and transduces the signal for cognate activation of B cells. *Proc Natl Acad Sci U S A* **89**, 6550-6554 (1992).
201. Z. Shulman *et al.*, Dynamic signaling by T follicular helper cells during germinal center B cell selection. *Science* **345**, 1058-1062 (2014).

202. D. Liu *et al.*, T-B-cell entanglement and ICOSL-driven feed-forward regulation of germinal centre reaction. *Nature* **517**, 214-218 (2015).
203. R. A. Cubas *et al.*, Inadequate T follicular cell help impairs B cell immunity during HIV infection. *Nat Med* **19**, 494-499 (2013).
204. L. Mesin, J. Ersching, G. D. Victora, Germinal Center B Cell Dynamics. *Immunity* **45**, 471-482 (2016).
205. S. L. Swain *et al.*, From naive to memory T cells. *Immunol Rev* **150**, 143-167 (1996).
206. M. S. F. Soon *et al.*, Transcriptome Dynamics Reveals Progressive Transition from Effector to Memory in CD4⁺ T cells. *bioRxiv*, 675967 (2019).
207. T. Ciucci *et al.*, The Emergence and Functional Fitness of Memory CD4(+) T Cells Require the Transcription Factor Thpok. *Immunity* **50**, 91-105 e104 (2019).
208. H. D. Marshall *et al.*, Differential expression of Ly6C and T-bet distinguish effector and memory Th1 CD4(+) cell properties during viral infection. *Immunity* **35**, 633-646 (2011).
209. D. J. Topham, P. C. Doherty, Longitudinal analysis of the acute Sendai virus-specific CD4+ T cell response and memory. *J Immunol* **161**, 4530-4535 (1998).
210. L. E. Harrington, K. M. Janowski, J. R. Oliver, A. J. Zajac, C. T. Weaver, Memory CD4 T cells emerge from effector T-cell progenitors. *Nature* **452**, 356-360 (2008).
211. M. Pepper *et al.*, Different routes of bacterial infection induce long-lived TH1 memory cells and short-lived TH17 cells. *Nat Immunol* **11**, 83-89 (2010).
212. M. Lohning *et al.*, Long-lived virus-reactive memory T cells generated from purified cytokine-secreting T helper type 1 and type 2 effectors. *J Exp Med* **205**, 53-61 (2008).
213. J. T. Chang *et al.*, Asymmetric T lymphocyte division in the initiation of adaptive immune responses. *Science* **315**, 1687-1691 (2007).
214. F. Sallusto, D. Lenig, R. Forster, M. Lipp, A. Lanzavecchia, Two subsets of memory T lymphocytes with distinct homing potentials and effector functions. *Nature* **401**, 708-712 (1999).
215. J. M. Schenkel, D. Masopust, Tissue-resident memory T cells. *Immunity* **41**, 886-897 (2014).
216. J. S. Hale *et al.*, Distinct memory CD4+ T cells with commitment to T follicular helper- and T helper 1-cell lineages are generated after acute viral infection. *Immunity* **38**, 805-817 (2013).
217. M. K. MacLeod *et al.*, Memory CD4 T cells that express CXCR5 provide accelerated help to B cells. *J Immunol* **186**, 2889-2896 (2011).
218. K. Luthje *et al.*, The development and fate of follicular helper T cells defined by an IL-21 reporter mouse. *Nat Immunol* **13**, 491-498 (2012).
219. A. Asrir, M. Aloulou, M. Gador, C. Perals, N. Fazilleau, Interconnected subsets of memory follicular helper T cells have different effector functions. *Nat Commun* **8**, 847 (2017).
220. D. Homann, L. Teyton, M. B. Oldstone, Differential regulation of antiviral T-cell immunity results in stable CD8+ but declining CD4+ T-cell memory. *Nat Med* **7**, 913-919 (2001).
221. M. A. Williams, E. V. Ravkov, M. J. Bevan, Rapid culling of the CD4+ T cell repertoire in the transition from effector to memory. *Immunity* **28**, 533-545 (2008).
222. H. D. Marshall *et al.*, The transforming growth factor beta signaling pathway is critical for the formation of CD4 T follicular helper cells and isotype-switched antibody responses in the lung mucosa. *Elife* **4**, e04851 (2015).
223. Y. Tian *et al.*, Unique phenotypes and clonal expansions of human CD4 effector memory T cells re-expressing CD45RA. *Nat Commun* **8**, 1473 (2017).
224. Y. S. Choi *et al.*, LEF-1 and TCF-1 orchestrate T(FH) differentiation by regulating differentiation circuits upstream of the transcriptional repressor Bcl6. *Nat Immunol* **16**, 980-990 (2015).

225. A. M. Siegel *et al.*, A critical role for STAT3 transcription factor signaling in the development and maintenance of human T cell memory. *Immunity* **35**, 806-818 (2011).
226. C. S. Ma *et al.*, Functional STAT3 deficiency compromises the generation of human T follicular helper cells. *Blood* **119**, 3997-4008 (2012).
227. E. J. Wherry, T cell exhaustion. *Nat Immunol* **12**, 492-499 (2011).
228. A. Schietinger, P. D. Greenberg, Tolerance and exhaustion: defining mechanisms of T cell dysfunction. *Trends Immunol* **35**, 51-60 (2014).
229. A. Crawford *et al.*, Molecular and transcriptional basis of CD4(+) T cell dysfunction during chronic infection. *Immunity* **40**, 289-302 (2014).
230. Y. Dong *et al.*, CD4(+) T cell exhaustion revealed by high PD-1 and LAG-3 expression and the loss of helper T cell function in chronic hepatitis B. *BMC Immunol* **20**, 27 (2019).
231. S. Hwang, D. A. Cobb, R. Bhadra, B. Youngblood, I. A. Khan, Blimp-1-mediated CD4 T cell exhaustion causes CD8 T cell dysfunction during chronic toxoplasmosis. *J Exp Med* **213**, 1799-1818 (2016).
232. X. Tian *et al.*, The upregulation of LAG-3 on T cells defines a subpopulation with functional exhaustion and correlates with disease progression in HIV-infected subjects. *J Immunol* **194**, 3873-3882 (2015).
233. P. Penaloza-MacMaster *et al.*, Vaccine-elicited CD4 T cells induce immunopathology after chronic LCMV infection. *Science* **347**, 278-282 (2015).
234. J. C. Beltra *et al.*, Developmental Relationships of Four Exhausted CD8(+) T Cell Subsets Reveals Underlying Transcriptional and Epigenetic Landscape Control Mechanisms. *Immunity* **52**, 825-841 e828 (2020).
235. S. D. Blackburn, H. Shin, G. J. Freeman, E. J. Wherry, Selective expansion of a subset of exhausted CD8 T cells by alphaPD-L1 blockade. *Proc Natl Acad Sci U S A* **105**, 15016-15021 (2008).
236. T. Wu *et al.*, The TCF1-Bcl6 axis counteracts type I interferon to repress exhaustion and maintain T cell stemness. *Sci Immunol* **1**, (2016).
237. S. J. Im *et al.*, Defining CD8+ T cells that provide the proliferative burst after PD-1 therapy. *Nature* **537**, 417-421 (2016).
238. L. M. McLane, M. S. Abdel-Hakeem, E. J. Wherry, CD8 T Cell Exhaustion During Chronic Viral Infection and Cancer. *Annu Rev Immunol* **37**, 457-495 (2019).
239. I. Siddiqui *et al.*, Intratumoral Tcf1(+)PD-1(+)CD8(+) T Cells with Stem-like Properties Promote Tumor Control in Response to Vaccination and Checkpoint Blockade Immunotherapy. *Immunity* **50**, 195-211 e110 (2019).
240. D. S. Thommen *et al.*, A transcriptionally and functionally distinct PD-1(+) CD8(+) T cell pool with predictive potential in non-small-cell lung cancer treated with PD-1 blockade. *Nat Med* **24**, 994-1004 (2018).
241. K. E. Pauken *et al.*, Epigenetic stability of exhausted T cells limits durability of reinvigoration by PD-1 blockade. *Science* **354**, 1160-1165 (2016).
242. F. Alfei *et al.*, TOX reinforces the phenotype and longevity of exhausted T cells in chronic viral infection. *Nature* **571**, 265-269 (2019).
243. C. Yao *et al.*, Single-cell RNA-seq reveals TOX as a key regulator of CD8(+) T cell persistence in chronic infection. *Nat Immunol* **20**, 890-901 (2019).
244. O. Khan *et al.*, TOX transcriptionally and epigenetically programs CD8(+) T cell exhaustion. *Nature* **571**, 211-218 (2019).
245. A. C. Scott *et al.*, TOX is a critical regulator of tumour-specific T cell differentiation. *Nature* **571**, 270-274 (2019).
246. H. Seo *et al.*, TOX and TOX2 transcription factors cooperate with NR4A transcription factors to impose CD8(+) T cell exhaustion. *Proc Natl Acad Sci U S A* **116**, 12410-12415 (2019).
247. H. W. Virgin, E. J. Wherry, R. Ahmed, Redefining chronic viral infection. *Cell* **138**, 30-50 (2009).

248. X. Zhou, S. Ramachandran, M. Mann, D. L. Popkin, Role of lymphocytic choriomeningitis virus (LCMV) in understanding viral immunology: past, present and future. *Viruses* **4**, 2650-2669 (2012).
249. K. Laposova, S. Pastorekova, J. Tomaskova, Lymphocytic choriomeningitis virus: invisible but not innocent. *Acta Virol* **57**, 160-170 (2013).
250. B. Eschli *et al.*, Identification of an N-terminal trimeric coiled-coil core within arenavirus glycoprotein 2 permits assignment to class I viral fusion proteins. *J Virol* **80**, 5897-5907 (2006).
251. W. Cao *et al.*, Identification of alpha-dystroglycan as a receptor for lymphocytic choriomeningitis virus and Lassa fever virus. *Science* **282**, 2079-2081 (1998).
252. P. Borrow, M. B. Oldstone, Mechanism of lymphocytic choriomeningitis virus entry into cells. *Virology* **198**, 1-9 (1994).
253. D. D. Pinschewer, M. Perez, J. C. de la Torre, Role of the virus nucleoprotein in the regulation of lymphocytic choriomeningitis virus transcription and RNA replication. *J Virol* **77**, 3882-3887 (2003).
254. K. J. Lee, I. S. Novella, M. N. Teng, M. B. Oldstone, J. C. de La Torre, NP and L proteins of lymphocytic choriomeningitis virus (LCMV) are sufficient for efficient transcription and replication of LCMV genomic RNA analogs. *J Virol* **74**, 3470-3477 (2000).
255. M. Perez, R. C. Craven, J. C. de la Torre, The small RING finger protein Z drives arenavirus budding: implications for antiviral strategies. *Proc Natl Acad Sci U S A* **100**, 12978-12983 (2003).
256. J. E. Gairin, E. Joly, M. B. Oldstone, Persistent infection with lymphocytic choriomeningitis virus enhances expression of MHC class I glycoprotein on cultured mouse brain endothelial cells. *J Immunol* **146**, 3953-3957 (1991).
257. M. Matloubian, S. R. Kolhekar, T. Somasundaram, R. Ahmed, Molecular determinants of macrophage tropism and viral persistence: importance of single amino acid changes in the polymerase and glycoprotein of lymphocytic choriomeningitis virus. *J Virol* **67**, 7340-7349 (1993).
258. A. Bergthaler, D. Merkler, E. Horvath, L. Bestmann, D. D. Pinschewer, Contributions of the lymphocytic choriomeningitis virus glycoprotein and polymerase to strain-specific differences in murine liver pathogenicity. *J Gen Virol* **88**, 592-603 (2007).
259. S. N. Mueller *et al.*, Viral targeting of fibroblastic reticular cells contributes to immunosuppression and persistence during chronic infection. *Proc Natl Acad Sci U S A* **104**, 15430-15435 (2007).
260. J. C. de la Torre, M. B. Oldstone, Selective disruption of growth hormone transcription machinery by viral infection. *Proc Natl Acad Sci U S A* **89**, 9939-9943 (1992).
261. R. Ahmed *et al.*, Genetic analysis of in vivo-selected viral variants causing chronic infection: importance of mutation in the L RNA segment of lymphocytic choriomeningitis virus. *J Virol* **62**, 3301-3308 (1988).
262. A. Bergthaler *et al.*, Viral replicative capacity is the primary determinant of lymphocytic choriomeningitis virus persistence and immunosuppression. *Proc Natl Acad Sci U S A* **107**, 21641-21646 (2010).
263. S. C. Smelt *et al.*, Differences in affinity of binding of lymphocytic choriomeningitis virus strains to the cellular receptor alpha-dystroglycan correlate with viral tropism and disease kinetics. *J Virol* **75**, 448-457 (2001).
264. L. Flatz, A. Bergthaler, J. C. de la Torre, D. D. Pinschewer, Recovery of an arenavirus entirely from RNA polymerase I/II-driven cDNA. *Proc Natl Acad Sci U S A* **103**, 4663-4668 (2006).
265. M. Kunzli *et al.*, Long-lived T follicular helper cells retain plasticity and help sustain humoral immunity. *Sci Immunol* **5**, (2020).
266. B. Rissiek, F. Haag, O. Boyer, F. Koch-Nolte, S. Adriouch, P2X7 on Mouse T Cells: One Channel, Many Functions. *Front Immunol* **6**, 204 (2015).

267. B. Rissiek, F. Haag, O. Boyer, F. Koch-Nolte, S. Adriouch, ADP-ribosylation of P2X7: a matter of life and death for regulatory T cells and natural killer T cells. *Curr Top Microbiol Immunol* **384**, 107-126 (2015).
268. H. Borges da Silva, H. Wang, L. J. Qian, K. A. Hogquist, S. C. Jameson, ARTC2.2/P2RX7 Signaling during Cell Isolation Distorts Function and Quantification of Tissue-Resident CD8(+) T Cell and Invariant NKT Subsets. *J Immunol* **202**, 2153-2163 (2019).
269. H. Borges da Silva *et al.*, The purinergic receptor P2RX7 directs metabolic fitness of long-lived memory CD8(+) T cells. *Nature* **559**, 264-268 (2018).
270. R. Stark *et al.*, T_{RM} maintenance is regulated by tissue damage via P2RX7. *Science Immunology* **3**, eaau1022 (2018).
271. F. Scheuplein *et al.*, NAD+ and ATP released from injured cells induce P2X7-dependent shedding of CD62L and externalization of phosphatidylserine by murine T cells. *J Immunol* **182**, 2898-2908 (2009).
272. L. Wooldridge *et al.*, Tricks with tetramers: how to get the most from multimeric peptide-MHC. *Immunology* **126**, 147-164 (2009).
273. P. G. Ritvo *et al.*, High-resolution repertoire analysis reveals a major bystander activation of Tfh and Tfr cells. *Proc Natl Acad Sci U S A* **115**, 9604-9609 (2018).
274. M. D. Buck *et al.*, Mitochondrial Dynamics Controls T Cell Fate through Metabolic Programming. *Cell* **166**, 63-76 (2016).
275. L. Wu *et al.*, Selective metabolic redundancy of Gpi1 allows for specific inhibition of inflammatory Th17 cells. *bioRxiv*, 857961 (2019).
276. M. Ralser *et al.*, A catabolic block does not sufficiently explain how 2-deoxy-D-glucose inhibits cell growth. *Proc Natl Acad Sci U S A* **105**, 17807-17811 (2008).
277. M. Berard, D. F. Tough, Qualitative differences between naive and memory T cells. *Immunology* **106**, 127-138 (2002).
278. A. F. Ochsenbein *et al.*, Protective long-term antibody memory by antigen-driven and T help-dependent differentiation of long-lived memory B cells to short-lived plasma cells independent of secondary lymphoid organs. *Proc Natl Acad Sci U S A* **97**, 13263-13268 (2000).
279. M. K. Slifka, M. Matloubian, R. Ahmed, Bone marrow is a major site of long-term antibody production after acute viral infection. *J Virol* **69**, 1895-1902 (1995).
280. P. A. Chervenick, D. R. Boggs, J. C. Marsh, G. E. Cartwright, M. M. Wintrobe, Quantitative studies of blood and bone marrow neutrophils in normal mice. *Am J Physiol* **215**, 353-360 (1968).
281. R. Schofield, L. J. Cole, An erythrocyte defect in splenectomized x-irradiated mice restored with spleen colony cells. *Br J Haematol* **14**, 131-140 (1968).
282. L. H. S. M. L. Clayton, Distribution of injected 59Fe in Mice. *Experimental Hematology* **20**, 82-86 (1970).
283. E. Hammarlund *et al.*, Plasma cell survival in the absence of B cell memory. *Nat Commun* **8**, 1781 (2017).
284. C. Brand *et al.*, The involvement of the spleen during chronic phase of Schistosoma mansoni infection in galectin-3-/- mice. *Histol Histopathol* **27**, 1109-1120 (2012).
285. S. G. Tangye, Staying alive: regulation of plasma cell survival. *Trends Immunol* **32**, 595-602 (2011).
286. L. H. Thai *et al.*, BAFF and CD4(+) T cells are major survival factors for long-lived splenic plasma cells in a B-cell-depletion context. *Blood* **131**, 1545-1555 (2018).
287. J. M. Stolley *et al.*, Retrograde migration supplies resident memory T cells to lung-draining LN after influenza infection. *J Exp Med* **217**, (2020).
288. J. Choi *et al.*, Bcl-6 is the nexus transcription factor of T follicular helper cells via repressor-of-repressor circuits. *Nat Immunol* **21**, 777-789 (2020).
289. D. L. Hill *et al.*, The adjuvant GLA-SE promotes human Tfh cell expansion and emergence of public TCRbeta clonotypes. *J Exp Med* **216**, 1857-1873 (2019).

290. J. M. Reynolds, G. J. Martinez, Y. Chung, C. Dong, Toll-like receptor 4 signaling in T cells promotes autoimmune inflammation. *Proc Natl Acad Sci U S A* **109**, 13064-13069 (2012).
291. S. Alam, A. J. Sant, Infection with seasonal influenza virus elicits CD4 T cells specific for genetically conserved epitopes that can be rapidly mobilized for protective immunity to pandemic H1N1 influenza virus. *J Virol* **85**, 13310-13321 (2011).
292. A. M. Cooper *et al.*, Disseminated tuberculosis in interferon gamma gene-disrupted mice. *J Exp Med* **178**, 2243-2247 (1993).
293. J. L. Flynn *et al.*, An essential role for interferon gamma in resistance to Mycobacterium tuberculosis infection. *J Exp Med* **178**, 2249-2254 (1993).
294. T. H. Ottenhoff, D. Kumararatne, J. L. Casanova, Novel human immunodeficiencies reveal the essential role of type-I cytokines in immunity to intracellular bacteria. *Immunol Today* **19**, 491-494 (1998).
295. M. D. Tameris *et al.*, Safety and efficacy of MVA85A, a new tuberculosis vaccine, in infants previously vaccinated with BCG: a randomised, placebo-controlled phase 2b trial. *Lancet* **381**, 1021-1028 (2013).
296. A. O. Moguche *et al.*, ICOS and Bcl6-dependent pathways maintain a CD4 T cell population with memory-like properties during tuberculosis. *J Exp Med* **212**, 715-728 (2015).
297. X. Zhang *et al.*, Unequal death in T helper cell (Th)1 and Th2 effectors: Th1, but not Th2, effectors undergo rapid Fas/FasL-mediated apoptosis. *J Exp Med* **185**, 1837-1849 (1997).
298. B. Corre *et al.*, Type I interferon potentiates T-cell receptor mediated induction of IL-10-producing CD4(+) T cells. *Eur J Immunol* **43**, 2730-2740 (2013).
299. M. Saraiva *et al.*, Interleukin-10 production by Th1 cells requires interleukin-12-induced STAT4 transcription factor and ERK MAP kinase activation by high antigen dose. *Immunity* **31**, 209-219 (2009).
300. I. A. Parish *et al.*, Chronic viral infection promotes sustained Th1-derived immunoregulatory IL-10 via BLIMP-1. *J Clin Invest* **124**, 3455-3468 (2014).

6. APPENDIX

CURRICULUM VITAE

Personal information

Name:	Marco David Künzli
Email:	marco.kuenzli@unibas.ch
Address:	Matthäusstrasse 11, 4057 Basel, Switzerland
Nationality:	Swiss
Date of birth:	March 10th, 1991
OrcID:	https://orcid.org/0000-0001-7699-779X
Google Scholar ID:	https://scholar.google.com/citations?hl=en&user=saeLhqMAAAAJ

Education

01/2016 – 10/2020	Doctor of Philosophy in Immunology (Advisor Prof Dr. Carolyn King): "Heterogeneity and plasticity of the CD4 T cell compartment in viral infections" University Hospital of Basel, University of Basel, Department of Biomedicine (Switzerland)
09/2015	Swiss Federal Diploma for Pharmacists
09/2013 – 07/2015	Master of Science in Pharmacy (Grade: 5.6 out of 6) University of Basel (Switzerland)
01/2014 – 06/2014	Masters thesis: "Studies of phosphoinositide 3-kinase δ-selectivity using reciprocal mutagenesis and identification of new selective inhibitors" (Mark: 5.5/6, with 6 being the best mark) Monash University, Melbourne (Australia)
09/2010 – 07/2013	Bachelor of Science in Pharmaceutical Sciences University of Basel (Switzerland)

Employment history

01/2016 – 10/2020	Doctor of Philosophy in Immunology (Advisor: Prof. Dr. Carolyn King) University Hospital of Basel, Department of Biomedicine (Switzerland) Project #1: Long-lived T follicular helper cells retain plasticity and help sustain humoral immunity My role in this project was to participate in the conceptualization of the project, designing experiments, and I was the main executer of the experiments. Additionally, I was involved in data analysis and contributed to writing the manuscript. Project #2: The impact of TCR signal strength on CD4 T cell differentiation in acute and chronic viral infection My role in this project was to design experiments and I was the main executer of the experiments. Subsequently, I was involved in data analysis and writing the manuscript.
10/2015 – 01/2018	Pharmacist (part-time, 10%) Stedtli Apotheke, Laufen (Switzerland)

	Deputy pharmacy store manager responsible for a team of 8 people and all subject-specific decisions.
09/2014 – 07/2015	Assistance year as Pharmacist Stedtli Apotheke, Laufen (Switzerland)

Supervision of students/junior researchers

09/2018	Lara Kroczek, intern

Teaching activities

03/2020	Lecturer in the Microbiology and Immunology block course at the Biozentrum of the University of Basel (Bachelor's degree).
04/2019	Assistant in the practical course of the Microbiology and Immunology block course at the Biozentrum of the University of Basel (Bachelor's degree).

Active memberships in scientific societies

06/2017 – present	Member of the Swiss Society for Allergology and Immunology (SSAI)

Prizes, awards, fellowships

05/2020	Freiwillige Akademische Gesellschaft Basel (7'000 CHF)
04/2020	Nikolaus und Bertha Burckhardt-Bürgin foundation (33'000 CHF)
11/2019	Keystone Symposia scholarship (1'200 USD)
04/2018	University of Basel travel fund for early career researchers (1'810 CHF)

Personal skills

Languages	German (native language), English (fluent), French (basic)
IT skills	MS Office: Word, PowerPoint, Excel Pages, Keynote, Numbers GraphPad Prism (Statistics) FlowJo (Flow cytometry data analysis) Python (basics) Inkscape R (basics, hands-on experience in scRNA-Seq, bulk RNA-Seq & ATAC-Seq analysis)

Contributions to international conferences

2020	**Keystone, Banff, Canada**: Poster presentation "Survival and fitness in the TFH memory compartment"
2019	**SSAI Annual Congress, Lugano, Switzerland**:Poster presentation "Survival and fitness of the TFH memory compartment"
2018	**Keystone, Austin, USA**: Poster presentation "Long-lived T follicular helper cells retain plasticity and help sustain humoral immunity"

Publications

Long-lived T follicular helper cells retain plasticity and help sustain humoral immunity

Marco Künzli, David Schreiner, Tamara C. Pereboom, Nivedya Swarnalekha, Ludivine C. Litzler, Jonas Lötscher, Yusuf I. Ertuna, Julien Roux, Florian Geier, Roman P. Jakob, Timm Maier, Christoph Hess, Justin T. Taylor and Carolyn G. King

Science Immunology, 2020 March 6. doi: 10.1126/sciimmunol.aay5552
Link: https://immunology.sciencemag.org/content/5/45/eaay5552

Opposing effects of T cell receptor signal strength on CD4 T cells responding to acute vs chronic viral infection

Marco Künzli, Peter Reuther, Daniel D. Pinschewer, Carolyn G. King

bioRxiv, 2020 August 06, doi:10.1101/2020.08.06.236497
Link: https://www.biorxiv.org/content/10.1101/2020.08.06.236497v1

Development of single and mixed isoform selectivity PI3Kδ inhibitors by targeting Asn836 of PI3Kδ.

Michelle S. Miller, Simon J. Mountford, Jo-Anne Pinson, Zhaohua Zheng, **Marco Künzli**, Vanit Patel, Simon J. Hogg, Jake Shortt, Ian G. Jennings, Philip E. Thompson.

Bioorg Med Chem Lett. 2016 Oct 1;26(19):4790-4. doi: 10.1016/j.bmcl.2016.08.028.
Epub 2016 Aug 11.
Link: https://www.sciencedirect.com/science/article/pii/S0960894X16308496?via%3Dihub

Redefining CD4 T cell residency: Helper T cells orchestrate protective humoral immunity in the lung

Nivedya Swarnalekha, David Schreiner, Ludivine C. Litzler, Saadi Iftikhar, Daniel Kirchmeier, **Marco Künzli**, Carolyn G. King

bioRxiv, 2020 February 28. doi: https://doi.org/10.1101/2020.02.28.963280
Link: https://www.biorxiv.org/content/10.1101/2020.02.28.963280v1

Resident Memory T cells Escape 'Home Quarantine'

Marco Künzli, Carolyn G. King

Trends in Immunology, 2020 May 06. doi: https://doi.org/10.1016/j.it.2020.04.010
Link: https://www.cell.com/trends/immunology/fulltext/S1471-4906(20)30094-6